2011-12-10

Web-based Medical Imaging Simulation System for Education and Research

Xiping Li
University of Miami, x.li11@umiami.edu

UNIVERSITY OF MIAMI

WEB-BASED MEDICAL IMAGING SIMULATION SYSTEM FOR EDUCATION AND RESEARCH

By

Xiping Li

A DISSERTATION

Submitted to the Faculty
of the University of Miami
in partial fulfillment of the requirements for
the degree of Doctor of Philosophy

Coral Gables, Florida
December 2011

UNIVERSITY OF MIAMI

A dissertation submitted in partial fulfillment of
the requirements for the degree of
Doctor of Philosophy

WEB-BASED MEDICAL IMAGING SIMULATION SYSTEM FOR EDUCATION AND RESEARCH

Xiping Li

Approved:

_____ Weizhao Zhao, Ph.D. Associate Professor of Biomedical Engineering	_____ Terri A. Scandura, Ph.D. Dean of the Graduate School
_____ Jorge Bohorquez, Ph.D. Assistant Professor of Biomedical Engineering	_____ Mike Georgiou, Ph.D. Associate Professor of Radiology
_____ Fabrice Manns, Ph.D. Associate Professor of Biomedical Engineering	_____ Xiaodong Wu, Ph.D. Professor of Radiation Oncology

LI, XIPING (Ph.D., Biomedical Engineering)

Web-based Medical Imaging Simulation System for Education and Research. (December 2011)

Abstract of a dissertation at the University of Miami.
Dissertation supervised by Professor Weizhao Zhao.
No. of pages in text. (140)

Based on the development of information and communication technology, especially in the wireless communication field, cloud computing becomes a solution to rapidly escalating service demand in more and more areas. In this work, a major effort has been made to establish an Internet accessible system for medical imaging simulation as a convenient service under the cloud computing environment.

First, an Internet accessible, medical imaging education platform has been developed. It includes teaching and dynamic assessment tracking system for five commonly used imaging modalities. Each imaging modality is delivered by interactive modules. Students' learning gain and/or instructors' teaching effect can be evaluated by assessment questions and other feedback methods. The system is integrated by the open source MySQL database software that manages updating materials and also tracks students' learning engagements, which allow the reliability and appropriateness of the on-line teaching material and assessment methods to be optimized. Instructor gets instant feedback on the topic delivered through his/her lecture when students work on the system. Since 2007, 103 students had used it as an assistant learning platform. The evaluation results have shown increased learning gains promisingly.

Second, a prototype simulation service platform has been established. This platform can manage different simulation applications. It is based on a job-oriented work flow to provide different kinds of service to users to perform medical imaging simulation.

These simulations not only include the straightforward CT data reconstruction based on Radon transform, but also the sophisticated PET imaging simulation based on GATE, an open source software, as well. To perform nuclear medicine imaging simulation, QGATE designer, a GUI-based GATE system, has been developed in this work. The QGATE designer provides users a graphical environment where a simulation design is simply achieved by "drag-and-drop objects" and "choose-and-modify parameters". The scripts that used to be manually entered to the GATE system will be automatically generated and complied by the system. The QGATE system can be installed on individual computers so that multiple users can work on their simulation projects individually and simultaneously by using the graphical designing tools. The QGATE's client-server configuration can manage the GATE system to queue and monitor the submitted simulation scripts and return simulation results. The system is suitable for classroom training and easy to use for students or new users to the field of nuclear medicine imaging simulation.

Finally, based on the developed simulation platform, a simulation study on PET imaging has been carried out. Event-based dynamic justification method has been tested based on the phantoms generated by NCAT associated with different breathing signals. The results show its potential capability of motion correction for PET data acquisition.

The education and simulation service platform is a useful tool for medical imaging. Further developments will enable the established system to expand its application fields and serve for e-learning under cloud computing environment.

ACKNOWLEDGEMENTS

First and foremost, I would like to express my sincere gratitude to my advisor, Dr. Weizhao Zhao, an extraordinary mentor and friend, for his continued guidance, encouragement, and support during my doctoral program. It is my privilege to work in his outstanding research team to obtain both professional knowledge and research experiences from him. Without him, this study would not have been possible.

I would also like to thank the committee members, Dr. Jorge Bohorquez, Dr. Mike Georgiou, Dr. Fabrice Manns and Dr. Xiaodong Wu, for their time, knowledge, invaluable suggestions and help on various aspects of this dissertation.

Thanks to all my friends, especially Dr. Ta-Cheng Chang and Zhuang Nie for their constant help during my study.

Most importantly, I want to express my deepest appreciation and love to my parents, my sisters and their family members. Without their unconditional love and continued encouragement, I would never have the opportunity to accomplish this dissertation.

Finally, I would like to thank my wife Dr. Xiaoping, Mo and my son, Xinghan, for all of their love and support.

Xiping Li

December 2011, Miami, Florida

TABLE OF CONTENTS

LIST OF FIGURES

LIST OF TABLES

CHAPTER 1 INTRODUCTION

1.1 BACKGROUND

Since 2006, cloud computing [1] has always been a hot topic and become more and more popular in these years. Though there is no standard and unified definition of this concept, the key idea behind is still "service". However it is more than a service concept. It gives a clear perspective technology trend on how to provide flexible, on-demand, dynamic, economic solutions and scalable infrastructure for different applications to different customers [2]. As a pioneer and a leader in cloud computing, in 2006, Amazon launched its cloud computing services: Simple Storage Service (S3) [3] and Elastic Computing Cloud (EC2) [4]. It is a typical example of the Infrastructure as a Service (IaaS). In 2008, Google announced its Python-powered Google App Engine (GAE) [5] as the Platform as a Service (PaaS). Microsoft also introduced its own PaaS: Windows Azure Platform (WAP) to help its customer to build, debug, test and distribute web services quickly and inexpensively as well as with minimal on-premises resources [2]. Another important application of cloud computing is the Software as a Service (SaaS), in this category, the most representative examples are Google Apps [6], and Microsoft Office Live [7] . Those kinds of software are running on a cloud platform. Users can check them out on-demand any time, at any terminal with internet connection such as PC, Netbook, smart phone and tablet computer.

Besides applications in business and IT field, knowledge based education and scientific computation also have been expanded in cloud computing field. In 2009, Delic K, et, al [8] proposed their Enterprise Knowledge Cloud (EKC) model to manage, share and deploy data, information and knowledge among company's employee, clients,

customers, partners and suppliers. Elastic-R [9] , in brief R, is an open platform for scientific computing. R, as a special language and environment, provides data analysis functions through running virtual machines on a cloud platform. R has also cross-platform capabilities, very powerful graphical system and interfaces to other popular scientific tools such as Scilab [10] and ROOT [11] .

Based on analysis of these successful cases and the common used ontology of cloud computing, in this work, a prototype of simulation service model for medical imaging is proposed. With a distributable education software package together, they are two major contributions of this work. Both of them have client-server structure and can be easily deployed to or hosted on a cloud computing environment. They can offer different education and specific research services in medical imaging field.

1.2 MOTIVATION

As an interdisciplinary science, medical imaging combines physics, mathematics, electrical engineering and computer engineering and provides students with a broad view of an integration of different technologies applied to biology and medicine. Various curricular settings are designed for different levels of student's learning objective. Commonly used clinical imaging modalities (X-ray, Computed Tomography, Magnetic Resonance Imaging, Nuclear Medicine Imaging and Ultrasound) are often taught through a series of courses, emphasizing the physics and signals, reconstruction and systems, or advanced topics. Meanwhile, medical imaging techniques are now ubiquitous in clinical and research laboratories. Medical imaging opens career opportunities for students in

fields of medical equipment or instrument manufacturing, medical imaging, signal software engineering, or even medical physicists after further training.

Recognizing the broad impact of medical imaging education, to deliver the knowledge efficiently and evaluate the education output, there comes a motivation to start an on-line learning and simulation platform. And it was originated from the idea, "A picture is worth/better than a thousand words", i.e., using pictorial description would be superior to the text-only description. We extended the idea, "A moving picture is better than a static picture," Furthermore, we added, "An interactive moving picture is better than a simple moving picture." Ultimately, our goal is to develop an online user-interactive teaching/learning system, as well as a software package which can be easily distributed, featuring animations and simulations for physical principles, mathematical derivations and engineering implementations, so as to fulfill the medical imaging education and simulation research tasks optimally. Eventually educators and students in medical imaging field may benefit from this project.

Since medical imaging is an important research field, there are many topics in PET (Positron Emission Tomography), SPECT (Single Photon Emission tomography), and CT (Computed Tomography). To the students who are interested in medical imaging field, it is crucial to bridge learning and research together. By using simulation, they can easily understand the physics principle of some medical instruments which are clinical commonly used. On the other hand they also can visualize these instruments, even design their own instrument. At the same time, they can also process the collected data to view

the result of different operations. Obviously, online interactive simulation services fit the purpose.

When conducting simulation, Monte Carlo methods are commonly used in PET. Several open source software packages are also available, such as SimPET and GATE [12] (Geant4 [13] Application for Tomographic Emission). However these kinds of open source software written in C++ need more experience to setup, configure and use. Meanwhile these kinds of software are not web-accessible such that they are uncommon to students and researchers. Also it is impossible to distribute them directly as a service on a cloud computing environment.

GATE [12] is a well-recognized PET simulation software. However, as a Linux application, in order to make it work, a series of supporting software must be compiled first. It is not easy for beginners and some researchers who do not have much programming experience. Whereas it may not be necessary for a temporary user (e.g. students) to build a working application by himself/herself, if he/she just wants to learn the principle behind PET using simulation method. Besides, the first step of the simulation based on GATE is to create a simulation script, therefore if a user is not familiar with the commands to generate many kinds of objects with hundreds of properties; it's hard to say he/she can run a simulation successfully.

In addition, simulations based on GATE [12] are extremely time-consuming, hard disk space capacity-consuming as well as high calculation capability demanding procedures. There is a need for a simulation service which has enough resources to

alleviate this requirements and at the same time, can be remotely accessed by different users at any time, any place with any terminal with network connection.

Meanwhile the platform that provides simulation services should have capabilities to handle different simulation applications. For example, a reconstruction simulation service can take different inputs from users. A PET simulation service could let users choose different virtual PET instrumentations, phantoms, and define source activity to carry out a specific research. In addition, it should be easily deployed to a cloud computing environment and reduce cost.

1.3 SUMMARY OF MAJOR WORK AND CONTRIBUTIONS

According to previous analysis, in this work, two web-based software packages for medical imaging education and simulation have been developed. Their common character is that they are distributable. This is one of most important features that should be considered in the first place. Both of them can be easily deployed to different network environments.

Introducing a user-oriented simulation service model is another important feature. Cloud computing is not only a technology trend in the future, but italso is a new business model. On-demand simulation service can give developers or content providers many opportunities to expand functions and features which users or the market really need. Meanwhile, these services can be accessed on convenient service nodes, no matter where they are located in public, private or hybrid cloud environment (Figure 1).

Here major work and contributions are summarized as follows,

1. Implementation of a distributable education software package for medical imaging, which includes two parts:

1) Based on the needs of curriculum, instructors and students, an Internet accessible, interactive module-based MITS (Medical Imaging Teaching System) has been built. The content granularity of each topic in each medical imaging modality has been defined to make sure MITS can be re-organized easily and is suitable for different level students.

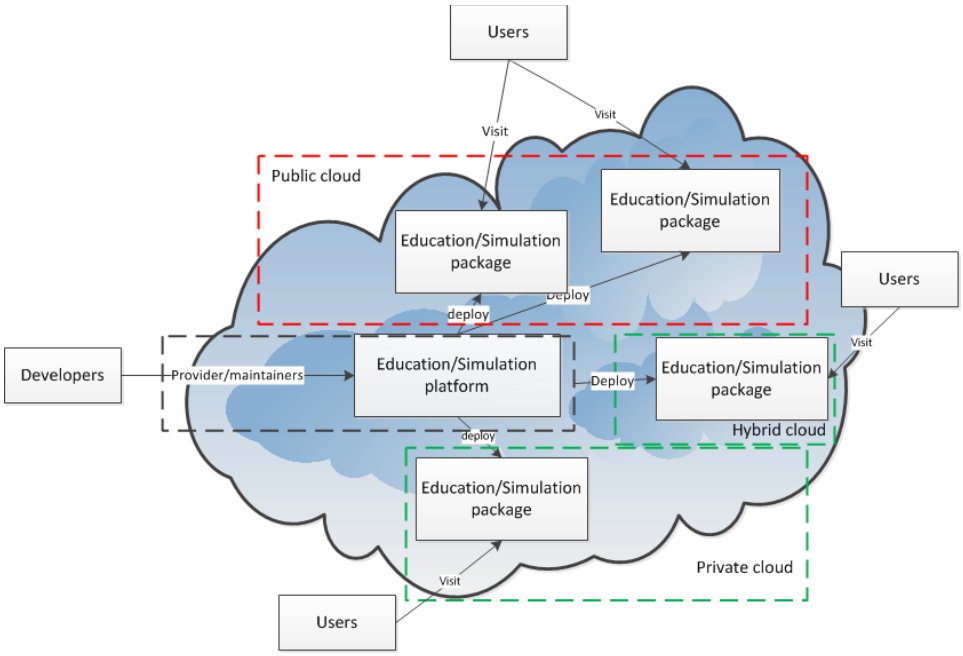

Figure 1: Relationship between developing, deployment and service in cloud computing environment

2) A DATS (Dynamic Assessment Tracking System) has been built, the following features have been included:

a) The on-line accumulative collected data can help evaluate the teaching efficiency of instructors and the learning effectiveness of students, the

feedback of the analysis result can help instructor boost efficient teaching to some degree.

b) The DATS also can provide meaningful information for assessing the content of each imaging modality to help build a successful medical imaging curriculum for students at different levels.

c) Through analyzing the questions' reliability, the questions can be made more reasonable and match the needs of assessment and evaluation. When enough information has been accumulated, those questions used in the test which have more reliability and are related to the basic concept of a medical imaging curriculum, can help found a medical imaging concept inventory.

d) MITS and DATS is a distribution package, any institutions who are interested can install it locally, and the information collected by those institutions may be shared among institutions

2 Implementation of a prototype of a simulation service platform which has following features:

1) It can wrap different medical imaging simulation applications in one distributable package. One of the most important features of MITS is using interactive simulations to help student to understand some fundamental concepts in medical imaging. Simulations created using Matlab [14] are very difficult to distribute with MITS and DATS. Besides Matlab [14] is a very expensive commercial software with a high license fee even in the academic

field, and a serious disadvantage is that they are not exactly network applications even though they have a network interface. This means that if some students operate these simulations almost at the same time, maybe they cannot get the correct result that should be. The simulation service platform overcomes those disadvantages. It is a guideline to help develop and deploy medical imaging simulation applications. Meanwhile it becomes a bridge to connect users and those simulation applications.

2) An innovation method in this simulation service platform is to introduce the "job" concept to manage and coordinate the input from different and the output from different simulation applications. Each job can save the input and output values and has its job status which can be checked by the user. Service server uses multi-thread programing technology to encapsulate different simulation applications in different threads. Running exception from single simulation application will not influence other simulation applications. This makes the simulation platform more stable, and gives it the capability to adjust itself against the server resource deficiency, for example, memory shortage, hard disk shortage and so on.
3) As a development example and guideline, in this work, a simulation application of Radon transform is realized. Under the simulation service platform, it can do Radon transform and inverse Radon transform to the images submitted by different users simultaneously, and users can select

their own transformation parameters and configuration, such as filter, filtering sonogram or filtering reconstruction image, etc.

4) QGATE, a complete simulation application for PET based on GATE, has been developed and wrapped in the simulation service platform. Unlike light-weighted simulation applications, QGATE needs much more server resources and always needs much more times to complete a simulation job. In order to reduce errors and exceptions during the simulation as well as help the user understand GATE, a designer client which has GUI (Graphic User Interface) has been developed based on Qt4.60 [15]. It can help users to design part of or a whole simulation script based on the rule of WSWG (what you see is what you get). Especially. It can help design different virtual PET instrumentations which have different geometrical structure, different crystal material and structure. wGate, an application running on Microsoft Windows platform, has been migrated from Linux platform based on the source code of GATE to help users to check out the simulation script before submission to the simulation server, it can also be used to complete a light-weighted simulation job locally.

3 Another important work is a simulation study based on GATE and the simulation service platform. Reducing or suppressing respiratory impact on PET imaging is always a hot topic. Numerous efforts have been devoted to this field including instrumentation improvement (PET/CT) [16], [17], [18], [19], [20], [21], [22], [23], [24], [25], data acquisition method improvement (List-mode [26], [27],

[28], [29], [30], [31] , Gated-mode [23] , [32], [33]) and post-processing (De-convolution [34], [35], [36]). Based on these efforts, several dynamic phantoms are designed using 4D NCAT (NURBS (Non-Uniform Rational B-Spline) -based Cardiac-Torso) [25] to simulate different respiratory status such as normal breathing, drinking or swallowing, coughing, and hiccupping. These phantoms have the physiology data source and can provide simulated human organs' location and movement according to the external movement signal which is used to simulate respiration. Pre-generated lesions with different volume and different activity distribution have been merged into phantoms. A new proposed motion correction method is tested based on these phantoms.

1.4 DISSERTATION OVERVIEW

The dissertation is organized as follows. In Chapter 2, the background of developing on-line medical imaging education software package is described. Design principle, evaluation rules, and assessment workflow are provided. The statistics and comparison results of data are given.

Chapter 3 describes the design and implementation of a prototype simulation service platform and related applications. Using a simulation application as an example, which can realize a Radon transform, inverse Radon transform, and FBP (Filtered back projection), a working mechanism of the multithread core is given. In Chapter 4, the backgrounds of PET and GATE [37], [38] are reviewed. The design, implementation of QGate designer and several design examples are presented.

Chapter 5 covers the PET simulation study. First breathing mechanics and motion correction methods in PET imaging are reviewed. Second, realistic phantoms based on NCAT [25] are generated and optimized. A new method of motion correction is proposed and tested.

Chapter 6 summarizes the works of this study and gives some suggestions of further developing direction of the education package and the prototype of simulation service platform for medical imaging.

CHAPTER 2 WEB-BASED EDUCATION PLATFORM FOR MEDICAL IMAGING

2.1 BACKGROUND AND SIGNIFICANCE

Biomedical engineering (BME) education has developed as an interdisciplinary engineering training area in the last 30 years. The *ASEE College Profiles* show that BME has become one of the most rapidly growing undergraduate engineering majors in the last decade (undergraduate enrollment has tripled from 1999 to 2010) [39], and is one of the only three engineering majors (with aerospace engineering and nuclear engineering) that have been monotonically increasing since 1999. Figure 1 depicts the trend of the enrollment of BME undergraduates in USA colleges.

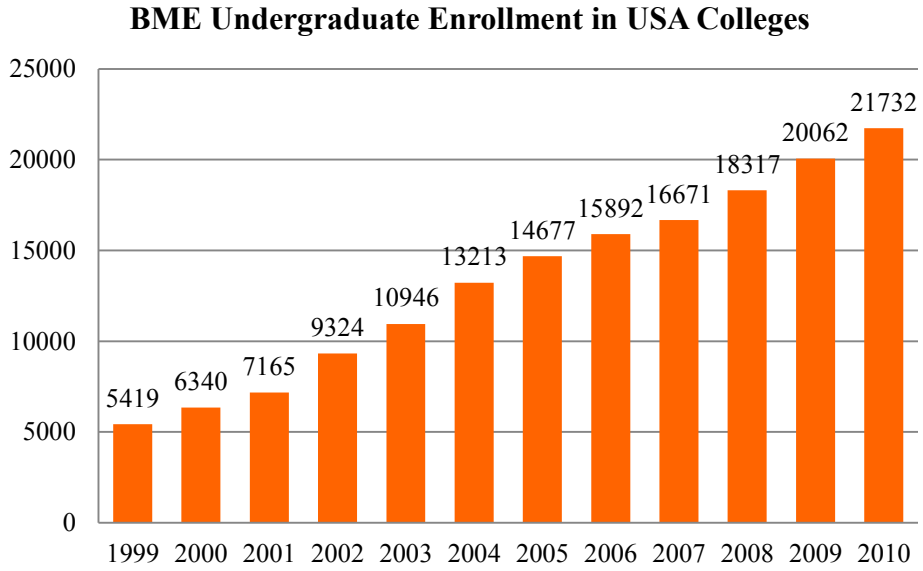

Figure 2: Statistics result of BME undergraduate enrollment in USA colleges from 1999-2010

As an important training area for BME students, the broad impact of medical imaging education is recognized. More and more institutions have established such a curriculum. Comprehensive discussion for undergraduate medical imaging education has

been published [40]. According to Whitaker Foundation database 2007 [41], there are 119 universities or colleges that have BME programs. Based on the list, a two-month survey was conducted through Internet in summer 2008. Figure 2 is the concise version of the survey result. Detailed information can be downloaded from our MITS website (http://mis.eng.miami.edu). 80 of them offer graduate level medical imaging courses, and 68 offer undergraduate level medical imaging courses. There are 51 institutions having *Internet-available* medical imaging teaching materials; most of them have one or two imaging modalities, and among them 15 institutions have *Internet-active* (but not interactive) animations or simulations. There are no systematic on-line programs to provide interactive simulation of any medical imaging modality.

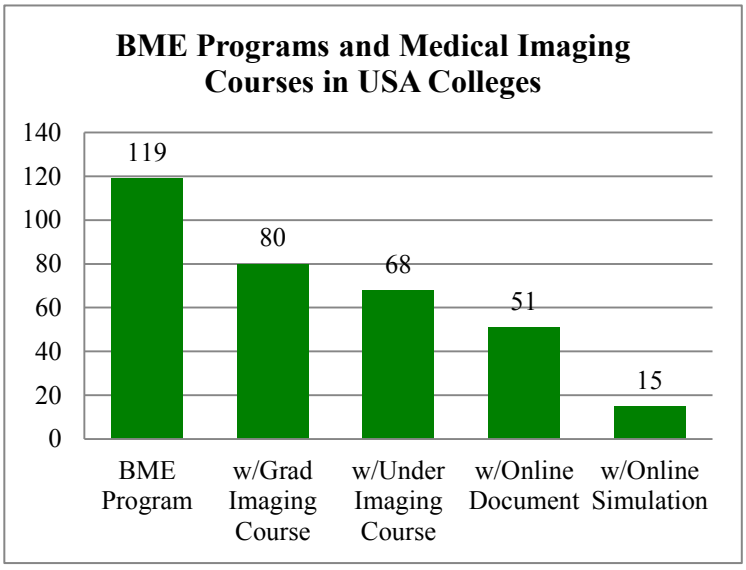

Figure 3: On-line survey result of BME in summer 2008

From the survey result, we can realize more and more colleges provide BME programs, but there are a few that provide online animation materials and simulation programs to help student learning medical imaging courses. Meanwhile, in the

Department of Biomedical Engineering at the University of Miami, six courses related to medical imaging are offered to students in different levels. These courses combine physics, mathematics, electrical engineering and computer engineering and provide students with a broad view of an integration of different technologies applied to biology and medicine. This provides us an opportunity as well as challenge to explore how to deliver these courses. Table 1 gives some basic information of the curriculum.

	Title	Topic	Other Information
BME 330	Foundation of Medical Imaging	Physics, basic technology	Required Junior
BME 520	Medical Imaging Systems	Non-invasive imaging modalities, Reconstruction	Elective Senior/Graduate
BME 521	Medical Imaging Application	Invasive imaging modalities, Image processing	Elective Senior/Graduate
BME 629	Advanced Medical Imaging	Advanced reconstruction Research topics	Elective Graduate
BME 645	Biomedical Optical Imaging and Diagnostics	Optical Coherence Tomography (OCT), Optical Microscopy, laser Doppler flow metry, etc	Elective Graduate
BME 681	Radiation Therapy Physics	Modern physics , basic modalities and instrumentations of radiation therapy	Elective Graduate

Table 1: Courses offered in BME department of University of Miami

Medical imaging involves various physics principles, diverse mathematic derivations for image generation, recognition and reconstruction, special system configurations and specific applications for different modalities. The tremendous amount of information and rapid changes in the medical imaging field require teaching material to be more flexible to fit into the available class hours. Efficient teaching for faculty and effective learning for students are crucial to the success of medical imaging education [42],

[43]. Along with the progress of other engineering education [44], [45], [46], medical imaging also seeks the best way to deliver knowledge to students. Internet/web-based education (a major subcomponent of the broader term "e-learning") is one of the tools with which education is popularly delivered [47], [48], [49], [50]. Education through the Internet makes it possible for more individuals than ever to access knowledge and to learn in new and different ways. Efforts have been made in different aspects, such as image reconstruction techniques varying from the very theoretical [51], [52], [53], to the math-intensive [54], [55], to algorithm efficiency and to image quality improvement [56], [57]. However, limited efforts actually describe, step-by-step, the process of the generation of image data, which is the fundamental education component of medical imaging. Hyper-textbooks are a source of "dynamic" online education that provides additional multimedia elements, as opposed to "text-picture" only textbooks. Several hyper-books [58], [59] are popularly used for medical imaging courses. Most hyper-textbooks provide a "one-way" active teaching model without interactivity.

Meanwhile, concept related animations and interactive simulation programs are becoming widely recognized as important tools. They can help students establish scientific and correct reflection of those concepts which include the basic knowledge of medical imaging. Without doubt, they will benefit from these correct understanding in their future study.

Interactivity among instructor, teaching material and students, is proven as an effective way to improve teaching efficiency [60], [61], [62]. Interactive learning environments can provide multiple means of representation and expression for the learner

through text and graphic modes, animated simulations and other combinations of the media. Interactive education aids in increasing the student's comprehension, motivation level and perception of learning [63]. Interactive modules allow students to tailor presentations to suit their own exact needs with sound, animation and video capturing the viewer's attention and conveying explanations more effectively [64]. Interactive medical imaging education has primarily been used for medical professionals [65], [66], or for developing programming skills for radiologists [67], [68]. On the other hand, the Internet's interactive feature is usually utilized well but its advantage to learning evaluation is often neglected. For example, the Internet provides the teaching-learning process, an efficient and automatic way to receive unbiased feedback by designed assessment functions [69], [70]. A dynamic tracking system embedded in the Internet accessible interactivity teaching software is highly desirable to use the Internet's unbiased and online feedback feature to influence evaluation.

Above all, as an online learning environment, MITS, has already been found to be useful to help successfully deliver these medical imaging curriculums. Meanwhile, to obtain a reasonably adequate perspective of student's performance, to evaluate teaching efficiency and assess student learning gain, an online tracking platform, DATS is also needed.

2.2 DESIGN PRINCIPLE OF MITS AND DATS

For MITS and DATS, we not only try to match student's learning style [71], "I hear and I forget, I see and I remember, I do and I understand." But also based on the rule of Kolb's experiential learning theory [72], [73] and the idea behind the theory of Convent

Inventory) [74], the content and material of MITS are organized and similar assessment methods are adopted.

2.2.1 PEDAGOGICAL MOTIVATION

The motivation to start this project was originated from the idea, "A picture is worth/better than a thousand words", i.e., using pictorial description would be superior to the text-only description. We extended the idea, "A moving picture is better than a static picture," (by using Adobe Flash Player or Media Player). Furthermore, we added, "An interactive moving picture is better than a simple moving picture," (by adding interactivities). Based on this idea, an online user-interactive teaching/learning system can be built, featuring animation and simulation for physical principles, mathematical derivations and engineering implementations, so as to fulfill the medical imaging education tasks optimally.

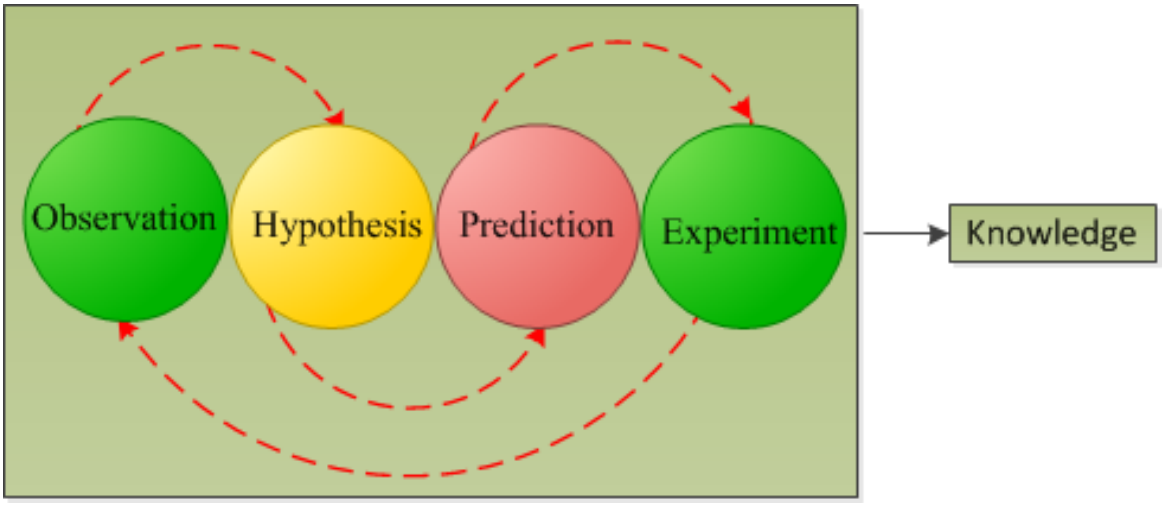

Figure 4: Four phases of scientific research method

2.2.2 KOLB'S LEARNING CYCLE THEORY

As we all know, the process of human knowledge will be achieved through four phases (Figure 3), first we observe the natural world around us, and find a phenomenon or problem, based on the knowledge we already have, we propose a hypothesis and utilize it to make some predictions and design appropriate experiments to test them, if the results of those experiments match well with those predictions. The new finding will be identified and integrated in the knowledge pool. This iterative process is so called the scientific research method [75], [76].

Similar with the scientific research method, Kolb [72], [73] proposed his learning cycle theory in 1984. This theory describes the personal studying process. The cycle is divided in four different stages which combine experience (feeling), perception (watching), cognition (thinking) and action (doing). Every stage can be the start point or the end point, the learner progresses learning through a cycle. In each cycle, a new concept will be introduced based on what he felt and observed in the previous cycle, new experience and new observation will be gained and will lead to further experiment. The cyclic learning process will make the learner advance in a specific field if he is more deliberately engaged in. Now it has already become the foundation of constructivist learning theory, and is always used as the guide to design instructional material.

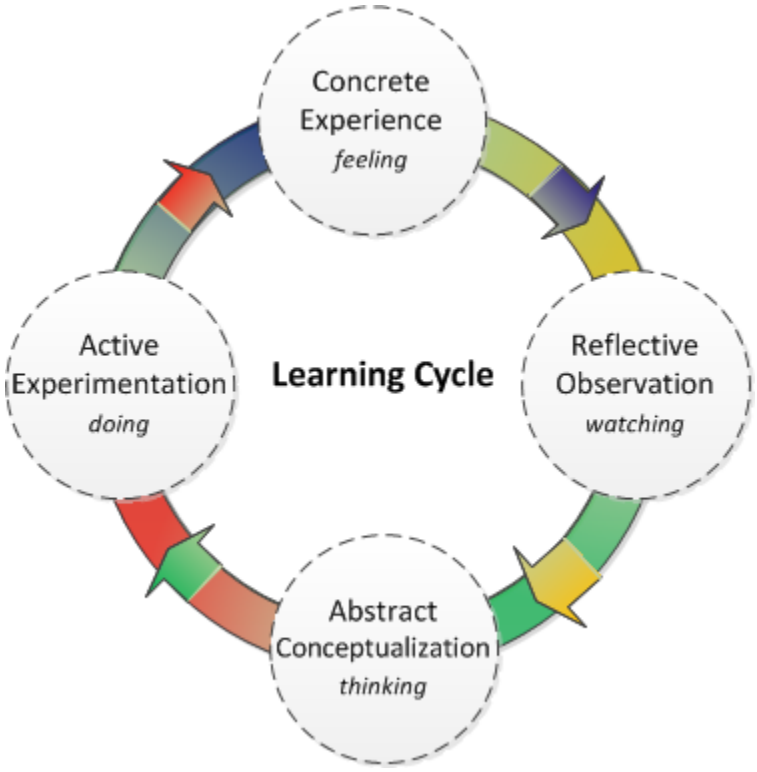

Figure 5: Illustration of Kolb's learning cycle

2.2.2 CONCEPT INVENTORY

Simply speaking, CI (Concept inventory) is a method and theory to assess education output based on human common sense. Since the first one, FCI (Force Concept Inventory) [74], published in 1992, several kinds of concept inventory in different field have been developed and proved their ability to evaluate students' learning performance. They are SSCI (The Signals and Systems Concept Inventory) [77], SCI (The Statistics Concepts Inventory) [78], GCI (Genetics Concepts Inventory) [76], SOMCI (Strength of Materials Concept Inventory) [79], CGI (The Chemistry Concepts Inventory) [80], [81], WCI (The Wave Concepts Inventory) [82] etc. Especially, a pilot version of an inventory of biomedical physics elements-of-competence for diagnostic radiography education in

Europe was developed in 2005 [83]. The design idea based on competence levels is also adopted in DATS.

The key idea of CI is to design serial questions related to a special curriculum. These questions only focus on the basic concepts, and avoid real complexities as far as possible. They require little or no computation. Students can solve these questions using their commonsense. Two tests including the same concepts/questions will be given to students, one is at the beginning, and the other is at the end. Through analyzing the result of the two tests, student's overall understanding of those basic concepts can be evaluated. Teaching performance and effect can be assessed. The result can motivate the teacher to change their teaching method and skill, stress specific concepts in the next cycle, and update their lecture content.

2.3 EVALUATION METHODS OF DATS

2.3.1 NORMALIZED GAIN

CI is not only another test; it can be viewed 1) As a diagnostic tool, 2) For evaluating instruction, and (3) As a placement exam [74]. The main assessment method of CI is normalized gain $\bar{g}$ [77], it is defined as follows:

$$\bar{g} = \frac{G_{post} - G_{pre}}{100 - G_{pre}} \qquad (2\text{-}1)$$

Where G_{post} is the post-test grade of a student, and G_{pre} is the pre-test grade. The normalized gain has advantage of supplying a more systematic and complete profile of the understanding of basic concepts.

2.3.2 COEFICIENT ALPHA

Kuder and Richardson [84] are pioneers in quantifying test reliability. The KR-20, coming from their equation 20, is commonly used to evaluate dichotomous scoring tests. The equation is given below:

$$r_{tt} = \frac{n}{n-1}\left(1 - \frac{n\overline{p_i q_i}}{\sigma_t^2}\right),\ i = (1,2,\ldots\ldots,n) \quad (2\text{-}2)$$

where r_{tt} is the reliability of the test, n is the total number questions in the test, σ_t^2 is the variance of the total score in the test. p_i is the proportion of students who answer the question correctly, q_i is the proportion of students who answer the question incorrectly.

Cronbach [85], [86] further gave a generalized equation, Eq.(2-3). It can be used in the test if all the questions are equally-weighted graded. Guttman [87] also derived this equation independently. It makes the value α have different names. Sometimes it is referred as Cronbach' alpha or coefficient alpha. It is also called as Guttman-Cronbach alpha in psychometric literature.

$$\alpha = \frac{n}{n-1}\left(1 - \frac{\sum V_i}{\sigma_t^2}\right), i = (1,2,\ldots\ldots,n) \quad (2\text{-}3)$$

where $\sum V_i$ is the sum of the variances of each question.

Kirk Allen [88] further proved, for dichotomously scoring questions, V_i reduced to $p_i q_i$, so the same value can be obtained . So the definition of the alpha value in Eq. 2-3 can be used. If the contribution of a question makes the alpha value increase, the question can be viewed as a "good" one and vice versa. The equation is given in the following:

$$\Delta\alpha = \alpha_n - \alpha_{n-1} \quad (2\text{-}4)$$

Where $\Delta\alpha$ is the change of alpha value when a question's contribution is removed, α_n is the overall alpha value when all questions are taken into account, α_{n-1} is the alpha value when the specific question is removed.

A "good" question will lower the alpha value when it is removed from the calculation, a "bad" one will have opposite effect to the alpha value, the $\Delta\alpha$ will be positive for a "good" one, and a " bad" one will have a negative alpha value changes.

Another parameter to evaluate the question used by Kirk Allen [88] is "gap", it quantifies the effect on total score variance of a specific question. In this work, the same idea is adopted, but we use the following equation to calculate the "gap" of the *i*th question,

$$g_i = \frac{\left(\frac{\sum^k x}{k}\right)_{i,correct} - \left(\frac{\sum^j x}{j}\right)_{i,incorrect}}{100} \quad (2\text{-}5)$$

Where g_i is the "gap" of question *i*, $\left(\frac{\sum^k x}{k}\right)_{i,correct}$ is the average score of students who answer the question *i* correctly, and $\left(\frac{\sum^j x}{j}\right)$ is the average score of students who answer the question *i* incorrectly.

2.4 SOFTWARE TOOLS FOR MITS AND DATS

In order to construct an online learning environment, besides a computer with static IP binding with a fixed domain name, several software tools are necessary, which can be freely used if the application is a non-commercial program under GPL (GNU Public License) and FOSS (Free/Libre and Open Source Software). They are Apache [89],

PHP (Personal Home Page) [90] and MySQL [91]. Furthermore, they are all cross-platform software which matches the distribution requirement of MITS.

Apache is a popularly used, fast growing, open source web server. It is the first web server software which supports HTTP (Hypertext Transport Protocol). Since the first version was released in 1995, it has become more powerful and stable. Based on the survey of www.netcraft.com, on May 2011, there are 203,609,890 among 324,697,205 web sites based on Apache [89]. It is about 62.71% of the total websites. Microsoft web server is in the second position which is about 18.37% of the total. Apache Server can be downloaded from www.apache.org, it supports several script languages, such like PHP [90], Perl, and Python, etc. A flexible configuration file gives user more freedom to choose the script language to develop their web page. The major version of Apache server we used is the latest version 2.2.

MySQL[91], like Oracle, Microsoft SQL server and IBM DB2, is a relational database server. It is a very reliable and faster database system. Applications written in different languages, such like PHP, C++ or C, can connect to the server. Using SQL language, clients not only can store the data securely but also can create, delete, query, sort, and analyze the storage data. It is also open-source software and can be run on Microsoft and Linux platform.

More and more web developers use PHP to develop their web page since it was introduced in 1995. At least 20 million web server support PHP. It is simple, fast and easy to use script language under PHP environment. In the PHP5 release, some new features have been introduced to enhance its function and performance, such as object-

oriented programing, error handling using exception, etc. Especially PHP5 supports the new extension of MySQL. We use PHP version 5.3.6 in this work. Many popular bulletins or forums are written in PHP, for example, Discuiz [92] and phpBB [93], which also are good references to construct the on-line learning platform.

2.5 STRUCTURE OF MITS AND DATS

Supported by previous NSF and institution funds, MITS has accumulated more materials related to medical imaging. Based on the design principles and evaluation methods, a database was first introduced in 2007, and then DATS was added to the on-line learning platform. In 2008, mainly based on the handout of BME 520, the learning materials were re-organized. The new version MITS established a relatively complete medical imaging curriculum, serving six courses mentioned above. Figure 6 illustrates the "hierarchy" of MITS. It is constructed by Imaging Modalities (level 1), i.e., imaging techniques (X-ray, CT, MRI, Ultrasound, and Nuclear Medicine Imaging (NMI)), Learning material are categorized according to their imaging modality MITS and their information are stored the database.

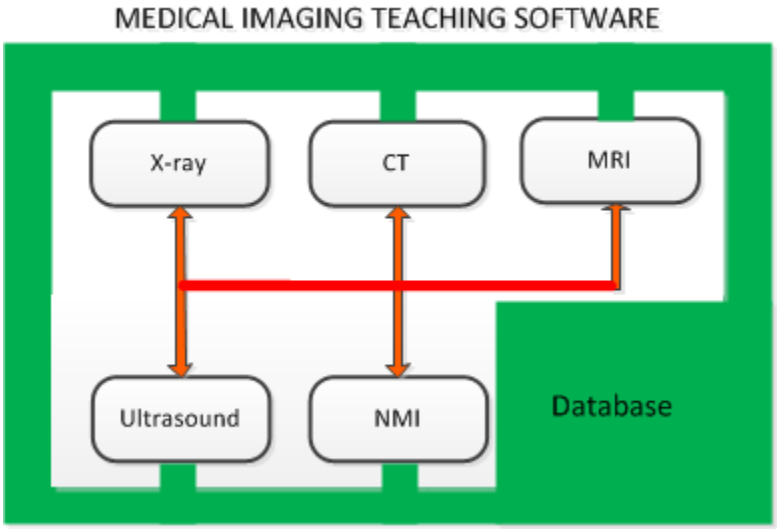

Figure 6: The "hierarchy" of the medical imaging teaching software (MITS)

Teaching modules have been built for each imaging modality in MITS. Fig.7 describes the relationship between modules, supporting components and dynamic assessment units. The second level in MITS is module units, equivalent to the teaching or learning topics within a modality. Supporting components are level 3 units in MITS (Fig.8). They mainly cover methods to deliver a module. These supporting components include Background Review, Text/Figure Description, Cartoon/Movie Animation, Program Simulation, and Application Demonstration. As an independent unit, Dynamic Assessment Unit can work behind other modules or components. These modules correspond to the “levels” of understanding, sequentially from physics, math, electric circuits, computer software, to system integration. The multi-level module-based design enables selected modules to be fitted into the course setting appropriately. It is highly desirable that one system can be applied to multiple courses.

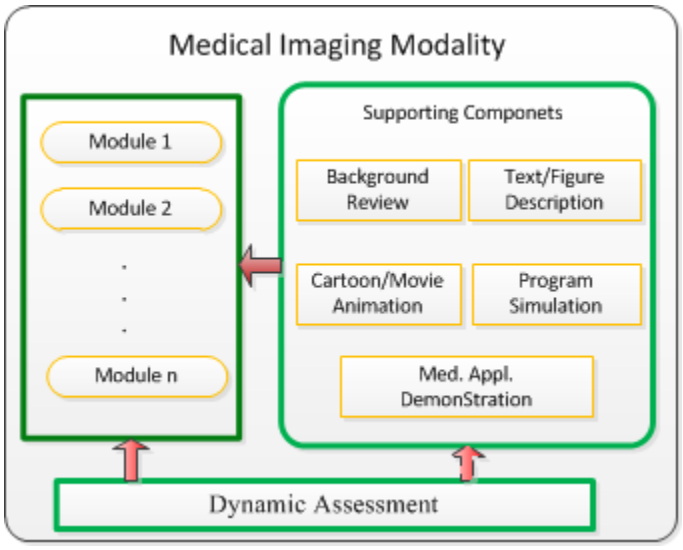

Figure 7: Relationship between Modules, Supporting Components and Dynamic Assessment Unit

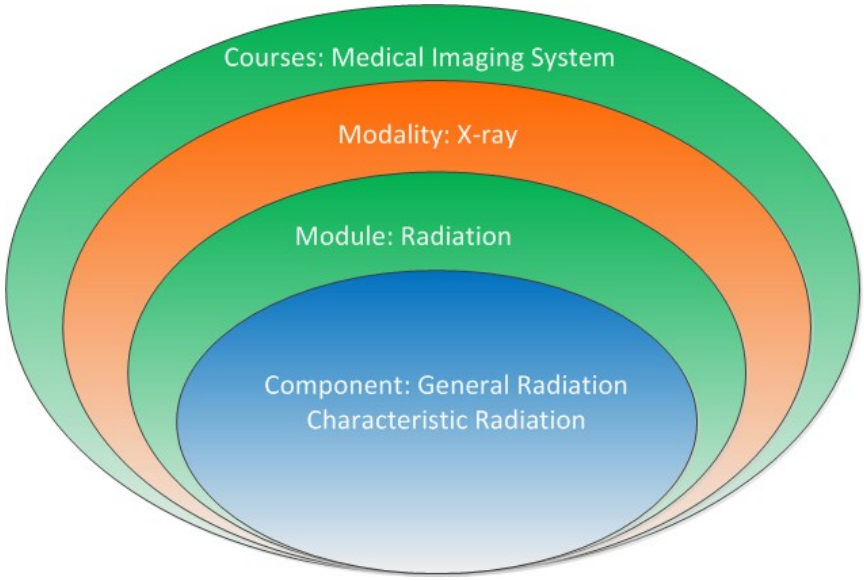

Figure 8: Four levels in hierarchy of MITS

Besides, an instructor can also pre-define his own modules using different components to meet his own education purpose. Each module may include the following components: 1) Historical and background review, 2) Text and figure illustration, 3)

Interactive animation, 4) Interactive and dynamic simulation (upload and download enabled), 5) Application demonstration, and etc. Many components are interactive by animation or simulation.

Similarly, a dynamic assessment unit can be added to a specific module, and includes several questions which are randomly selected from the database. Like CI, these questions will be given twice as pre-/post-test. The learning gain can be calculated to help improve the module later.

2.6 DATABASE DESIGN AND IMPLEMENTATION

As a relational database system, MySQL use *Database*, *Table* and *Field* arrangement to store data. InnoDB [94] is one of the table types supported by MySQL. It can provide required security and allow many users to simultaneously make changes of the data. It fits the purpose and application environment of MITS and DATS. Therefore it is chosen as the default table type.

Making a simple and efficient website which can be easily maintained and extended is the guide line to design MITS and DATS. Convenient distribution to a cloud computing environment as a software package is another consideration. Though designer experience and iterative procedure can help a lot to a good design, some of the common rules are considered and adopted initially. These rules include 1). Repetitive data should not be stored; 2). Flexibility and extendibility must be stratified, a field which needs smaller storage requirement should be used; 3). Frequently accessed tables and fields can be queried efficiently.

Tables	Purpose
mis_user	store user related information
mis_record	save test and learning record of users
mis_setting	save the setting of different courses, instructor, etc.
mis_module	store modules' information
mis_component	store components' information
mis_xray	standard questions for x-ray
mis_ct	standard questions for CT
mis_mri	standard questions for MRI
mis_nmi	standard questions for nuclear medicine imaging
mis_ultra	standard questions for ultrasound
mis_quiz	standard questions related to components, instructor

Table 2: Tables of MITS and DATS

A new database named "misdats" is created for MITS and DATS. Table 2 shows several important tables used to store different information. In order to make it more convenient for distribution, the questions are stored in different tables according to their modality. The data saved in *table mis_record* can be analyzed by instructors or administrators later using the tools developed for DATS. *Table mis_module* stores the webpages information which contains several components' ID. PHP scripts can organize a new web page for the user when it is browsed or visited for the first time. This page will be cached and its external link will be saved in *table mis_module* to accelerate browsing speed when it is visited next time. The role of *table "mis_component"* is to store the information of components of MITS and DATS, its fields are listed in Table 3:

ID field stores the identity of a component which is a unique integer value. *Name* field stores the component's short name which includes 255 characters. *ModalityID* field

stores the value of the modality identity which the component belongs to. *Title*, *Subtitle* and Content field stores the text description of a component. *Figure field* stores the external link of a binary data, e.g. pictures, figures, photos, movies and flash files etc. Similarly, field *Simulation* stores the external link of a simulation component. PHP scripts can organize the component in different ways according to the value in *Style field*, for example, how to arrange the pictures and text descriptions in a webpage. *Link field* saves the external link of these components when a cached component description is created. *Field Weight* represents the level of a component; it is useful when the website runs in a random mode according to the students' level. Comparatively speaking, *Status* is an important flag, because each bit of the flag indicates a state of the component. For example, the bit 0, if the value is 1, it indicates the external link of this component is available. PHP scripts can omit other bits and fields, just read the external link from *Link field*, and put the content in the web page of a module. If the value of this bit is 0, then there is no external link yet, PHP scripts must construct the component file first based on other values in several fields. After assembly is finished, this external file will be saved in the corresponding folder and the information will be updated in *field "Link",* the value of this bit will be set to 1.

2.7 DATS DESIGN AND IMPLEMENTATION

In order to track and assess student's performance, collect the feedback and timely manage MITS, DATS is built to serve as an online evaluation toolbox. A special component which can run interactively can be added to any module to serve the evaluation process. Besides providing the instructor with several basic management,

assessment and analysis tools, DATS can also help students do self-testing using the questions in the database. Figure 9 illustrates the configuration of DATS, where green blocks are medical imaging modalities described above, while orange blocks are the dynamic tracking system organized by the MySQL database. The assessments include required information about the engagement, performance (pre-/post-test), or open-end feedback during the teaching/learning for the modality (on a module-basis or modality basis).

Field	Data Type	Function
ID	*SERIAL, 64Bit*	Unique identification of a component
Name	*VCHAR(255),255 Char*	The component's name
ModailtyID	*TINYINT(4) , 4Bit*	Which modality this component belongs to
Title	*VCHAR(255)*	The title of the component
Subtitle	*TINYTEXT,2^{16}-1 Char*	The subtitle of the component
Content	*LONGTEXT,2^{32-1} Char*	Text description of the component
Figure	*TINYTEXT,2^{16}-1 Char*	The external links of Picture , photos and animation
Simulation	*TINYTEXT,2^{16}-1 Char*	The external link of a simulation component
Question	*TINYTEXT,2^{16}-1 Char*	Questions ' ID related to this component
Style	*TINYINT , 8Bit*	How to organize the component in a module
Link	*TINYTEXT,2^{16}-1 Char*	external link of a cached component
Weight	*TINYINT(4) , 4Bit*	Which level course
Status	*INT, 32 Bit*	a value to verify a components' status, e.g. cached
Author	*VCHAR(255)*	Who created this component
Date	*DATETIME,8Byte*	Creation time

Table 3: Main fields of table mis_component and their MySQL data type

DATS enables independent administrator control. The system allows new instructors to join the system from the same or different institutions as site administrators. This system is username/password protected and Internet accessible. The assessment of student performance can be acquired by the instructor through the online database. An instructor from any institution can apply for an "instructor" account (as a site-administrator) through the Website. A new site-administrator has the privileges: 1), to add new users (students). Email address or student number (partial or complete) can be used as user ID and "group-add" is allowed (by inserting a list, one user per line), 2), to search and delete users, and 3), to access and generate reports of users. Site-administrators from different institutions are independent and do not interfere with each other. Administrators and instructors can access the designed tracking information from the system which includes username, gender, ethnic information, institution, level (junior, senior or graduate, major, and sign on/off times, etc. The contents of assessments include questions of concept understanding (true/false or multiple choice), questions of problem solving, program testing for simulation, and anonymous open-end feedback, even how long does a student spend on learning a module.

Using modality management (Figure 10), an instructor can turn on or turn off a modality. The number of questions for post-test of this modality can be chosen too. The total numbers of questions are shown in the last column. The module management page works in the same way (Figure 11). An instructor can also turn on or turn off the pre-defined modules according to his/her teaching progress. In addition, new assessments can also be uploaded by site-administrators. A site-administrator can either manually search

the database to generate a report or setup a query based on teaching/learning progress, or time duration.

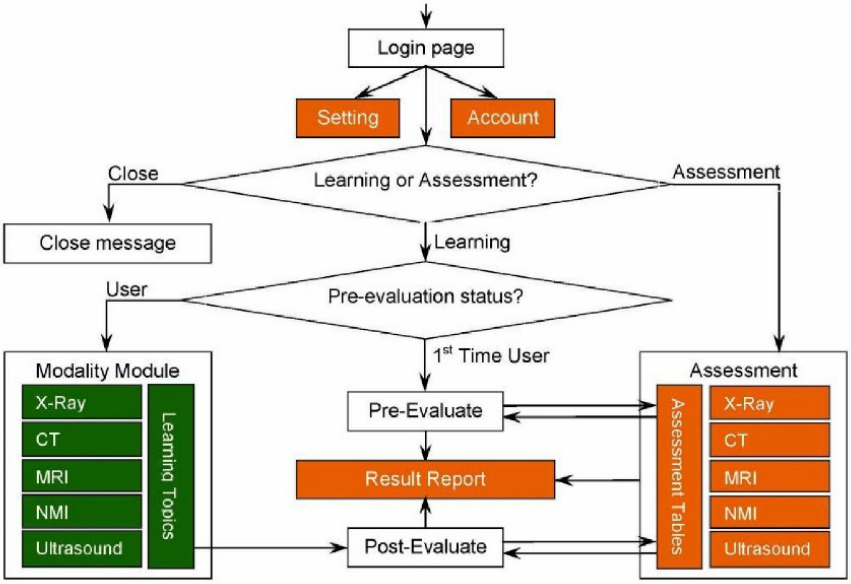

Figure 9: Work flow of DATS

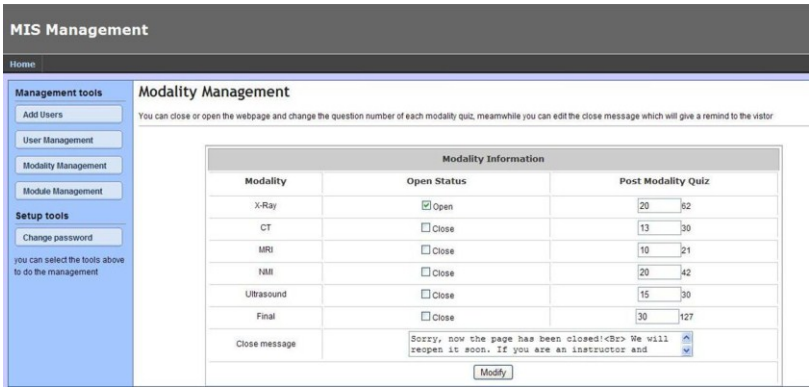

Figure 10: Modality configuration page

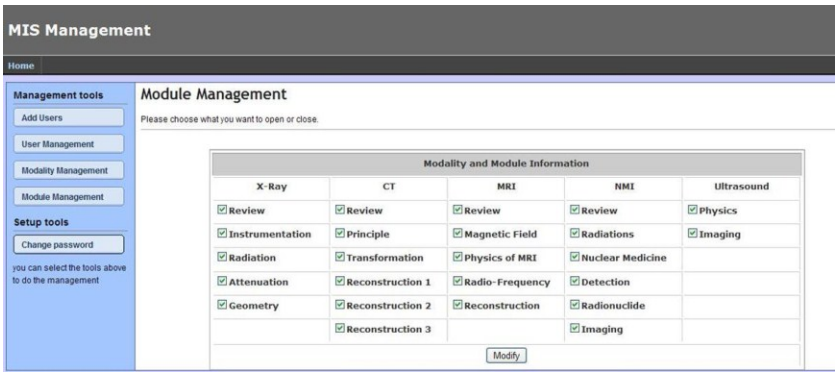

Figure 11: Pre-defined modules configration page

2.8 EVALUATION QUESTIONS DESIGN AND IMPLEMENTATION

Pre/Post modality questions come from "Review of Radiologic Physics" [95] and are stored in different database tables. Based on the concepts in literature of each module, in 2008, 4 to 6 questions were designed for each pre-defined module. A total of 98 questions were added in MITS. These questions can be classified in two categories. One is true/false questions, the other is multi-choice questions. Like CI, each question only represents one basic concept. The purpose is to check whether students have the right understanding of a concept or not. Questions can be answered based on common sense. Here we give two questions as example:

Question 1: If ^{19}F is in a 1 Tesla magnetic field, what is its precessional resonance frequency?

(A) 40 Hz
(B) 40 kHz
(C) 40 MHz
(D) 40 GHz
(E) 40 THz

Using this question, we try to test whether the student grasps the dimension range of resonance frequency (Lamar frequency) of a specific useful element, at the same time this question also can help them memorize the unique value of the gyromagnetic ratio of

this particular element. Through changing elements or changing the strength of external magnetic field or both, similar questions can be given.

Question 2: If ultrasound passes through the following tissues, which one has the highest speed?

(A) Lung
(B) Fat
(C) Liver
(D) Muscle
(E) Skull bone

This question can test whether students have the concept of the relationship between the propagation speed of a specific frequency ultrasound and the material density of that medium. Obviously, this question includes an implicit question to test whether the students know about the basic knowledge of the composition of different tissues, e.g. Lung is full of air, so lung density is the lowest; fat, liver and muscle have a density similar to that of water. Bone includes more calcium, therefore it has the highest density as well as the highest propagation speed. If the lowest propagation speed is asked, it can also test the same concept.

2.9 LEARNING CONTENT

The learning material of medical imaging can be dynamically constructed by MITS based on its three-level hierarchies. Figure 12 gives an example. The left column shows the current selected modality: *X-ray* and current selected module: *Instrumentation*, the center part express as the content of the module, which may include several components.

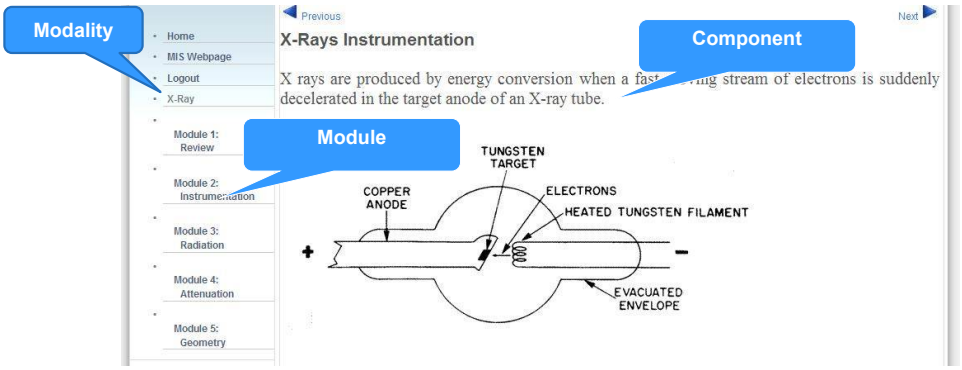

Figure 12: A dynamitic webpage based on the modality, module and component hierarchy

MITS is mainly focus on the development of animations for physics/chemistry principles as well as simulations for engineering implementations. Figure 12 above shows some components from X-ray or CT imaging modality as examples to describe the principal learning material in the system. These components are described in detail in following paragraphs.

2.9.1 BACKGROUND REVIEW

Background review contains reviews of related physics and math background (such as modern physics for X-ray, Fourier transform for CT) and historical review of the modality's evolution (such as radiation's discovery, evolution of CT's generations). Our class teaching experience and other reports [42] indicate that students' learning interest is very much stimulated by the stories of scientific discoveries and inventions. Links to websites relating to the scientists or scientific inventions (such as the "Virtual Nobel e-Museum" [50]) are also included in this component.

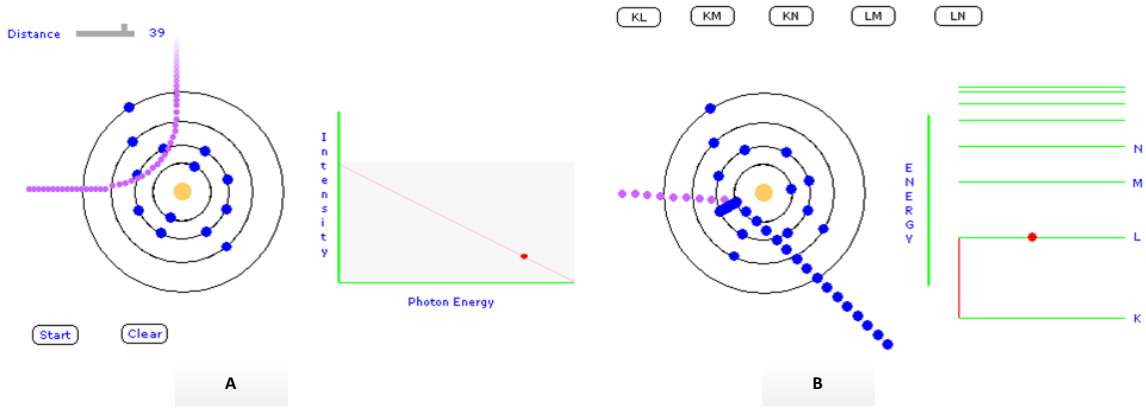

Figure 13: An example of delivery of the concepts of general radiation and characteristic radiation, A). General radiation; B). Characteristic radiation

2.9.2 CARTOON AND MOVIE ANIMATION

Animation provides students an interactive environment to *visualize* a "dynamic" physical process or a "live" instrument (by Adobe Flash Player, Windows Media Player, or even MS Power Point Presentation). Figure 13 shows X-ray's generation by animation. The left panel is the "general radiation" animation. It can let the user change the electron's distance to the nucleus (on the top left corner of the middle panel) and displays the output X-ray energy level. When a user clicks the *Start* button, he/she can see a *flying particle* (animating an electron) *pass around* the nucleus with a changed direction; and the extra energy emitted (i.e., X-ray) is marked on the right side (a continuous function). In the right panel, the "characteristic" radiation animation shows the user how the radiation relates to the nucleus' electron binding energy. When a user clicks the *KL* button, he/she can see a "physical reaction" sequence in which *a flying particle knocks out* an electron in the K-shell (the most inner shell in the figure) of the atom; then an electron in the L-shell (the shell next to the K-shell) replaces the vacancy in the K shell; and the output X-ray

energy is shown by an energy transition on the right side (a discrete function). The purpose of an animation is to generate a dynamic visualization "picture" for a basic and fundamental physics (chemistry or biology) concept or principle.

2.9.3 PROGRAM SIMULATION

Simulation is the core training for each modality. Different from animation, simulation is the engineering component of the teaching/learning process. A system parameter, such as sampling frequency, processing tools, such as student-designed filter, and images (as original data to be simulated) can be interactively entered (or uploaded) to the system and a computational simulation can be executed and the results can be viewed through the Internet.

We give one example of teaching medical imaging by simulation. Figure 14 shows the simulation of CT reconstruction by Radon transform. The Radon transform (projection) converts a signal from the object domain (a brain phantom) to the ray-sum domain (signal received by radiation sensors). One of its expressions can be written as:

$$p(x',\theta) = \Sigma f(x\cos\theta + y\sin\theta, y')\ \forall y' ,$$

where *(x,y)* is the coordinate in the object domain, *(x',y')* is the coordinate in the rotated object domain with θ degree, i.e., $x' = x\cos\theta + y\sin\theta$; *f* and *p* are the object function and projection function respectively. The transform can then be done by different ration angle θ (increment of sampling angle) and *x'* (increment of sampling distance) to simulate CT's X-ray tube rotation and sensor arrangement. These parameters are *interactively* adjustable by users. When the button "Radon Transform" is clicked, a *live projection sinogram* is generated column-by-column (up left). A single rotation angle projection profile can also

be observed (Figure 15). Similarly for the Inverse Radon transform (back projection), CT reconstruction can also be simulated by selecting different θ and *x'* values and designing appropriate filters (practice of programming).

2.9.4 MEDICAL APPLICATION

Medical application is a library that posts a variety of medical imaging applications for the corresponding modality. For instance, for the MRI modality, this component displays MRI images (with brief descriptions) of different parts of the body, organs, in normal or abnormal conditions, under different acquisition/processed parameters (such as T1-, T2-weighted, or ADC, DTI maps).

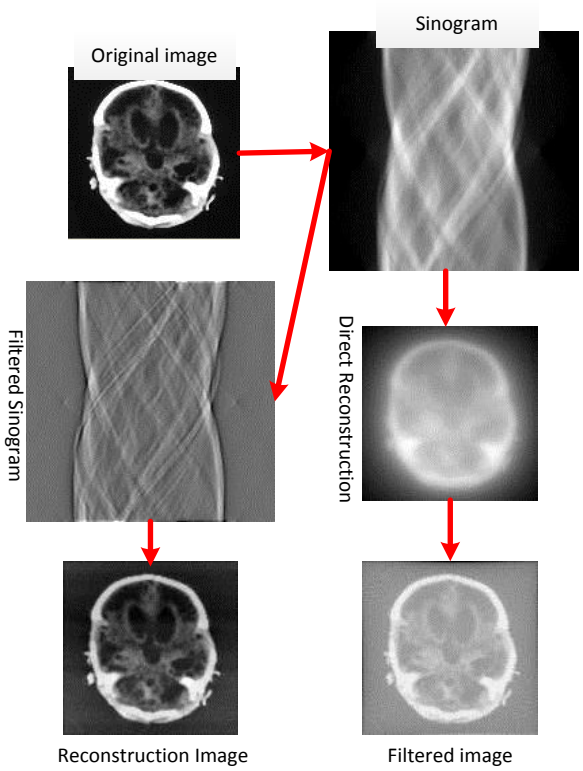

Figure 14: Illustration of work flow of Radon transform simulation

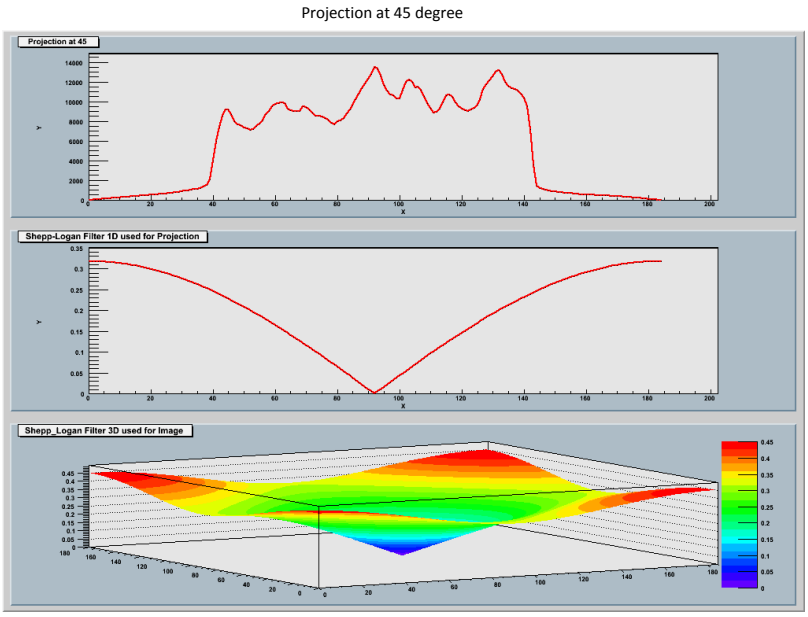

Figure 15: A projection at a certain degree and a filter used in Radon transform simulation

2.10 RESULT OF STATISTICAL COMPARISON

2.10.1 STATISTICAL COMPARISON RESULTS WITH AND WITHOUT MITS

Table 4 shows results from one medical imaging class (BME520, Medical Imaging System) for students learning X-ray and computed tomography (CT). Students who enrolled the class were senior undergraduates (60-70%) or graduate students. Students' academic, and course records (mean ± SD) without using MITS (n=23, top row) and using MITS (n=21, bottom row) are listed in the table below: where problems in the tests and exams were "standardized" questions from the book "Review of Radiologic Physics" [95] and other reference books [58], [59], [96]. Projects for X-ray and CT simulations were the same for both years. Statistical comparison (ANOVA, Single factor) of students'

cumulative GPA shows no difference between two years ($^{*1}p\leq0.7$), indicating similar background for all students.

Condition	Students	GPA	All problems	Concept Problems	Projects
Traditional, Without MITS	23	3.42±0.34	82±9%	76±5%	82±5%
Traditional, With MITS	21	^{*1}3.46±0.44	^{*2}89±8%	^{*3}91±6%	^{*3}90±6%

Table 4: The result of statistical comparison based on the data of students who had used the MITS and those who had not.

Statistical comparison of students' correct percent rate for all questions shows no significant difference; however, the p-value ($^{*2}p\leq0.1$) implies a "trend" of increased understanding to all questions (conceptual and computational). Students' understanding improved most in conceptual questions and in their projects. The statistical comparisons show significant differences (both $^{*3}p\leq0.05$) between the pre-/post-applications.

2.10.2 STATISTICAL ANALYSIS RESULTS BASED ON COLLECTED DATA

Since DATS was introduced in MITS in the fall semester of 2007, and has been used to collect data. And by spring 2011, there have been 145 users, 103 of them have had records of learning one modality at least. These data are considered as the effective records. All the statistical results are based on the data. In total, 72 students used the new designed questions in their on-line test. Figure 16 gives detailed information on the students that had used MITS from fall 2007 to spring 2011.

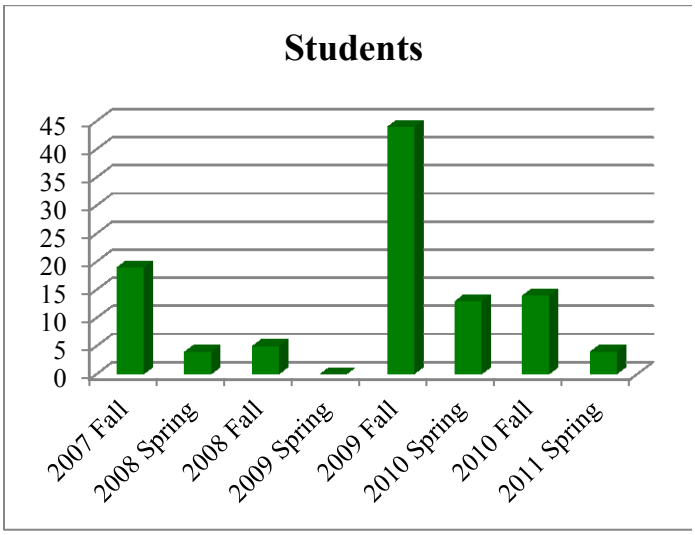

Semester	Number
2007 Fall	19
2008 Spring	4
2008 Fall	5
2009 Spring	0
2009 Fall	44
2010 Spring	13
2010 Fall	14
2011 Spring	4
Total	**103**

Group	Students	Gender	Students	Major	Students	College	Students
Undergraduate	57	Male	76	BME	98	UM[1]	97
Graduate	39	Female	27	EE/CE	2	FAU[2]	5
Instructor	5			Medicine	2	FIU[3]	1
other	1			Other	1		
Total	**103**		**103**		**103**		**103**

[1]UM: University of Miami; [2]FAU: Florida Atlantic University; [3]FIU: Florida International University

Figure 16: The number of effective records from 2007 fall semester to 2011 spring

Associating with the application of the MITS/DATS system in course-work, a test was also conducted to examine the student's understanding of imaging principles through the system directly. A preliminary calculation of the students' learning gain by the normalized equation was performed. A concept problem was given before a student started a module and the same or a similar concept problem was given immediately after the student finished the module. Students were informed to finish the module in one logon session so that the pre/post tests reflect the gain through the module only, regardless of students' knowledge from other sources. Through initial analysis, we found

that the average students learning gain (n=15) on 17 basic medical imaging concepts was 0.38+0.18 (Figure 17).

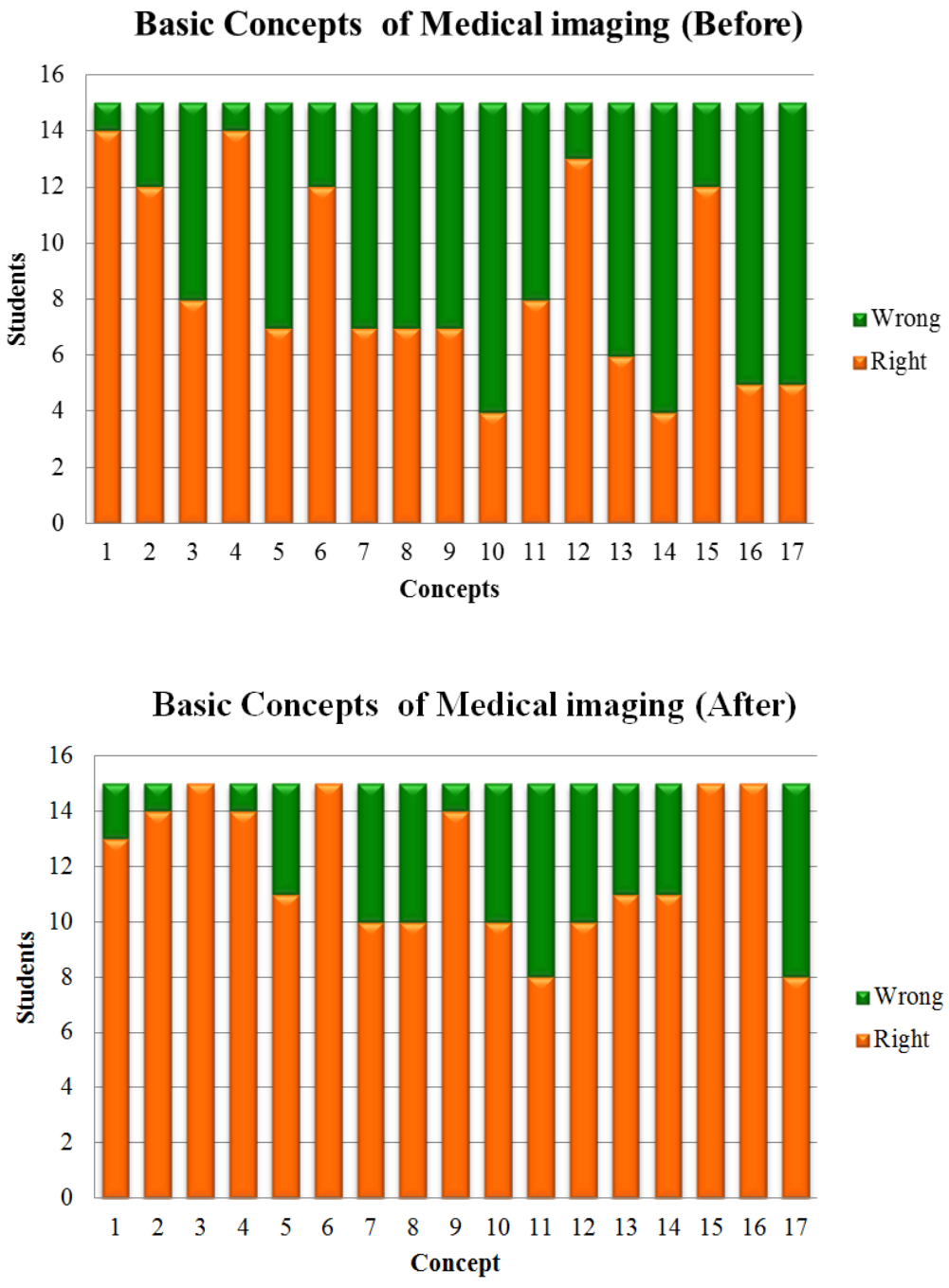

Figure 17: Statistic results of 17 basic concepts of medical imaging in pre/post module test .

Test	Questions			Correct		$\bar{\alpha}$
	Total	Mean	STD	Mean	STD	
New Designed Questions						
Modality /Pre	47	23.0	14.8	15.9	13.5	0.67
Module /Pre	44	29.5	13.1	19.6	12.2	0.55
Module /Post	39	28.4	16.4	14.3	11.5	0.57
Questions from Review of Radiologic Physics						
X-Ray /Post	62	16.9	3.4	7.3	3.5	0.33
CT /Post	30	15.4	6.2	7.8	3.1	0.83
MRI/Post	21	20.9	3.2	9.6	3.4	0.95
PET/Post	42	20.5	3.5	8.7	4.6	0.58
Ultrasound/Post	30	18.5	2.5	6.9	3.0	0.73

Test	Students	Questions		Score	
	Total	Mean	STD	Mean	STD
New Designed Questions					
Modality /Pre	72	15.4	6.2	49.9	19.3
Module /Pre	72	18.6	6.6	65.3	16.5
Module / Post	72	15.9	6.2	68.0	15.9
Questions from Review of Radiologic Physics					
X-ray / Post	53	20	0	42.8	19.6
CT / Post	43	13.2	0.7	39.7	29.5
MRI/Post	44	10	0	45.7	31.8
PET/Post	43	20	0	42.6	18.7
Ultrasound/Post	37	15	0	37.1	19.2

Table 4: Overall statistical result of data from DATS

Unlike a traditional test, questions of each test in DATS are randomly chosen from the database. The number of questions can be pre-setup by instructors. So each

question may not be equally accessed. None of tests were due-time assignments. Students can access them at any time they prefer and also can stop in the middle, and continue at the next convenient time. Though we encouraged students to take part, not all students were motivated to perform at their best in each test. This is an important reason which makes that the overall performance of each test not good enough. In addition, questions from "Review of Radiologic Physics" [95] do not relate too much to the materials on the learning web-site. Some of them are a little bit difficult for some students; some questions need to be solved with calculation. Because there is no penalty to student due to his/her online performance, some students may have randomly chosen the answers of some question and finished each question in very short time.

In Table 4, in the upper part, the first column shows the name of tests. Each of the tests was conducted in several parts at different times by different students from different groups. Data in the table show the overall results. *Questions* column includes 3 parts, *Total* shows how many questions in the test. *Mean* under *Questions* represents average access times of each question. Their standard deviations (STD) are also given. *Correct* column shows the mean value and STD of questions which had been correctly answered in that test. The last column gives the value of coefficient alpha calculated by Eq. 2.6. In the bottom part in Table 4, *Students* column show how many students had taken part in that test. *Questions* column gives the mean value and STD of questions students had answered. The last column shows the mean value and STD of scores in the test. In DATS, the questions of a test were randomly selected for students. Based on the

definition of coefficient alpha in equation 2.3, in order to reflect the real contribution of each question in a test, equation 2.3 is modified as the following:

$$\bar{\alpha} = \frac{\bar{n}}{\bar{n}-1}\left(1 - \frac{(\frac{\bar{n}}{M})^2 \sum V_i}{\sigma_t^2}\right), i = (1,2, \ldots \ldots, M) \quad (2.6)$$

where $\bar{n}$ is the mean value of the number of questions , M is the total number of questions in a test.

Test	Mean	STD	Median	Min	Max
New Designed Questions					
Modality /Pre	0.1693	0.2424	0.1058	-0.6780	0.8153
Module /Pre	0.1009	0.0881	0.1006	-0.0667	0.4460
Module / Post	0.1144	0.0870	0.1216	-0.1560	0.3053
Questions from Review of Radiologic Physics					
X-ray / Post	0.1720	0.1031	0.1682	-0.1061	0.3906
CT / Post	0.4057	0.1684	0.4310	0.0985	0.7615
MRI/Post	0.4264	0.1184	0.4091	0.2640	0.6833
PET/Post	0.1756	0.0960	0.1577	0.0236	0.4417
Ultrasound/Post	0.1683	0.0897	0.1708	0.0051	0.3400

Table 5: Statistical result of questions' "gap" values of different test

According to the coefficient alpha value, there are two aspects to determine whether a test is reliable or not. One is score variance of the entire group. The bigger the score variance, the more reliable a test tends to be. The other one is the difficulty of questions. Questions should be kept in the same level. For example, if all the students did equally well in a test, the variance σ_t^2 would be zero, and any little disturbance in $\sum V_i$ would make the alpha value go to negative infinity. Only when all the questions are

equally selected correctly, the alpha value will be zero. Though perhaps the overall performance of some tests is not good, the tests themselves may still be reliable.

The mean score of a test and the "Gap" value of each question together can be used to analyze the consistency of questions' difficulty level. If a question has a big gap value, it means it tended to be easier to those students who did well in a test. To some other students who did not do well, it could still be a difficult question, especially when the overall mean score of that test was low. If the gap value is small, it is possible that it was a difficult question to most students. In some cases, when a question has a negative value which is far away from the mean value, it indicates the question itself may be incorrect.

In Table 5, the statistical results are given. They include the mean value, STD, median value, minimum value and maximum value of each test. Figure 18 shows the gap value distributions of each question. From the figure, we can see that the new designed questions in the three tests show better difficulty consistency. Most questions fall in the range [0, 0.2], except for a few questions. However, the gap values of questions in post modalities have larger range. Some questions also have bigger gap values. That means that on one side, they are too easy for one group students, on the other side, they are too difficult for other students. It is better to separate them into different levels

In Table 6, question 8 in CT modality is listed as an example. 15 students had answered this question. 5 of them answered correctly, 10 students made a mistake. Its gap value is 0.761.

CT Question 8				
Which of the following **cannot** be used to process CT images?				
a	Window/level adjustment			
b	Multiplanar reformatting			
c	Phase encoding			
d	Volume rendering			
e	Shaded-surface display			
User ID	Questions	Correct	Score	Time (s)
Answer correctly				
113	13	11	84.6	564
116	13	13	100	782
130	15	15	100	1199
133	15	15	100	462
134	15	15	100	323
Avg.	14.2	13.8	96.9	666
Answer incorrectly				
56	13	1	7.7	228
70	13	4	30.8	492
72	13	2	15.4	211
74	13	1	7.7	108
84	13	5	38.4	262
97	13	0	0	362
110	13	5	38.4	178
111	13	3	23.1	211
112	13	6	46.2	223
115	13	0	0	203
Avg.	13	2.7	20.8	247
gap	0.761			

Table 6: A question example which has big gap value

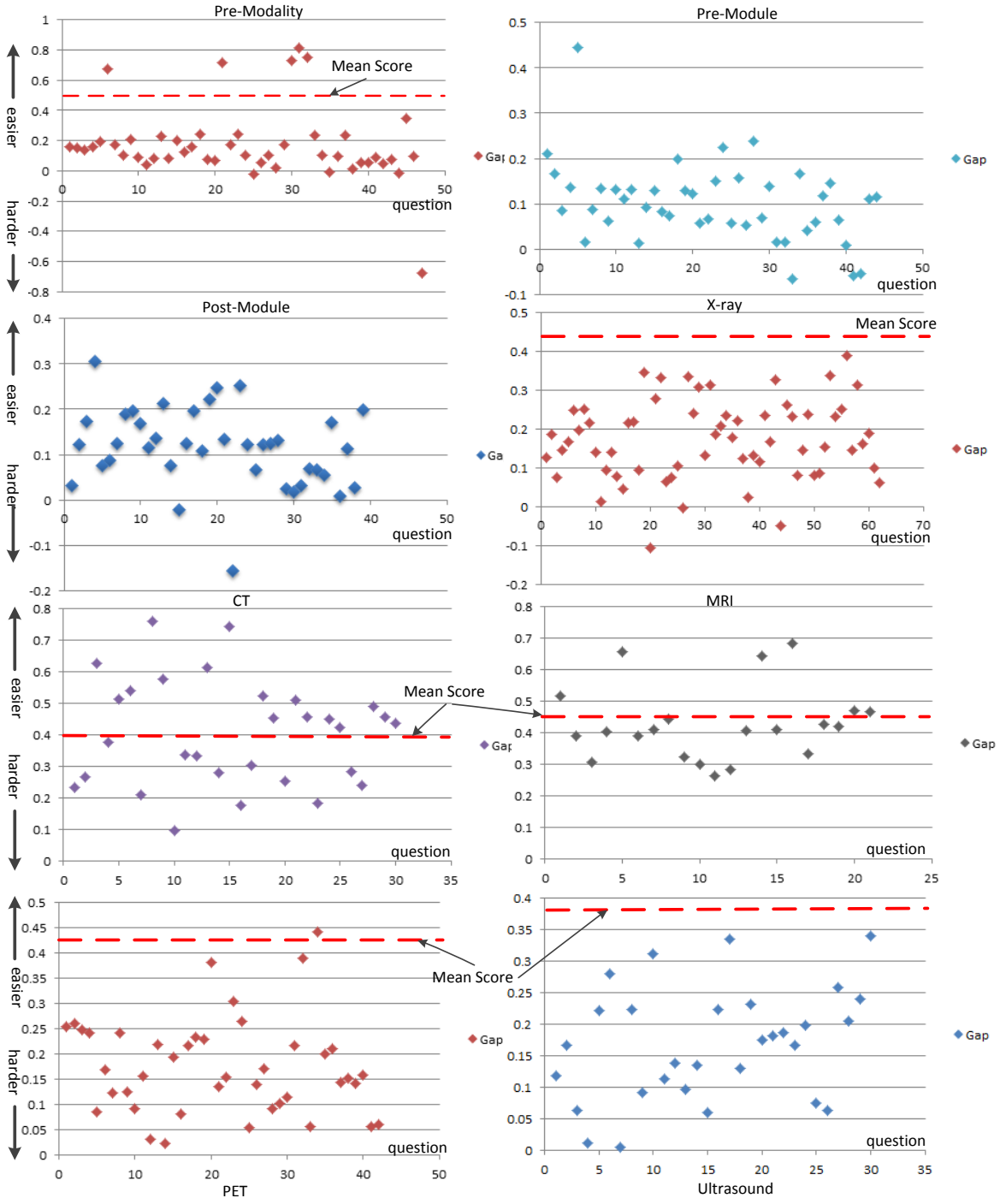

Figure 18, "Gap" value of questions in different test

. From Table 6, we can see that if some questions are too difficult for some students, they are inclined to answer them randomly and try to finish the quiz as soon as possible. So the average time they use is much less than students who are confident to answer those questions correctly.

In addition, from the information in Table 4, the method of delivering questions in DATS is reasonable and reliable. All the questions in the database had been chosen.

2.10 CONCLUSION AND DISCUSSION

Based on the outcomes and the evaluations of different assessments, we conclude that the developed MITS/DATS system is convincingly suitable and applicable for medical imaging education to undergraduates. It is feasible to scale up the development through the efforts by multi-institutions or a cloud computing environment to produce a professional medical imaging teaching product that can be adopted by interested academic institutions. The updated MITS/DATS system can be distributed to institutions that are interested in delivering medical imaging education through this teaching approach. In order to let the medical imaging education community to use the system, a major challenges must be considered, i.e., the software upgrading.

The software upgrading means the future "sustainability". Establishing an online teaching system is a "one-time" effort (we acknowledge that it is a time-consuming effort). However, the system must be sustainable. A "live" teaching system must be an upgradeable (continuous-optimizing) system. Our solution is as follows. During teaching a specific module of an imaging modality, we assign students or recruited interns a project that requires students to create an animation or simulation for a specified

physical/math/engineering concept. In the end of the semester or internship, each student presents his/her work to the class or other interns. The instructor asks all students which animation/simulation gives the most thorough overview of the specified concept. Students then "evaluate" all presentations (including existing work) and "vote" for their favorite animation/simulation. The best animation/simulation will replace the existing one for this concept. By implementing such a method, the MITS/DATS system will not only be sustainable but also upgradeable. At the same time, both hardware and software will be controlled by the institution locally. Among institutions that use the MITS/DATS system, application experiences can be exchanged under difference training environments such as large class size, community college, other engineering or medical students, and the system can be synchronized adaptively.

Th works in this chapter have been presented on several international education conferences [97], [98], [99].

CHAPTER 3 A PROTOTYPE OF SIMULATION SERVICE PLAFORM FOR MEDIACAL IMAGING

3.1 BACKGROUND AND SIGNIFICANCE

Comparative studies have demonstrated that simulation is an efficient, economic and important method to help students understand the physical principle behind the phenomena [100], [101]. Simulation applications can provide interactive methods to promote the learning and research interest of students who engaged in. For example, Foldit [102] is a multiplayer online game which can help researchers solve different protein-structure prediction problems. It attracted many players worldwide who may not have background in biochemistry. Their solutions for a specific protein have been published in a scientific journal [103]. This also inspires us to develop a simulation service platform in medical imaging field which can connect education and research together. Since the deployment of MITS, a prototype based on the service-oriented model has been proposed and developed.

3.1.1 DISADVANTAGES OF MATLAB-BASED SIMULATION COMPONENTS

The more distributable and expandable a platform is, the more users can have chance to access its service, therefore it can gain more opportunity to expand itself and have longer life cycle in the future. However, most simulation components embedded in MITS are developed based on Matlab. This makes MITS very difficult to distribute because of these simulation components. One important reason is the high license fee of Matlab. Though Matlab is a very powerful and commonly used software in scientific computation and research field, as a commercial software, it is also very expensive.

Matlab R2011, a package including an individual academic license, signal, imaging processing and developing tool boxes is about $3000 [14], according to the quote on June 2011. This price is almost twice higher than the overall price of MITS including hardware. Another disadvantage is that these simulation components are not exactly network applications, though they have a network interface based on MITS. This means that when different users submit their simulation parameters at almost the same time, only the last ones will be accepted, others' will be discarded either by webserver or by the simulation applications. The result that a user gets may not be what it should be. Before version R2007 of Matlab, a program named *matweb* had been provided to help users demonstrate their projects and development through a web server. Like simulation components in MITS, except for the network interface, the application still acts like a normal stand-alone application: First in, First out (FIFO). It cannot handle different users' input at the same time either. Moreover, *matweb* cannot work if the host computer is not in login status. In addition, the new version Matlab does not support the *matweb* program anymore. Obviously other simulation applications in MITS face the same problem. A new solution should be explored.

3.1.2 PROPOSED MODEL

In order to solve these kinds of problems, a new service-oriented model with extendable server-client structure is proposed (Figure 19). The main idea of this solution is to provide a simulation service platform to manage these applications. It can offer a network interface for each simulation application. Therefore users' input and application output can be connected together. The platform can provide service to different kinds of

simulation applications. Based on their relationships with the simulation service platform, those applications can be classified into two categories. One category is standalone executable applications which can fulfill special simulations independently. The other type of applications is part of the simulation server. Thus, the server can easily control them and give much more flexibility to users.

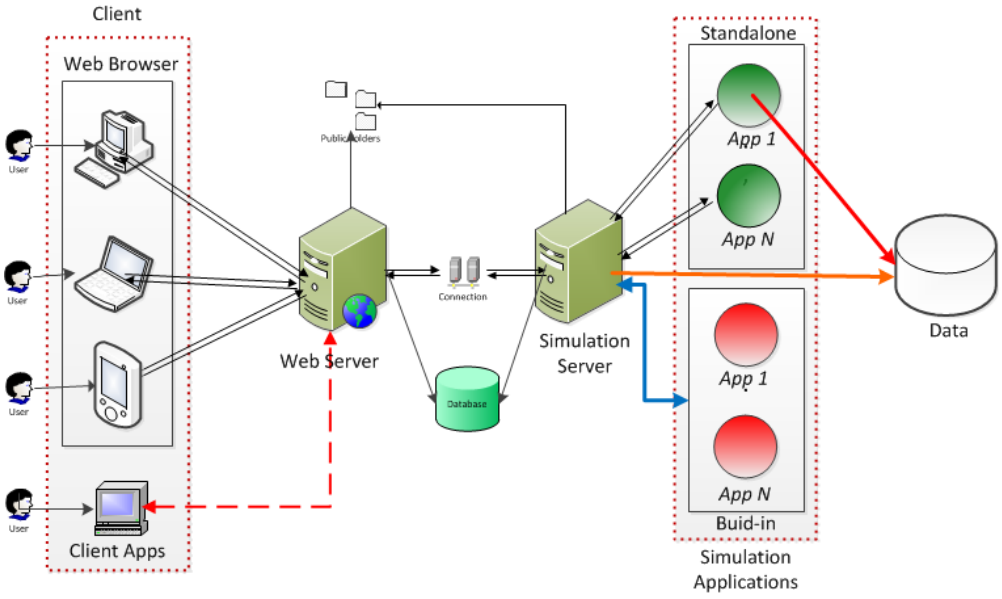

Figure 19: The working flow chart of a simulation service platform

A simulation server is the central part of a simulation service platform. It can coordinate the simulation applications and system resources to perform different simulations. Through communicating with the web server, the input from a user can also be managed and distributed to a related simulation application. The output from the simulation application will return to its corresponding user. Besides communicating through web browser, if it is required, a client, a special application on user terminal, can make the whole simulation service invisible to a user, like many APPs in a modern smart

mobile. To implement all these functions, a detailed communication protocol between client and simulation server must be designed.

3.1.3 CGI INTERFACE

CGI stands for Common Gateway Interface [104], [105], which is a protocol that Apache web server communicates with other applications hosted on the server side. In this work, it is our solution to make a connection between the web server and the simulation server. Applications developed following CGI protocol can be called by Apache web server. These CGI applications can be written using any language, such as, Perl, Python, C, and C++, even the PHP language. MITS and DATS can also be run in CGI mode. This flexibility allows developers to use their familiar developing language to write applications for the simulation service platform. The working directory and file extension of a specific CGI program can be configured in Apache web servers' configuration file, *httpd.conf*.

Specific CGI programs can be visited using any applications supporting HTTP, e.g. *Microsoft iexplorer, Google Chrome, Firefox and etc.* The unique identification information of the client can be transferred to the corresponding CGI programs by the web server. The output of these CGI programs, mainly a dynamic html page, will be relayed back to the client.

HTTP may be the most common protocol we touch in our daily life. When a web page is visited, a *request* will be sent to the web server. The input parameters from the client side can be sent through different methods. Two popular methods are *Get* and *Post.* Through appending users' input onto the end of the URL, the *Get* method can ask the

web server to provide corresponding resources. *Post* is a little bit different; it uses the HTML form to submit the input of a user. Thus an additional header is required to specify the content type and its length. Therefore when it is refreshed, the browser may send an error message if the page is expired and no cache are found.

The entire user's input will be relayed to and parsed by CGI programs. The response from the server is the output result of CGI programs plus an additional header section, but only the result will be displayed in the browser.

3.1.3 WORK FLOW ANALYSIS OF A SIMULATION APPLICATION

In chapter 2, a simulation component of the Radon transform is introduced. Now in this section, its whole procedure will be analyzed. Figure 20 describes its work flow. A simulation always starts at the client side. When the webpage designed for the simulation is visited, the user has to decide how to perform a simulation and prepare for necessary parameters used for this simulation. In the case of tomographic simulation, a picture or photo needs first to be selected as a phantom. It can be a photo stored in the server or a new one just uploaded by the user. Other parameters must be selected or fulfilled, such as projection angle, filter, and projection span, projection frequency, etc. After uploading all required information, the user can submit it as a simulation job and wait for the result. Now the control of the simulation job is transferred from the user to the webserver. The webserver will validate all the inputs and redirect them to the simulation server. Then the simulation server takes control. If the system and simulation application status are good, the simulation application (before it was a *Matlab* program) will be called and the real simulation procedure will be started. The image may need to

be resized to 128 × 128 to save calculation time. If it is a color image, converting to a gray scale image is also required. Then the simulation application calculates how many times the projection will be done. If more than one projection is required, all the projections can be utilized to create a movie clip and let the user view the whole procedure. During the reconstruction, different filters can be chosen. The whole procedure of reconstruction can also be saved as a movie clip.

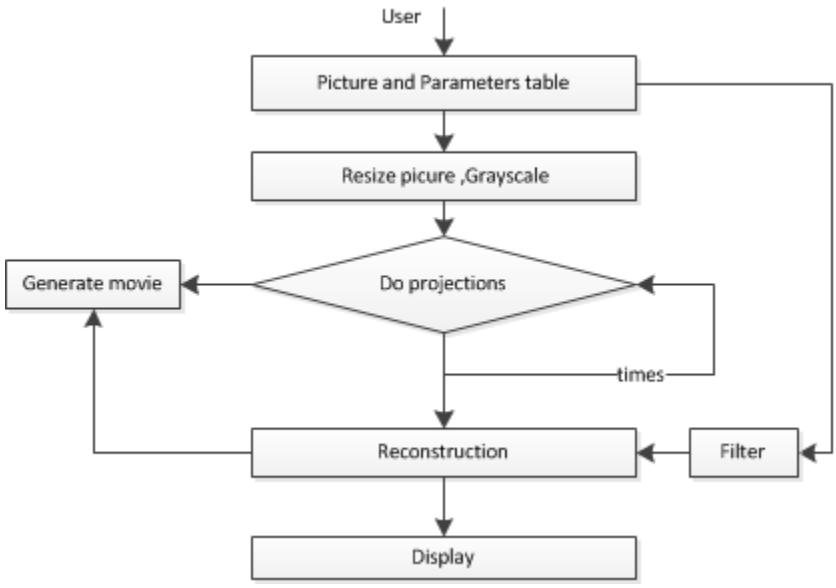

Figure 20: The processing flow of Radon transform simulation

Through the above analysis, a simulation service platform includes four different parts: UI (User Interface) , a webserver, a simulation server and simulation applications. Their relationships and functions can be identified by Figure 21. The bold dash line means the physical boundary of the four parts in a simulation system. First, a simulation always is initiated from a client. After the data has been provided through the UI, the data will be validated first by the validation module in the client side. Then the data will be

transferred to a CGI program using HTTP *Get* or *Post* method. The CGI program will package the data in a meaningful format and transfer it to the simulation server. The simulation server will decompose the package first, based on the information in the package, decide which simulation application will be called and how to store the input data and result, then start a new thread to run this simulation application. After the simulation application finishes its work, the thread will be terminated automatically and its status will be reported to the simulation server. The returned message will be packaged and relayed to the CGI program. Eventually the user receives the simulation result on the client.

Here we must emphasize that not all simulation applications can run fast enough to get the result immediately, especially those involving time-consuming tasks. In this situation, the simulation server will return a message to the CGI program to let the user know the job's status. The user can check back at a later time with a unique job-id assigned to this task to verify the status of the simulation.

3.2 SIMULATION SERVER DESIGN AND IMPLEMENTATION

The Simulation Server component is a background program under the Linux platform or a service under the Windows platform. When the Simulation Server starts, it will broadcast its own information in the local network and listen to the requesting information from a specific port. The client applications designed for this simulation server, located in the same network, can identify the Server and communicate with it through the Apache web server and CGI programs. As illustrated in Figure 22, the Simulation Server component has four modules.

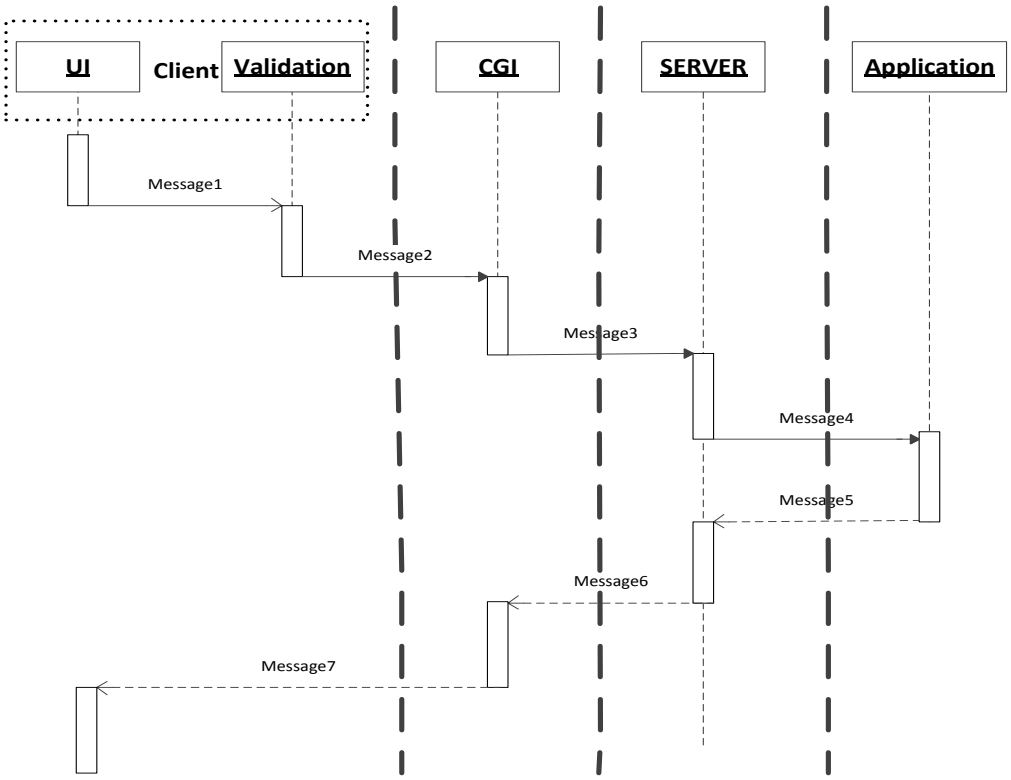

Figure 21: The message sequence chart of the whole simulation system

The *Job Manager* module treats every simulation task as a job. Each job is identified by the *job ticket* that contains the information specified by scripts. Each job is submitted by the user to either a specified shared folder in the high-performance computer (if the Client and the Server are located on the same local area network (LAN)) or Apache web service hosted on the Server side. The Job Manager monitors the shared folder or a port which is used to communicate with the Apache web server constantly. Based on the *job ticket's* description, the Job Manager prepares and forwards all required information to the *Simulation Controller* module to conduct the simulation.

Since the Server can face multiple users through multiple Clients, the *Job manager* module checks each job-sender's authentication and allocates data space for simulation results. Based on the job status, the *Job Manager* lists the job in the running queue, waiting queue or finished queue. When a job is submitted, a job object will be created. A unique ID will be assigned and the *Job Manager* will store all related information to the ID for backup. The *Job Manager* is also responsible for exporting simulation results processed by the *Post Processing* module. The *Simulation Controller* module monitors the waiting job queue, picks the job that has the highest priority or the first available on the queue, and feeds the required information to the simulation applications.

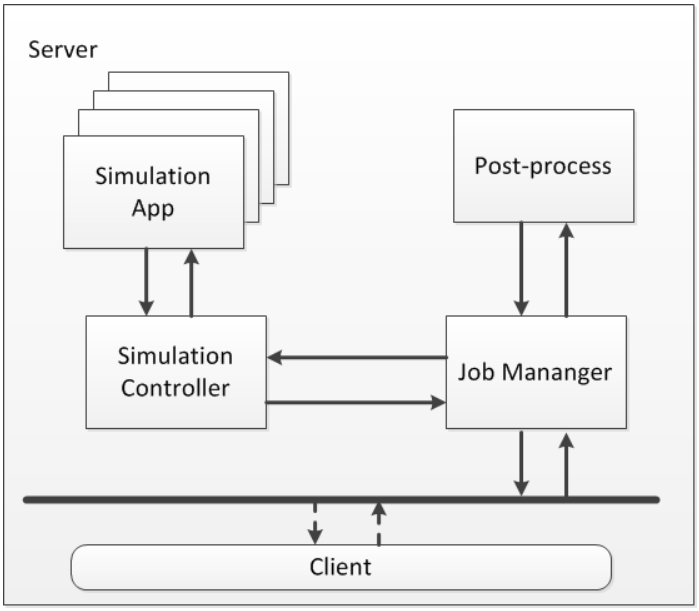

Figure 22: The modules in the simulation server

As the most important part of a simulation service platform, the simulation server is a multithreaded program. It can process parallel tasks concurrently. Therefore its performance can be speeded up. However, unlike single-threaded applications, multi-

threads perhaps will contend for the same resource at the same time. If the simulation server is not designed well, synchronization problems, such as dead lock, live lock, and starvation may happen and lead to unpredictable behavior. Sometimes it may cause unresponsive operation, even a program crash. It is a new challenge to coordinate those threads. When the simulation server is executed by an OS (operating system), such as Linux and Microsoft Windows, a process will be created. The main thread associated with the process will run first. Then other threads will be created by the main thread, such as the *Job Manager* thread, the *Simulation Controller* thread and other supporting threads (disk monitoring thread, memory monitoring thread, etc.). Since a thread is a unit of control in a process, it can fulfill a specific function. Meanwhile it can have its own sub-thread. In the following section, the detailed description of the design and implementation of the *Job Manager* and *Simulation Controller* is given.

3.2.1 JOB MANAGER MODULE

When the *Job Manager* thread is created, it will create a sub-thread to coordinate jobs and simulation applications (Figure 23). Meanwhile a counting semaphore object will be created. It can provide mutual exclusion and condition synchronization [106]. An associated integer value with the semaphore can be used to indicate how many jobs are waiting in the queue. After a job is submitted, its information is written into a database first. If a system failure happens, all job objects can be rebuilt to avoid losing jobs. Then a new job object will be created and inserted into the waiting queue. The insertion operation must be protected by critical sections. Critical sections can guarantee mutual exclusion between threads, so that only one thread can execute operations in its critical

sections. Failure to do so, may cause a fault named "data race" [107], because in a multi-user and multi-threading environment, when some users are submitting jobs, some threads or other users may be executing deletion operations. This will cause unpredictable behavior of the simulation platform which is difficult to trace and debug. The queue operation in critical sections must be finished as fast as possible to avoid a service time-out failure. After a job has been inserted into the queue, the integer value kept in the counting semaphore object will be increased by one, and the *Job Coordination* thread will be notified automatically and start to work. First it checks the system status. If there is no error status, it continues to check whether a job which has the same simulation application ID is being processed. If no job is found, the free space of the hard disk will be checked. If it is lower than the threshold, a system error will be raised. Before the space problem has been solved, no job can be simulated. The error can be checked by the user on the client side. If no error has been found, the job will be transferred to the *Simulation Controller*. The integer value in the counting semaphore will be decreased by one. After the job has finished, its status will be updated and the user can check out the result.

3.2.2 SIMULATION CONTROLLER MODULE

When the simulation server is executed, the *Simulation Controller* thread is created by the main thread. A thread is created for each external application utilizing its description information in the database, such as the application ID, the executable binary location, the input and output format, etc. If several different instances of an application are needed to speed up the simulation, the *Simulation Controller* can create a different

thread for each instance and assign a different sub-ID to help job coordination thread find an idle instance for a new coming job.

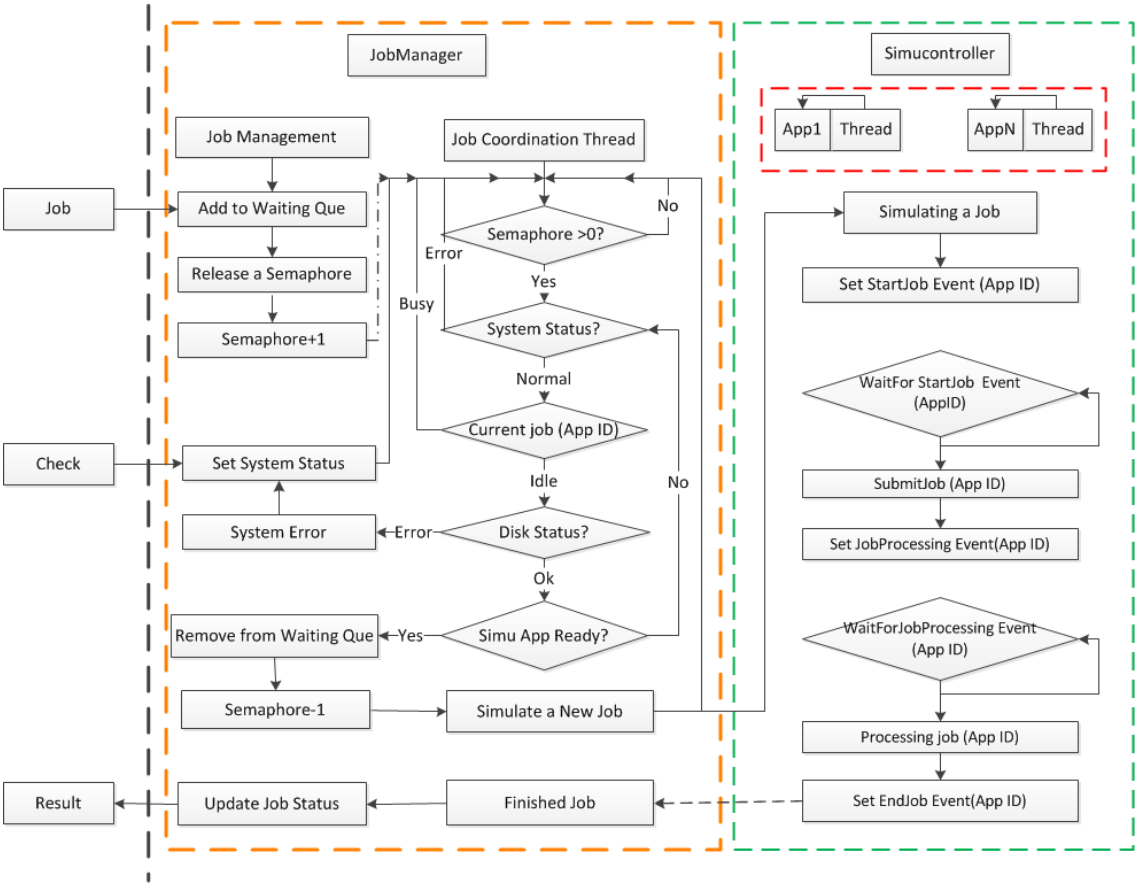

Figure 23: The detailed work flow of *Job Manager* and *Simulation Controller*

In the *Simulation Controller*, event objects are used to synchronize between threads. On Microsoft Windows platform, a thread can call *WaitForSingleObject*, an API (Application Interface), to wait for an event object and go to sleep. It can be waken up by another thread which is called *SetEvent*. After that, the event object will be left in signaled state, unless *ResetEvent* is called to clear its signaled state and let the thread sleep again. If no job comes in, no thread calls *SetEvent*, so the application thread will remain in sleeping status. After finishing a job, *ResetEvent* must be called to convert all

event objects to unsignaled state, so the next job can be served. Similar functions are realized on the Linux platform based on the POSIX [108] *PThreads* library.

Three event objects have been defined for each simulation application. They are *StartJob, ProcessingJob,* and *EndJob*. Using these objects, the *Simulation Controller* and *Job manager* can easily control each simulation application thread and get its status when necessary.

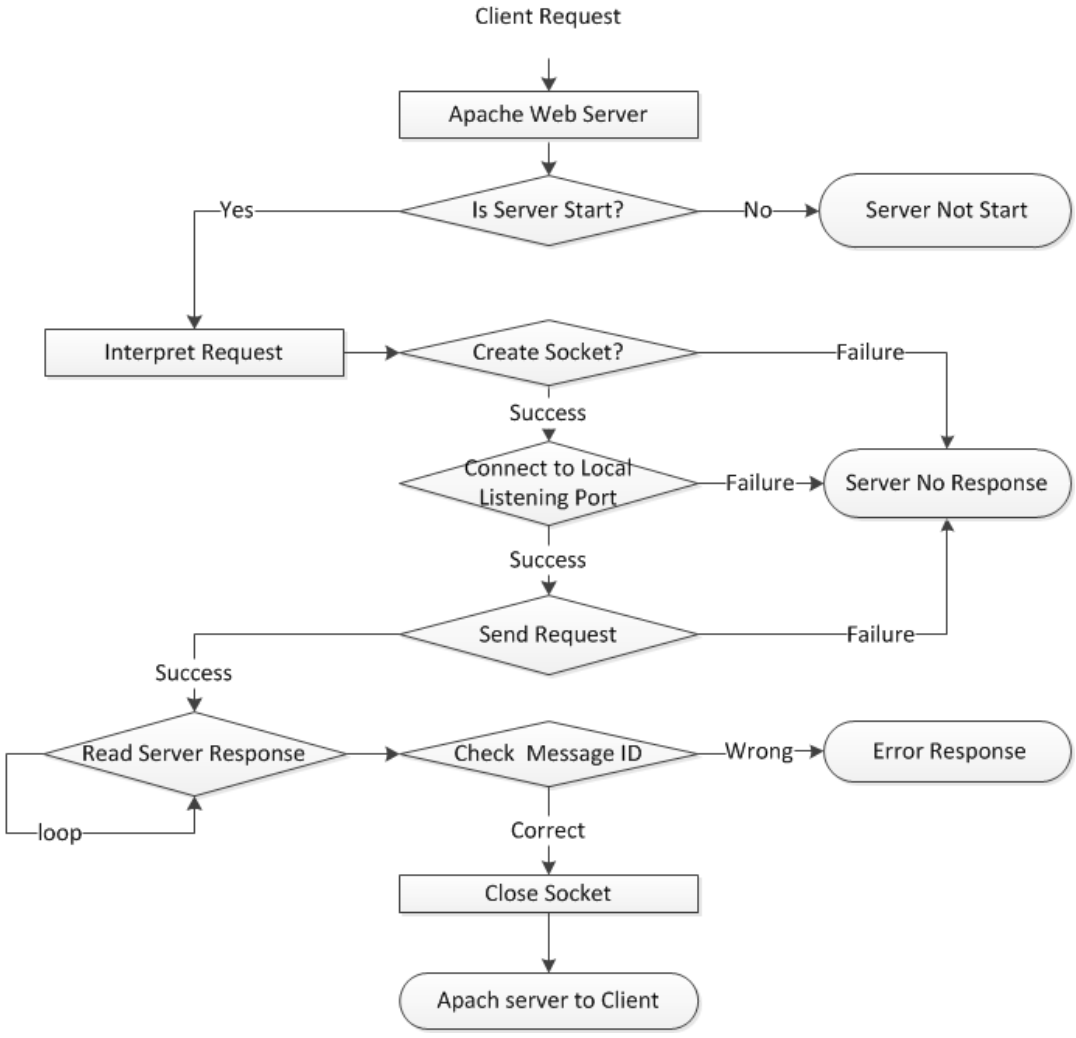

Figure 24: Work flow of a CGI program

3.3 FRAMEWORK OF CGI PROGRAMS

As described in section 3.1.3, CGI programs are responsible for communication between the web server and the service program. Each CGI program can fulfill a specific function. All CGI programs have similar framework. Figure 24 describes the detailed work flow.

Client operation can be divided into different kinds of request, such as submitting a job, deleting a job, etc. Each kind of request will be assigned a unique internal service ID. When a CGI program gets a client request from the web server, it will check the simulation server status. If the simulation server has no response, it will return an error message to the client immediately. Otherwise, it will analyze the parameters from the request, disassemble it and reconstruct a new package which can be recognized by the simulation server. After establishing network communication between the CGI program and the simulation server, the new package of client request will be passed to the simulation server. Until the simulation server finishes the operation of the request, it will return a message to the CGI program. Finally, the client gets the operation result. If any error happens in this procedure, the CGI program will be responsible for notifying the client.

3.4 INITIAL TEST METHOD AND RESULT

Figure 25 describes the UI for the Radon Transform based on the work flow described in section 3.1.3. The parameters for each simulation which the user selected

can be saved as a job. The users can take advantage of the administration page to manage their jobs. Using the job ID, the result can be checked at any time once it is available.

Unit tests and integrated tests are utilized to test thee simulation platform during the developing period. In addition, an application named "*Clickit*" has been developed to help testing CGI programs and the simulation server (Figure 25). It can simulate the mouse clicking operation on different areas of a computer screen at the same time or at any time interval (millisecond to hours) on a prescribed schedule. So, using several personal computers, one can test the system performance using many different operations at the same time. From the test result based on the Radon Transform simulation application, no failure has been found on the operations of submitting and deleting a job.

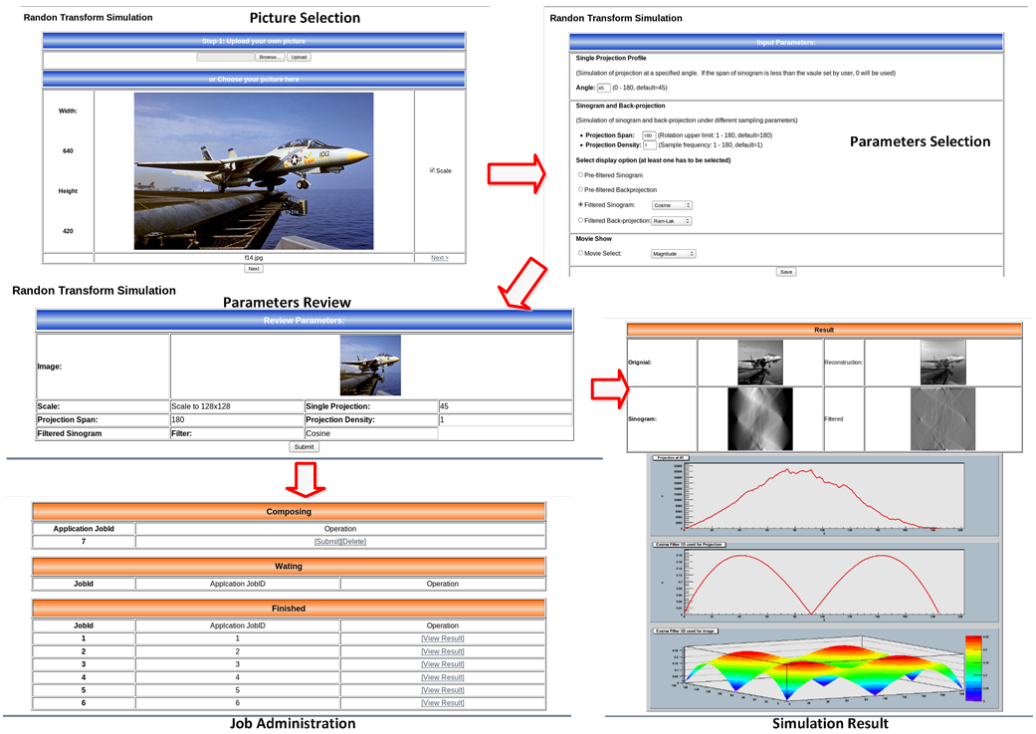

Figure 25: UI for Radon Transform simulation

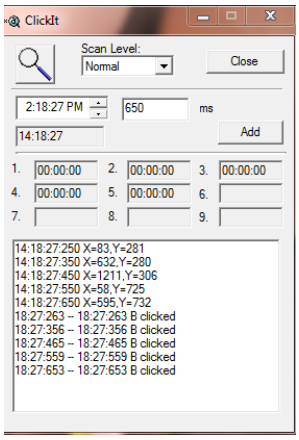

Figure 26: A testing tool for the simulation service platform

3.5 SUMMARY

This chapter described the design and implementation of a prototype simulation service platform. Initial test results indicate that its framework is reasonable and relatively stable. Its performance meets the design expectation. In the next two chapters, a PET imaging simulation method based on GATE will be described in detail. Unlike the light-weighted Radon transform, it is a relatively complex simulation procedure that brings more challenges to the service platform.

CHAPTER 4 PET IMAGING SIMULATION

4.1 PET BACKGROUND

PET, a nuclear medicine imaging modality, is commonly used to study biological functions in human and animals in clinical applications and experimental research. Radioisotope-labeled pharmaceutical compounds, such as 2-deoxy-2-^{18}Fluoro-D-Glucose (^{18}FDG), are usually administered to human beings or animals resulting in detectable photons produced by positron-electron annihilation. The detected photons, recorded as "counts" by radiation sensors, ultimately lead to the generation of a 2D/3D map of distribution of the radioisotope-labeled pharmaceutical compounds, the PET image, reconstructed using various algorithms. In the following parts, the background of PET will first be described.

4.1.1 POSITRON DECAY

In PET, the production of the positron is through the positron decay, when a proton (p^+) converts to a neutron (n) in an atomic nucleus, a positron (β^+) will be produced as well as a neutrino (υ) which has small mass and zero charge to take away the excess kinetic energy, and the equation is as follows:

$$p^+ \rightarrow n + \beta^+ + \upsilon \quad (4\text{-}1)$$

For example, ^{18}F will decay to ^{18}O, and emit a positron with kinetic energy in the range of 202 keV to 633 keV [109], it follows the equation 4-2:

$$^{18}_{9}F \rightarrow {}^{18}_{8}O + \beta^+ + \upsilon + E \quad (4\text{-}2)$$

where E is the kinetic energy of the positron. The emitted positron will lose its kinetic energy through interaction with the electron or nucleus in the matter, and eventually it

will annihilate with an electron. Because of the uncertainty of elastic and inelastic scattering in a specific material, the range which a positron can travel before annihilation is related to the source, its initial energy and the properties of the interaction material. For ^{18}FDG, in water, the maximum range is 2.4 mm, and the mean range is about 0.6 mm [110] . This is an important reason that PET imaging has limited spatial resolution. After annihilation, two 511keV photons are produced which travel in opposite direction through the matter. However if the positron, the electron or both have non-zero momentum at annihilation, photon pairs may not be emitted at strictly 180^{o} from each other. In water, the fraction of photons emitted at angles not from 180^{o} is as high as 65% by estimation [111]. This will further reduce the spatial resolution of PET image.

With reliable and economical distribution network support [112], ^{18}FDG is the most popular positron-emitting radionuclide for various clinical applications in PET procedure. It has the capability of imaging glucose metabolism with a half-life of 110 minutes. It is only an analogue of glucose, so it also has a short biological half-life. After administration in the patient, almost 50% of the original amount will be excreted by normal kidney function in 2 hours [113], because the nephrons poorly reabsorb the filtered FDG. This further decreases the effective half-life of ^{18}FDG.

Other positron emitters, such as ^{11}C (20.4 minutes), ^{13}N (9.96 minutes), ^{15}O (124 second), are also in great interest. Due to their short half-lives (in parentheses), they cannot be delivered or transported as ^{18}F, so they must be produced on site. Otherwise, the cost will be too high to be used in clinical or experiment studies. These emitters also

are more commonly choses to do simulation first before applied to clinics or research laboratories.

4.1.2 PHOTON INTERACTION

When the photon pairs traverse human tissue, there will mainly be three interactions: 1). Rayleigh scattering (Coherent scattering), 2). Photoelectric effect and 3). Compton scattering.

Rayleigh scattering occurs when the incident photon interacts with the whole atom. The scattered photon has the same energy as the incident one, but has different trajectory direction. So no energy is absorbed by the tissue. Rayleigh scattering only happens at very low photon energy level. For example when the photon energy is above 70keV, at most 5% scattering is due to Rayleigh scattering [114].

When the energy level is below 100keV, the photoelectric effect plays an important role. The incident photon will interact with an orbital electron, part of its energy is used to overcome the binding energy of this electron, and part of energy will pass to the electron as the electron's initial kinetic energy. Finally the photoelectric effect will produce an Auger electron and characteristic x-ray of the specific atom. The probability of Photoelectric effect is roughly proportional to $\frac{Z^{3.8}}{E^3}$ for low Z material, where Z is the atomic number and E is the energy of the incident photon [114]. The probability will reach a maximum when the energy of the incident photon is just higher than the binding energy of the electron, because human soft tissues are mostly composed by low atomic weight elements, such as H, C, O and N. The binding energy of orbital electrons is low; therefore incident photons of low energy (less than 100 kev) are preferred when

imaging soft tissues, because the photoelectric effect chiefly contributes to the imaging quality.

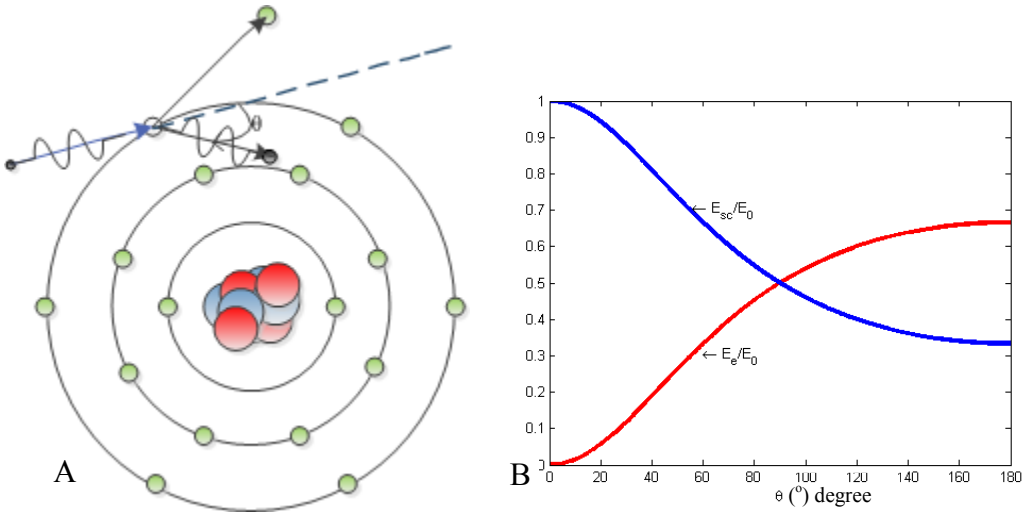

Figure 27: A) illustration of Compton scattering; B). The energy ratio of the scattered photon to the incident photon

In Compton scattering, the incident photon interacts with a free or a loosely bound electron of an atom in the medium, and causes the electron and itself to scatter independently. This interaction does not consume all the energy of the incident photon, the remaining energy of the scattered photon can be calculated through the following equation.

$$\mathrm{E}_{sc} = \frac{E_0}{1+\alpha(1-cos\theta)} \qquad (4\text{-}3)$$

where E_0 is the energy of the incident photon, $\alpha = \frac{E_0}{511(keV)}$, for the photon pairs produced by positron emitters , $\alpha = 1$; θ is the scatter angle, So the kinetic energy, E_e of the electron will be

$$E_e = E_0 - E_{sc} = \frac{1-cos\theta}{2-cos\theta}\, E_0 \qquad (4\text{-}4)$$

when θ =0, the photon does not lose any energy, when θ =180, the incident photon will lose 2/3 its initial energy. Figure 27 shows the energy ratio of the scatter photon and the electron to the incident photon. At the energy level of the annihilation photon pair (511 kev), Compton scattering is the most important interaction in human tissue.

4.1.3 SCINTILLATORS USED IN PET

After photon pairs pass through the human body or research object, they will be detected by PET scintillators. However, there is no scintillation material with properties that are all ideal for a PET scanner. All scintillation materials used by different commercial or experimental PET scanners have their own advantages and disadvantages.

The properties of six commonly used scintillators are listed in Table 7. Four most important properties are: 1. attenuation length at 511 keV; 2. signal decay constant; 3. light output; and 4. overall energy resolution. An ideal scintillator should have shorter attenuation length, shorter decay constant, and higher light output and higher energy resolution. BGO detectors have better detection efficiency due to their larger linear attenuation coefficient (0.9496 cm^{-1} at 511KeV [115]) and higher density. In order to get similar detection efficiency as systems using BGO detectors, a PET scanner using NaI (TI) detectors would be almost three times thicker than BGO's. But NaI(TI) gives better light output than BGO. Though LSO has higher density, higher light output, higher linear attenuation coefficient and shorter decay constant, due to its intrinsic structure, its energy resolution is poor. Lutetium has a natural radioactive isotope form ^{176}Lu (2.6% abundance) present in the material [116]. GSO has better energy detection and more uniform light output than LSO, but it has lower density, lower linear attenuation

coefficient and lower light output. BaF_2 has the shortest decay constant and is mainly used in time-of-flight research. YSO is a relatively new material and has better physical parameters, but nowadays it still has not been commercially adopted.

Property	NaI(TI)	BGO	LSO	GSO	YSO	BaF_2
Name	Sodium Iodide	Bismuth Germanate $Bi_4Ge_3O_{12}$	Lutetium Oxyorthosilicate Lu_2SiO_5:Ce	Gadolinium Oxyorthosilicate Gd_2SiO_5:Ce	Yttrium Oxyorthosilicate Y_2SiO_5:Ce	Barium Fluoride
Density($g.cm^{-3}$)	3.67	7.13	7.4	6.71	4.53	4.89
Effective Z	50.6	74.2	65.5	58.6	34.2	52.2
Attenuation length (cm)	2.88	1.05	1.16	1.43	2.58	2.2
μ (cm^{-1})	0.3411	0.9496	0.8658	0.6978	0.3875	0.4545
Decay constant(ns)	230	300	40	60	70	0.6
Light output (photons/keV)	38	6	29	10	46	2
Relative light output	100%	15%	75%	25%	118%	5%
Intrinsic ΔE/E (%)	5.8	3.1	9.1	4.6	7.5	4.3
ΔE/E (%)	6.6	10.2	10	8.5	12.5	11.4
Hardness (Mohs)*	2	5	5.8	5.7	5.8	3

Source: [111], * *from* [117]

Table 7: Scintillators used in PET Scanner

4.1.4 SINGLES, RANDOM AND TRUE COINCIDENCE

Positrons are emitted in all directions in the human body. After annihilation, only a small part of scattered or un-scattered photons can be detected by the scintillation detectors. If a single photon is counted by a PET scanner, it is named a *single* event. If two single events are detected in a very short time interval with nanoseconds, it is called a *coincidence event*. The time interval is named the *coincidence window*, and it can be predefined by the manufacturer based on the geometrical structure of the PET scanner. If

photon pairs of annihilation are detected by the PET scanner at an acceptable angle, it is called a *true coincidence* event, see Figure 28 for details.

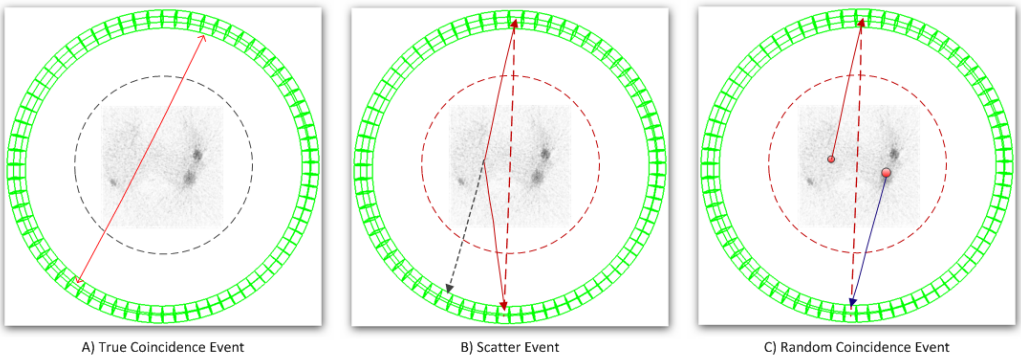

Figure 28: Different types of coincidence event

The line between two detectors of a coincidence event is called the line-of-response (LOR). Due to the scattering, photon pairs may change their trajectory, and the LOR is different to what it should be. This phenomenon is called a *scattered event*. Meanwhile some positrons may annihilate simultaneously or in a very short time interval. Photons come from different annihilations could perhaps be counted mistakenly as coincidence events. These events are named *random events*. The ratio of true coincidence events to singles is only 1%-10% for a specific PET scanner. If a PET scanner is operated in 2D mode, the ratio of scatter events to total events is about 10-20%. But if it is operated in 3D mode, the scatter may be significant larger to 35-60% [109].

4.1.5 COMMERCIAL PET SCANNERS

In Table 8, technical features of seven different commercial PET scanners from different manufacturers are given based on the work of Tarantola et al [118]. These data

can be used as the important reference when designing a new virtual PET scanner in the simulation.

The NEC (noise equivalent count) [119] can be used to compare the sensitivity of a PET scanner with another. It is defined as follows:

$$NEC = \frac{T^2}{T+S+KR} \qquad (4\text{-}5)$$

Where *T, S, R* is the count rate of true, scatter and random events respectively, and *K* equals 2 if the real-time random subjection method is used. The NEC curve can be obtained based on the standard NU2 2001 [120] NEMA (National Electrical Manufacturers Association) phantom to reveal the performance of a PET scanner. It is a simple phantom which includes a 20-cm diameter by 70-cm long cylinder. Figure 29 illustrates another commonly used phantom: NEMA 2-2001 IQ phantom. The script of Figure 29 is implemented by OpenGATE [12] collaboration, and the picture is rendered in QGate Designer (to be described in following sections).

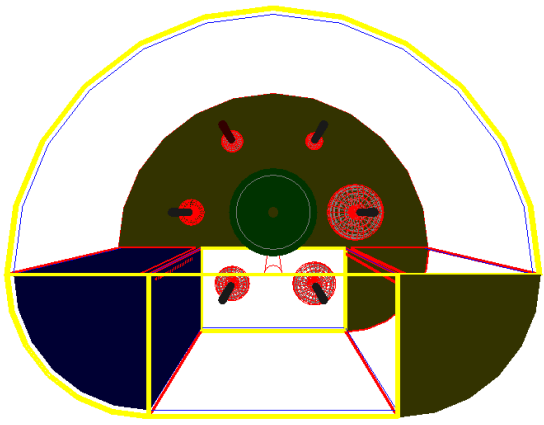

Figure 29: NEMA IQ Phantom in GATE

	Advance/ Advance Nxi	ECAT ACCEL	ECAT EXACT HR+	ECAT EXACT	ECAT ART	C-PET	ALLEGRO
Manufacturer	General Electric	CTI-Siemens	CTI-Siemens	CTI-Siemens	CTI-Siemens	Philips-ADAC	Philips-ADAC
Ring diameter(mm)	927	824	824	824	824	900	860
Number rings	18	24	32	24	24	N/A	29
Crystals number	12096	9216	18432	9216	4224	6	17864
Crystals size (mm)	4.0×8.1×30	6.45×6.45×25	4.05×4.39×30	6.29×6.29×20	6.29×6.29×20	500×300×25.4	4×620
Crystals /Block	36	64	64	64	64	N/A	No blocks
Crystals material	BGO	LSO	BGO	BGO	BGO	NaI (TI)	GSO
Energy window (kev)	300-650	350-650	350-650	350-650	350-650	435-665	435-650
Coincidence windows (ns)	12.5	6	12	12	12	8	8
Septa material	Tungsten	Lead	Lead	Lead	N/A	N/A	N/A
Septa dimensions (mm)	1×170	1×65	0.5×65	1×65	N/A	N/A	N/A
Transaxial FOV (mm)	550	585	585	583	600	576	576
Axial FOV (mm)	152	162	155	162	162	256	180
Number of Image planes	35	47	63	47	47	64/128	90
Slice thickness (mm)	4.25	3.375	2.46	3.375	3.375	2	2

Source: [118]

Table 8: Technical Features (Factory Data)

4.2 MOTIVATION AND SIGNIFICANCE

Due to ethical considerations, safety regulations, and/or economic considerations, clinical protocols or animal experiments using PET imaging are usually investigated through computer simulations prior to their application. However, the simulation is a sophisticated process due to the probabilistic nature of radioactivity in PET imaging as well as issues regarding designs and algorithms in data acquisition, signal processing and image reconstruction. Monte Carlo methods are commonly proposed to deal with this scenario. Among existing simulation software packages, the Geometry and Tracking 4

(Geant4) [13] system, has been widely used to simulate applications in many fields, such as medical physics, nuclear physics, and particle physics. It provides well-validated physics models, geometry modeling tools and efficient visualization utilities. Based on the Geant4 libraries and using C++ object-oriented language to achieve a modular, versatile, scripted simulation toolkit, the OpenGATE collaboration [12] developed the Geant4 Application for Tomographic Emission (GATE) [37], [121] system, which was dedicated initially to PET and single photon emission computed tomography (SPECT) simulations and has been extended to computed tomography (CT) and optical imaging simulations now.

The Monte Carlo method adopted by the GATE system has been validated [122], [123] through the comparison between the simulated data and the data collected from commercial systems, such as the ECAT EXACT HR+ system (CPS Innovations, Knoxville, TN, USA) and the dual-headed AXIS SPECT system (Philips Medical System, Cleveland, OH, USA). Simulation results obtained from the GATE system have also been verified by ^{111}In SPECT acquisitions through energy spectra, spatial resolution and sensitivity comparisons [124]. Data generated by the GATE simulation models were compared with data collected by the Siemens biographTM 6 PET scanner (Siemens Medical Solutions, Knoxville, TN, USA). A good agreement between the simulated and the experimental data sets for the scatter fraction and count rate measured at 1 kBq/ml concentration has been reported [125]. The simulation accuracy, reliability and applicability make the GATE system a validated platform for PET and SPECT applications, such as detector and scanner design [126], [127], [128], image reconstruction [38],

[129], [130], scatter and attenuation correction methods [131], [132], protocol optimization [133], and so on.

The GATE system has been frequently used as a simulation toolkit. The popularity of this system has been proven by the fact that more than 11,000 users [12] have registered on the GATE website. However, GATE does not provide users with a graphical user interface (GUI) for simulation-design and performance-administration, which is an obstacle for users with less experience in the field. In addition, in order to fully utilize the capability of GATE, further customization by editing and modifying the scripts is required. This work involves user's compiling and programming knowledge under the environments of C++, Roots Object Oriented Technologies (ROOT) [11], or Class Library for High Energy Physics (CLHEP). It is highly desirable to have an instrument that allows a user to construct his/her simulation by graphical tools without involving much programming and to manage the simulation jobs efficiently. An automated or semi-automated solution to the simulation needs would be appreciated by a number of users, especially those with less experience or non-programming background.

4.3 QGATE CLIENT DESIGN AND IMPLENTATION

4.3.1 DESIGN

The GATE simulation software is based on the so-called *script* commands through parameters entered by the user in an interactive fashion. An object in the simulation, such as a radiation detector, has a number of property parameters. If any of them had an error, such as a wrong property name, GATE would generate a wrong simulation result or an exception to terminate the simulation. We proposed a GUI client

interface to help the user design objects (e.g., box, sphere, cylinder, etc.), which can be selected from the *object table* provided by an *ObjectList* window. Each object's property parameters can be selected from the *property table* (e.g., geometric dimensions, material names, etc.). The names of the property parameters are defined in corresponding database files and linked to dropdown lists so that human errors can be effectively avoided. The client of the system will automatically generate the scripts for the simulation. Meanwhile, the 3D display of selected objects helps the user understand the simulation system intuitively. Under such an environment, the simulated PET/SPECT scanner and the simulated phantom can be directly conveyed to users. Figure 24 shows the functions associated with the client component.

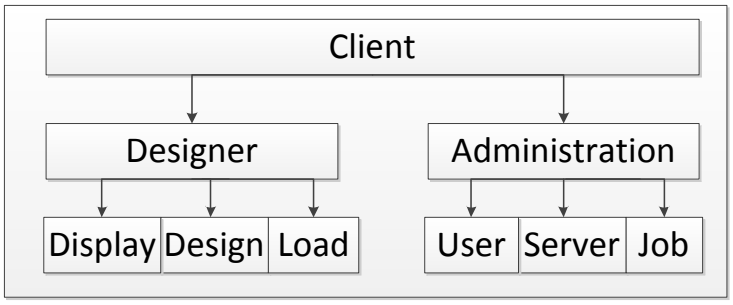

Figure 30: The modules of QGATE client

Since the GATE system is usually installed on a high-performance computer [134] and the simulation jobs are usually designed from the user's local computer, we proposed to build a server interface to host the GATE system on the high-performance computer. The client interface can remotely access the server interface and deliver the generated scripts to the server. The server manages the scripts to be queued, uploaded, or reused for the GATE system. The server can also return the simulation results to the client. By this way, users can get their simulation jobs done remotely and check their simulation results

individually. Figure 30 shows the functions associated with the client component. Based on these design principles, QGATE has been constructed as an integrated solution to simulation design and simulation education under the GATE environment.

4.3.2 IMPLEMENTATION

As a simulation software platform with client and server architecture, the QGATE system is written in C++. The current version of the QGATE Client is developed based on the open source software GATE 6.0, Geant 4.93 and Qt 4.60 [15]. Qt is a cross-platform GUI development toolkit. This single source (C++) compatibility makes the client run on different platforms without additional development. The QGATE Client has been tested under operating systems of Microsoft Windows XP, Microsoft Windows 7 (32 Bit) and Linux Fedora 10-14. The simulation server is also written in C++. It wraps GATE 6.0 as the core to interpret the simulation job.

Based on these design principles, the client component of the QGATE system can be installed on a remote computer (Figure 30). The *Designer* module in the client provides users with a GUI interface (Figure 31). However, converting a simulation design into the corresponding scripts is the key step to ensure the QGATE system's automation. We took the *open source* advantage of the GATE system and analyzed its workflow and running mechanism. From the source codes, we extracted and created the script templates for different objects and exported them to associate with graphical objects under the GUI environment. The objects' property parameters were linked to the property name database file. The *Designer* guides a user to select an object, to fill out required property parameters (if a parameter is omitted, a default parameter will be used), and to

choose/produce its lower/parallel hierarchical objects. The scripts will be generated by the embedded templates.

Figure 31 demonstrates how the QGATE system assists a user to complete a simulation design. The construction of a design starts from choosing a simulation system. A system component, i.e., an object, can be dragged from the *Gate Designer* window's Graphic (object) list and dropped to the *New Design* window. The object properties will be displayed by the *Object Inspector* window. These properties are specified by corresponding parameters for objects of sensor, crystal, digitizer, coincidence, random engine, output and so on. The user can edit the selected object's properties through the *Property Editor* window. A default property will be used if it is not defined by the user. When the user saves the design for the specified object(s), the script(s) will be generated by the QGATE system automatically. Since the GATE system has already built several internal pre-defined systems, such as Cylindrical PET, ECAT, these systems can serve as simulation templates for users. The QGATE Designer allows users to select these templates, modify them, and add new objects to them so as to build their own new designs. The QGATE system interprets the graphical design to be executable scripts and upload the scripts as outputs of the client. When the graphical elements, i.e., objects, are removed, duplicated or modified during the design, the scripts will also be updated accordingly. The *Administration* module in the client component plays the *manager* role for the QGATE system. The user-account is initiated by an *administrator* account that can add, remove and modify user accounts so that multiple users can sign on the client to design simulation tasks.

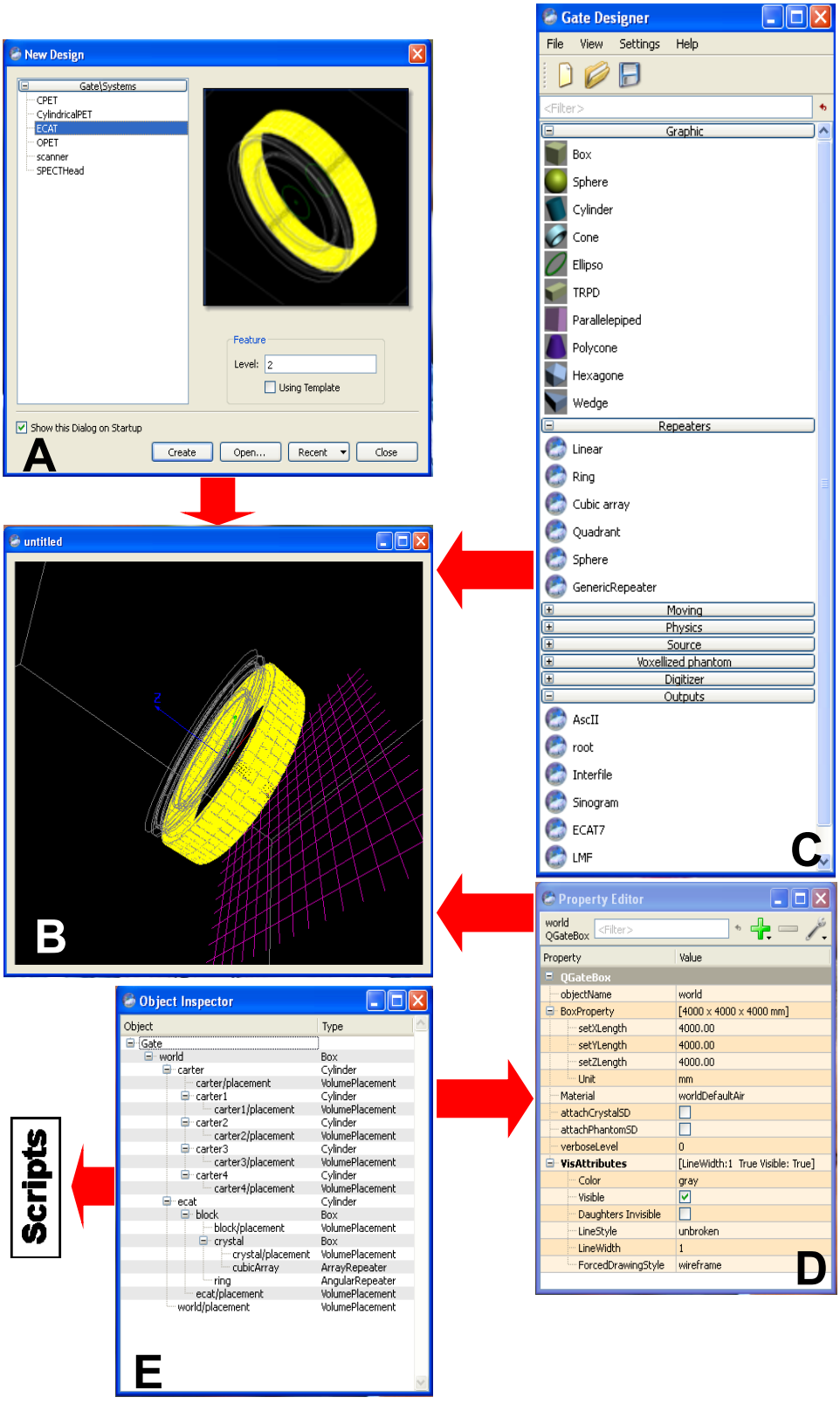

Figure 31: Designer modules and their functions

If more than one simulation task need to be executed, the *Administration* module will generate a *job ticket* for each task. According to the order of the *job tickets*, the server conducts simulation sequentially.In the QGATE system, each simulation is regarded as a job and each job is listed in one of three job queues: 1) the waiting job queue, 2) the running job queue, or 3) the finished job queue. The server will pick up a job from the waiting job queue and the client will update the queue statuses. The *Administration* module also helps the user to communicate with the server, such as uploading simulation scripts and related data files, getting simulation outputs, and checking simulation status.

4.4 DESIGN EXAMPLE AND RESULTS

The ECAT system is a pre-designed example included in the GATE system. Its scripts can be pulled out and modified to conduct specified simulations. However, a user must know all specifications in order to construct scripts. Here we give a design example by using the QGATE designer to build an ECAT family system (Figure 32).

When a new design is started, the QGATE *designer* will always create a new default object, a world. The world is a box object with air as default material. The world's geometric dimensions should be large enough so that all objects can be added later. The world's length, width and height can be changed in the *Property Editor* window. Other properties, such as line color, line thickness, or wire-form for display, can also be changed in the window (Figure 32 A and E). The user can then drag a cylinder object from the GATE Designer window's *Object List* (see Figure 31 C) and drop it onto the world (Figure 32 C). The cylinder can be named as "ECAT" (or other name) through

the cylinder's *Property Editor*. Similar to the world, other properties of the cylinder can also be modified. The user will next add a crystal block to the cylinder. The crystal's material can be chosen from the *Material Database* (Figure 32 F). The crystal block's dimension is defined by the similar way to the cylinder's. After the crystal block is designed, the user can drag a repeater object from the *Object List* (see Figure 31 C, *Repeater list*) and associate it with the already-selected crystal block. By editing the repeating numbers in x, y and z directions, the user can fill them in the 3D space inside the cylinder (Figure 32 D). The user can then save the design as scripts and export the file to the server (Figure 32 G and H). A brain phantom can be selected from the *Object List*. Figure 33 A and B shows the selected Hoffman digital phantom. Its location and radioisotope concentration can also be modified. Figure 33 C to E shows the resultant images returned through the QGATE Server through 100 second simulation by GATE.

The result will be updated immediately in the display panel. The QGATE designer will read the *material database* from its system folder. The database includes all materials defined in the GATE system. The QGATE Client serves the *interpreter* function for GATE and the simulation Server plays the *manager* role for GATE. In term of functionality, the QGATE system has so far focused on PET simulations. Objects related to PET simulation in GATE 6.0 have been wrapped in the QGATE Client. In terms of performance, the QGATE system has a very similar performance capability to the GATE 6.0 system. Functions and objects in GATE that are not related to PET simulations have not been included in the QGATE system.

The QGATE designer allows every object's properties to be modified graphically by clicking the object. Its associated *Property Editor* will appear. By modifying the visual properties, using QGATE Designer, it is easy to design different virtual PET scanners which can be used in GATE. Figures 35, 36 illustrate how to construct a similar virtual PET scanner based on the technical parameters listed in Table 8. First a block is defined which includes 6×6 crystal units. Then it is expanded 3 times in the *y* direction to construct an object, and the object is repeated 112 times along the whole ring which has a radius of 463.5mm. A virtual PET scanner which has similar geometrical structure as the GE Advance PET scanner can be constructed. Figure 35 is a simplified representation. Only one big block is repeated six times in a ring.

The script output from QGATE may also have errors that prevent execution in the server side. In order to help the user check the script further, *wGate* (Figure 34), an application on Microsoft platform, is migrated from the Linux platform based on the source code of GATE and Geant.

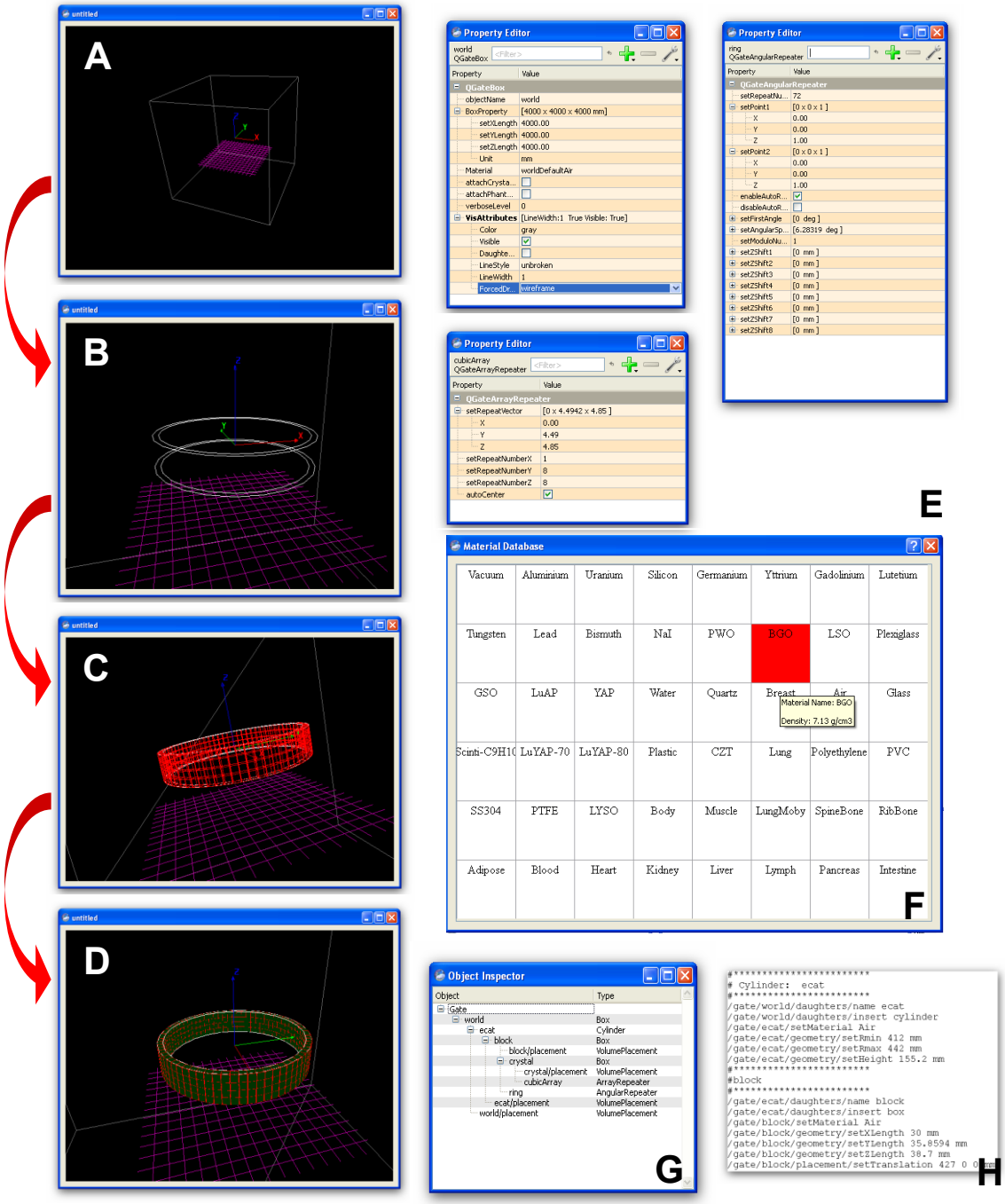

Figure 32: A design example of using QGATE designer

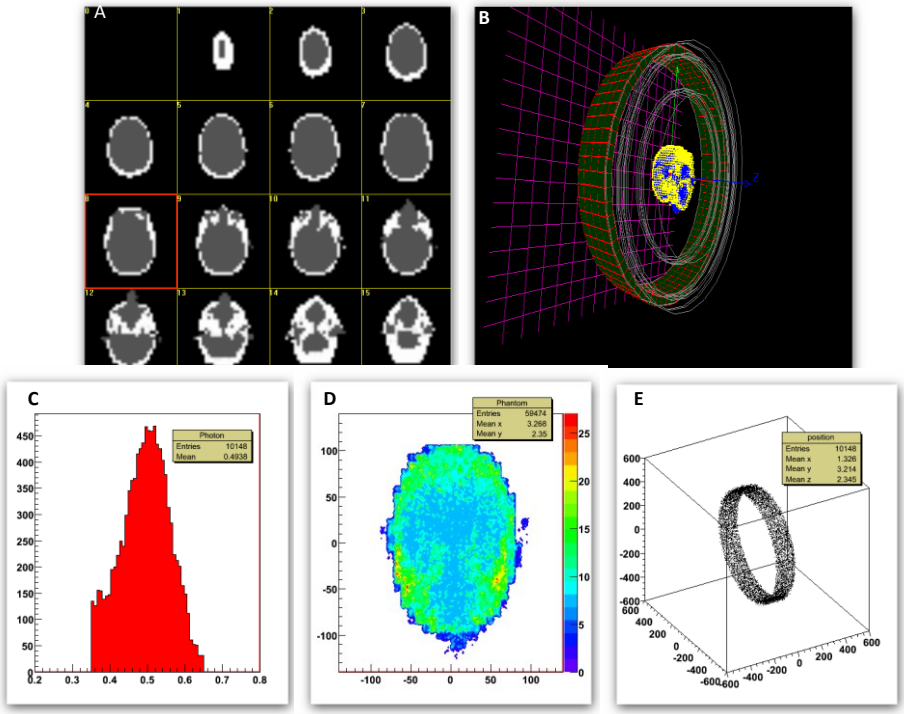

Figure 33: The result of a PET simulation

```
ROOT session
C:\upload\Geant493binary\Debug>wGate.exe
[G4]
[G4] ********************************************************
[G4]  Geant4 version Name: geant4-09-03    (18-December-2009)
[G4]                       Copyright : Geant4 Collaboration
[G4]                       Reference : NIM A 506 (2003), 250-303
[G4]                             WWW : http://cern.ch/geant4
[G4] ********************************************************
[G4]
[Core-0] Initialization of geometry
[Core-0] Initialization of physics
[Core-0] Initialization of actors
[Core-0]
[Core-0] ***************************************************************
[Core-0]  GATE version name: gate_v6
[Core-0]                    Copyright : OpenGATE Collaboration
[Core-0]                    Reference : Phys. Med. Biol. 49 (2004) 4543-4561
[Core-0]                    WWW : http://www.opengatecollaboration.org/
[Core-0] ***************************************************************
[Core-0] ***************************************************************
[Core-0] GATE Windows version:wgate_v6
[Core-0]                    WWW : http://qgate.eng.miami.edu/
[Core-0]                     by Xiping Li, bug report:x.li1 at umiami dot edu
[Core-0]                     a part of  our open source project of QGATE
[Core-0]                     which is an education platform and a  simulation automation solution
[Core-0]                     based on GATE and other simulation softwares
[Core-0] ***************************************************************
[Core-0]
[Idle>
```

Figure 34: wGate: a windows version GATE

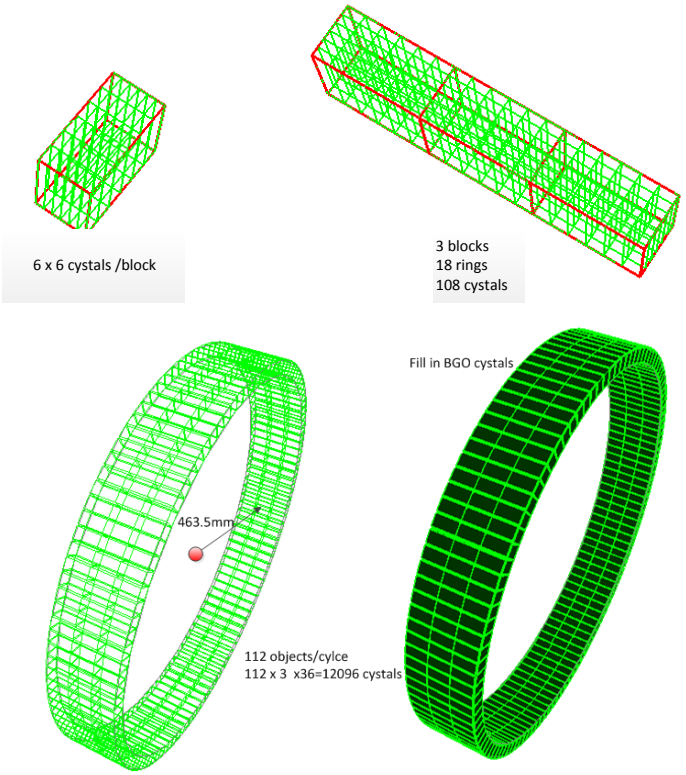

Figure 35: Illustration of constructing a virtual PET scanner in GATE based on GE Advance scanner

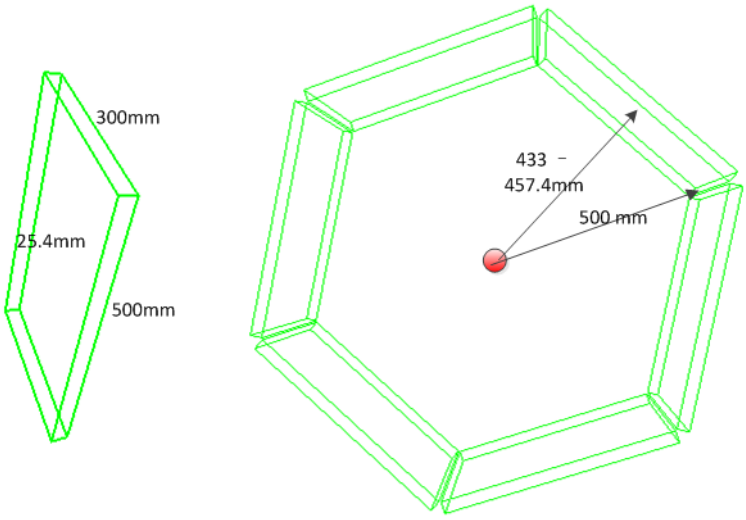

Figure 36: Illustration of constructing a virtual PET scanner in GATE based on C- PET Scanner

4.5 CONCLUSION AND DISCUSSION

The QGATE system has been developed as an educational or training tool kit to perform nuclear medicine imaging simulation. Considering the complexity of emission tomography, we developed this system aiming to ease the learning process for beginners or medical/biomedical students. The advantages of the system include the user-friendly graphical interface to avoid sophisticated scripts preparation, the multi-user/job management function, and the ability to remote-access the high-performance server. The GATE system is a powerful simulation tool kit. However, its full potential as a routine simulation system to beginners has not been fully exploited. The major obstacle is the composition of scripts, in terms of syntax, property names and importing/exporting scripts/results. One of our endeavors in this study is the "translation" (or interpretation) from text-based script composition to GUI-based design. Under the GUI environment, beginners in the field can easily build the simulation protocol by visually choosing a pre-designed model and editing the objects' properties without struggling on writing program-like commands. Another endeavor in this study is to separate the designer from the high-performance server. The QGATE Client-Server setup enables the designer (client) to be installed on different local computers due to the fact that the design process does not require much computational resource. Multiple users can do their design individually, such as in a training class setup. The QGATE client provides efficient methods to generate scripts and upload to a remote server. The user can easily design the simulation by using drag and drop tools, and immediately obtain the scripts corresponding to the graphical design. The user can also check the details of each

designed object by using zooming, rotating and on/off graphical tools. The QGATE client checks all objects' properties before exporting the scripts to the server. For example, material names are commonly mistyped and entered to the system. This specifically designed feature avoids user's mistake and misunderstanding the GATE commands, such as the command sequence and command name. The QGATE server, installed on the high-performance computer, manages the uploaded jobs and returns the simulation results by the order of job tickets. The QGATE is a graphical simulation application that helps the user to use and understand GATE and Geant4. It assists beginning users or students to get training in the field of the emission tomography simulation.

The works in this chapter have been presented on an international education conference [135] and published on "The Open Medical Imaging Journal" [136].

CHAPTER 5 PET SIMULATION STUDY

Besides for education purpose, as a simulation service platform, QGate, is also used in the research fields. Through providing pre-defined and stored virtual PET instrumentations and phantoms, the whole work flow in a particular research can be facilitated. As described previously, QGate can be executed by user-provided complete scripts from the client-server model. The research of PET imaging simulation can be further simplified into 3 steps: virtual PET instrumentation selection, phantom selection and source activity definition. In this chapter, we give more details about how to carry out PET imaging simulation research using different phantoms which are generated according to different respiratory signals.

PET measures the location of the line on which a positron is annihilated. After accumulating many such coincidence lines, line integrals of annihilation photon activity are produced and transmission tomography can be reconstructed. Commonly used ^{18}F-FDG, PET imaging provides unique physiologic and metabolic information about lesions and it is a routinely used tool for detecting, staging, and monitoring response to therapy of cancerous tumors in the lungs.

When performing PET imaging in patients with lung cancer, the exact location, shape and size of the lesions in the lungs may be distorted as a result of respiratory motion from the patient's regular breathing during the scan. Respiratory motion affects the image quality by reducing the target-to-background ratio and also degrades the spatial resolution by introducing image blurring. Respiratory motion results in artifacts that degrade accurate diagnostic characterization of the lung lesions, their spatial localization and also their quantitation. This has a negative impact on the management of the detected

lesions, particularly for small lesions in the lower level of the diaphragm, between the lung and the liver.

5.1 BREATH MECHANICS

A breathing cycle can be divided into two phases: inspiration and expiration. Normally, inspiration is active and expiration is passive. Respiration is the result of the combined work on two halves of the diaphragm, intercostal muscles, abdominal muscles and other muscles. In the inspiration phase, the diaphragm contracts and moves downward. Meanwhile, abdominal muscles will contract too and push the diaphragm up. In the expiration phase, both muscles tend to relax and return to the equilibrium position. The movement range of the diaphragm between the end of inspiration and the end of expiration normally is about 1 cm, but during acute breathing, e.g. coughing, this movement can reach up to 10 cm [137].

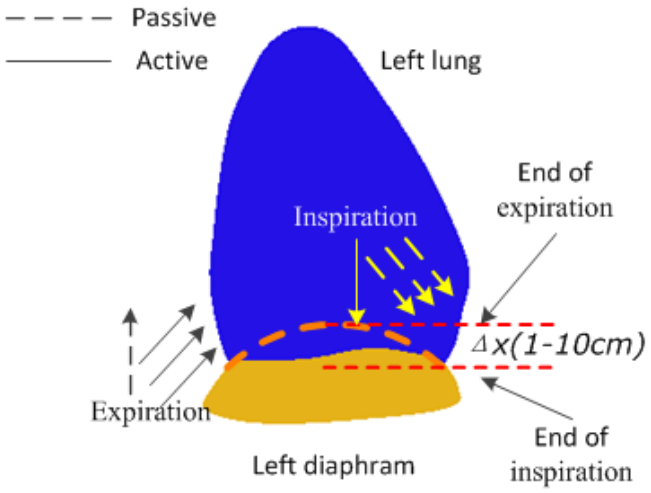

Figure 37: Lateral view of the relationship of lung and diaphragm in the breathing cycle

Besides the diaphragm movement, another breathing movement comes from the ribs movement due to intercostal muscles contraction and relaxation (Figure 37). During inspiration ribs are pulled upward and forward by external intercostal muscles, and rotate on an axis of their costal neck. Therefore this will increase their AP (Anterior-Posterior) and transverse diameters as well as the volume of thoracic cavity. In the expiration phase, internal intercostal muscles do the opposite action and decrease the volume of the thoracic cavity.

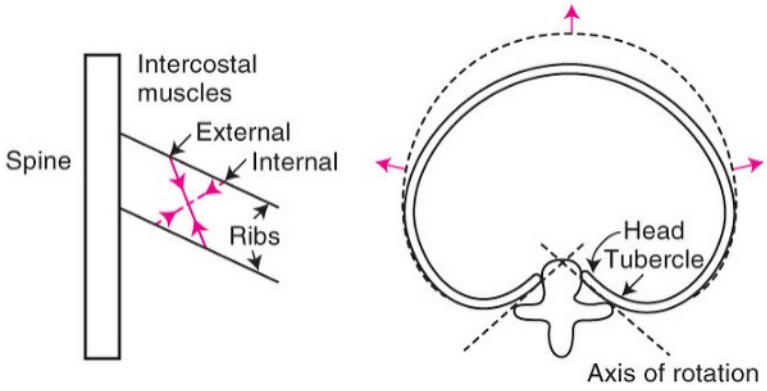

Figure 38: Ribs movement will expand or shrink the volume of the thoracic cavity [137]

The breathing signal can be recorded by many ways. In section 5.2.3, a detailed review will be given. Figure 39 shows the different breathing signals captured by PowerLab 4/10 ST (ADInstruments Pty Ltd, Bella Vista, Australia) with an elastic belt which has a pressure sensor fastened on the abdomen of a subject (Figure 40, D). Cough will lead to a forceful contraction of the chest and abdominal muscle. Therefore intense changes can be seen in the signal.

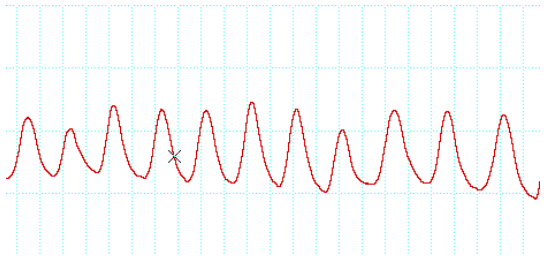

(a) Normal breathing

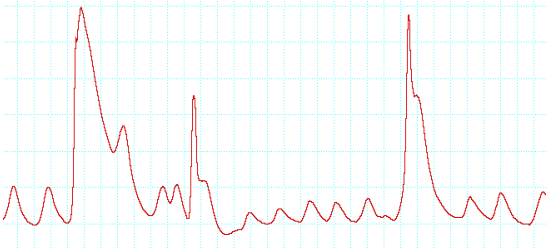

(b) Cough

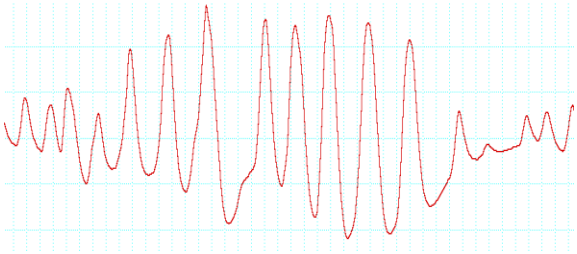

(c) Swallowing

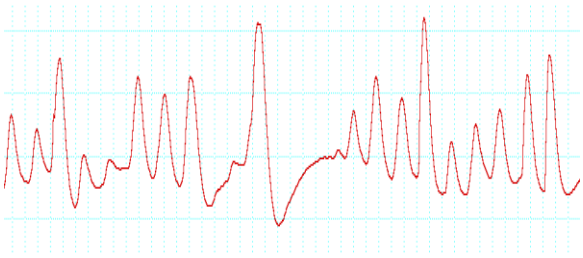

(d) Hiccup

Figure 39: Breathing signals recorded using abdomen elastic belt and PowerLab

Swallowing or drinking will also produce rapid abdominal muscle contraction, but the signal intensity is much lower than for cough. Hiccups are sharp, spasmodic contractions of the diaphragm [138]. Their signal has shorter period.

In some situations, the two halves of the diaphragm may not contract synchronously. In this study, only synchronous contraction is considered. Though the signals reflect the pressure changes due to AP expansion, they can be utilized to simulate AP movement. Relative regular signals of different respiratory status are sampled into a period signal and will be used to generate the phantoms in this study.

5.2 REVIEW OF MOTION CORRECTION IN PET IMAGING

Tremendous amount of effort has been devoted to the improvement of lesion localization, the standardized uptake value (SUV) estimation and attenuation correction in PET imaging. Investigations include utilizing new generation of PET/CT instrument, addition of data acquisition mode, external device assistance, software for post-acquisition processing and statistical simulation for data assurance. In order to provide better simulation on-demand service, first we review related works in this field.

5.2.1 IMPROVEMENT OF INSTRUMENTATION PET/CT

PET/CT is probably the most significant evolution for PET imaging. The PET scan detects the metabolic signal of actively growing cells (lesion) in the body and the CT scan provides a detailed picture of the internal anatomy that reveals the location, size and shape of the lesion. Normally, a low-dose CT scanning at 40 -50 mA [113] will be given first. Total scan time will be less than 30s. The axial field of view will cover 100

cm with a slice thickness which can be matched the PET scan. Patients will be asked to hold their breath during the CT scan. Alone, each imaging test has particular benefits and limitations but when the results of PET and CT scans are "fused" together, the combined image provides complete information on the lesion. Image fusion, originally termed for computer vision [139], [140]meaning the process of combining relevant information from two or more images into a single image, is now a common practice in PET imaging. Image fusion techniques, based on various image registration methods [16], have been routinely applied for PET/CT studies. In addition to the matching of PET and CT data to identify a lesion's anatomical location, CT data has also been used for attenuation correction, i.e., converting CT number to attenuation information. The basic objective is to match the 3D CT transmission data to 3D PET emission data [17], [18]. However, the CT data captured during a single moment (such as by breath-hold method) of a respiratory cycle does not match the PET data during different phases in many respiratory cycles. Several approaches have been proposed to solve this problem. 1) Averaging CT data sets over many respiratory cycles [19], [20], [21], [22], in the same way, PET emission data are an average over many respiratory cycles. Attenuation correction is improved but motion artifacts cannot be completely removed by this approach. 2) Using a cine CT scan lasting one or more respiratory cycles [23], [24]. Synchronization between acquired cine CT during one or more respiratory cycles and PET data acquisition in following respiratory cycles may induce mismatching by the approach. 3) Extending the CT data to a four dimensional domain. A typical application is to transform the CT data set into a 4D domain, in which a predefined 3D phantom [25] can be temporally modeled by a

respiratory motion. A four-dimensional transformation, defined as a 12-parameter global affine motion model (six parameters for rotation and translation, three for scaling and three for skewing) and resolved by minimizing iteratively squared voxel difference [141], makes the CT data from a fraction of the respiratory cycle fit into different respiratory phases. 4) Gating CT in a similar way that PET acquisition is gated [142], [143], [144]. 5) Interactive PET/CT data acquisition. This approach applies a deep-inspiration breath-hold manner during scanning. Patient training is required to ensure reproducibility [145].

5.2.2 IMPROVEMENT OF DATA ACQUISITION MODE: LIST-MODE

The list-mode has been another upgrade for PET data acquisition. In contrast to the conventional frame-mode PET, the list-mode data acquisition records annihilation in an event-by-event fashion. A comparison study [26] shows that the list-mode PET advances in higher frequency of data storage, higher temporal resolution, and higher flexibility of data manipulation but possibly fails to send data to the hard drive when a large amount of events occur in a very short time interval due to the limited of transferring bandwidth of hardware. The list-mode data can incorporate other detected events (such as respiratory signal) to form valid constraints for reconstruction. Re-bin data in list mode is an application to remove the blurring effect. Image reconstruction, its relationship to motion, motion compensation and other relevant problems have also been investigated through theoretical developments and computer simulations [27], [28], [29], [30], [31]. Post-processing is a common practice in list-mode PET. Motion detection can also be performed from list-mode PET even without using external devices. A feasibility study [146]demonstrates that using post acquisition of list-mode data acquired in different

short time bins, a lesion's center of mass in the z-direction corrects the respiration curve obtained with the external motion detection device. Two difficulties exist in list-mode PET. First, finite resolution and noise of real motion tracking systems can degrade the performance of the algorithms (such as reconstruction, deduction of motion effect). Second, computational cost is very high because data are also recorded in temporal domain. To fully utilize the data is usually time-consuming.

5.2.3 GATED DATA ACQUISITION: MOTION CORRECTION

Gated PET triggered by an external signal has been comprehensively investigated by many research groups. Gated acquisition mode has been widely used to deal with the rigid movement during PET scan. It can greatly improve the respiratory motion signal recovery and geometrical delineation. Motion corrected images have greatly improved resolution compared to non-gated images, but they do introduce some resolution degradation compared to gated images resulting from registration error. In the gated acquisition mode, each respiratory cycle was divided into short-time bins, defined to encompass the respiratory cycle. Pioneering work has been done by the group of Nehmeh et al. at Memorial Sloan-Kettering Cancer Center [23] , [32], [33]. They demonstrated the importance of compensating respiratory motion artifacts in lung ^{18}F-FDG PET studies and the feasibility of respiratory gated PET as a practical solution to this problem. They assessed lung motion artifacts in lung cancer and demonstrated more accurate quantitation and definition of PET lesions by dividing the breathing cycle into discrete time bins. In order to produce respiratory gating, they used the Real-Time Position Management (RPM) Respiratory Gated System from Varian Medical Systems (Palo Alto,

Ca), originally designed for radiation treatment. The RPM tracks the vertical motion of two passive reflective markers on a plastic box set on the patient's abdomen, by using an infrared video camera. An illuminator ring surrounding the video camera floods the room with infrared light. A PC with vendor software digitizes the video signal, tracks the respiratory motion and allows the user to select a trigger pulse at a specific amplitude or phase within the respiratory cycle [33]. The respiratory motion track of the RPM system relies on the vertical motion of two passive markers. This makes the system vulnerable to inaccuracies due to complex 3D respiratory movements during the patient's breathing. It also requires positioning a box on the patient's abdomen and it involves a somewhat elaborate instrumentation set-up with the video camera. Respiratory gated systems vary depending on hardware or algorithm designs. Applications include, 1) Using the Polaris^{TM} device (Northern Digital, Waterloo, Canada) that tracks the motion of a plate with 4 reflectors using infrared radiation [147] (Figure 40, A); 2) Using the Real-time Position Management (RPM) system (Varian medical Systems, Palo Alto, CA) that tracks the respiratory motion through the use of 2 passive reflective markers [32], [33], [148], [149](Figure 40, B); 3) Using a pneumatic bellow placed around the chest to obtain respiratory motion signal [150] (Figure 40, D); 4) Using temperature-sensitive respiratory gating device [151]; 5) Using LDS (Laser optical Displacement Sensor) [152], [153], [154] (Figure 40, C); 6) Using the NCAT phantom to simulate respiratory motion and binning data in different gating windows [155]; 7) Using nonlinear motion model to process respiratory motion in stages of inspiration and expiration separately [156]. The objective of

using all these gating signals is to remove, reduce or compensate motion effect from the PET data [147], [153], [154] , [155], [157], [158].

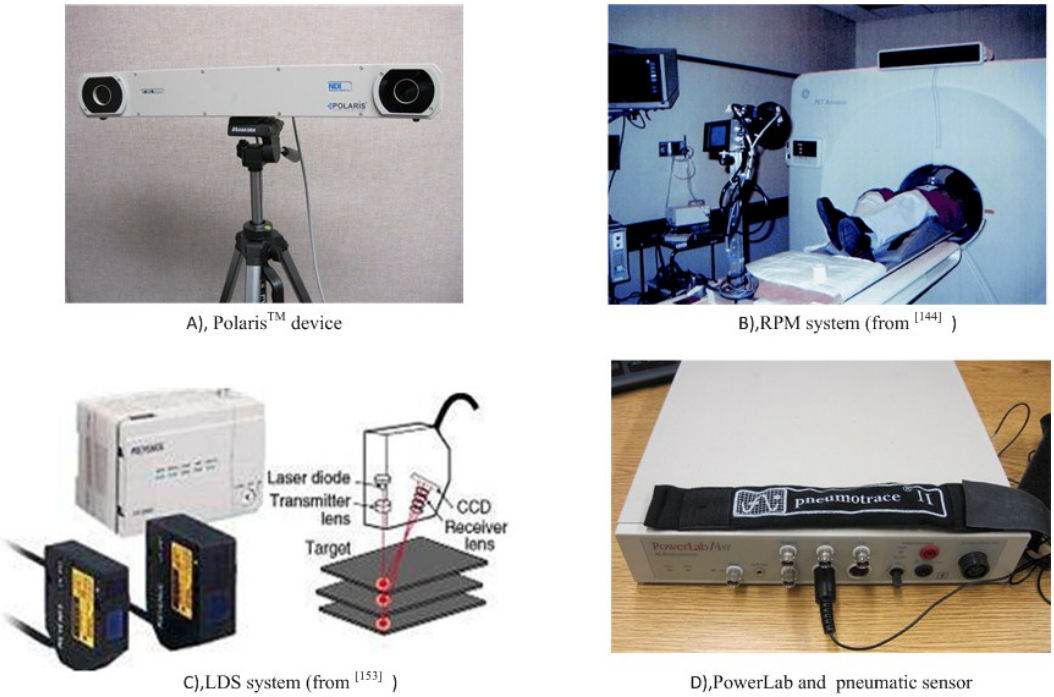

Figure 40: Different respiratory signal tracking system

More recently, Nehmeh et al. [159] developed a new method of respiratory-correlated dynamic PET (RCDPET) that allows the acquisition of 4D PET data without a respiratory tracking device. The RCDPET technique uses dynamic PET acquisition and an external reference point source attached to a rigid foam block placed on the patient's abdomen at the level of the lesion to track the respiratory motion. Then, PET data are retrospectively reconstructed at any phase or amplitude within the respiratory cycle. While this method has the advantage of not requiring a respiratory monitoring device for real time extraction of the respiratory signal, it involves positioning of the box with the

attached point source on the patient and into the field of view of the scanner, which may cause a degree of discomfort to the patient. This method required 200 times more memory per field of view than a standard emission scan (229 MB vs. 1.14 MB). It also has a longer time resolution compared to the respiratory-gated PET (1s vs. 0.013s) and requires computationally extensive and time consuming post-processing of the data [159].

5.2.4 IMPROVEMENT OF SOFTWARE: DECONVOLUTION POST-PROCESSING

Deconvolution, as a commonly used mathematical tool in signal and image processing [151], [160], has recently attracted researchers' attention in the field of CT and PET data processing. Since the annihilation collected by sensors in PET is influenced by respiratory motion, PET data acquisition can be presented as the result of a convolution between annihilation and respiration in both temporal and spatial domains. A post-processing deconvolution method applied to reconstructed PET images has been proposed by El Naqa et al. group. Several deconvolution methods have been tested in their studies [34], [35], [36], including methods which require little information about the breathing pattern motion of the tumor (only partially successful) to more accurate methods which require approximate tumor trajectories during breathing. The results show that the deconvolution approach is promising for either large or small tumors and indicate that using the wavelet based techniques and Bayesian estimation provided the best performance for motion deblurring. They model the resultant image as

$$g(x) = f(x) \otimes h(x) + n(x) \quad (5\text{-}1)$$

where *g* is the degraded image, *f* is the true image, *h* is the characteristic of the imaging system and *n* is the noise introduced. This type of problems is usually solved by the Wiener filter [161] or a modified Wiener filter when the spectrum of the SNR is not available. The modified Wiener filter requires tuning of a constant. When the 4D CT is available to estimate respiratory motion, the motion model (variable x in above equation) is derived from a linear mapping of the tidal volume and airflow space into a 3D space at different phases of the breathing cycle. By using expectation maximization method (EM) [162], [163], a similar alternative of the Wiener filter [161] they obtain the un-blurred image f after the k-th iteration

$$\hat{f}_{k+1}(x) = \hat{f}_k(x)\left[h(-x) \otimes \frac{g(x)}{h(x) \otimes \hat{f}_k(x)} \right] \quad (5\text{-}2)$$

where h is the motion-based tissue location probability function derived from 4D CT, g is the observed image. While the method restores the true PET image, it also unnecessarily amplifies the noise in PET data compared to other motion compensation techniques. When the motion is linear, spatially variant deconvolution filters have to be used, which increase not only the computational cost, but can also introduce other artifacts. In dealing with noise reduction (a criterion of convergence), they use the wavelet transform [164]. Other groups also have used wavelet-based noise reduction applications in the same or similar circumstances [34], [165]. The deconvolution approach is based on a system optimization consideration by post-processing. Nevertheless, at the present time progress is still being made to validate and standardize new methods for ^{18}F-FDG PET imaging for clinical use.

5.3 EVENT-BASED DYNAMIC JUSTIFICAION METHOD

As summarized in section 5.2, the list-mode approach can use a post-processing approach in order to remove unwanted parts of the acquired signal and to re-bin collected data based on the recorded respiration signal. The gating approach that takes "snapshots" data is based on the respiratory gating signal. The deconvolution approach that detaches motion effects from collected data sets is again based on the recorded respiration signal. These methods deal with the respiration signal differently. It is obvious that subject respiration causes trajectories of coincidence events off the radiation detectors which the trajectories of coincidence events are supposed to hit (to facilitate following description concisely, the word "trajectories" will replace the phrase "trajectories of coincidence events"). Figure 41 illustrates this phenomenon. In consequence, a blurred image is observed resulting from reconstruction of "misaligned" raw data. If the amount of trajectory offsets were known, re-arranging the trajectories back to their "original" locations would yield the motion-free signal collection on radiation detectors. The re-arrangement of trajectories is in fact to re-arrange the counting numbers in corresponding registers (see d_2 for implementation in Figure 41). However, the re-arrangement of trajectories must be performed simultaneously because the trajectories will overlap each other between respiration cycles. **Event-based dynamic justification** is the innovation for the proposed method.

The breathing motion of the chest and abdomen in axial-view can be represented by δ_x and δ_y components for a specific point in the contour. Figure 41 illustrates the "enlarged" respiration signals measured in two perpendicular directions at the moments

of beginning of expiration and beginning of inspiration. During inspiration, a lesion may move from p_1 to p_2, for general description, two pairs of radiation detectors (passing p_1 and p_2) are arbitrarily selected. Since the radiation is randomly emitted in three dimensions, we consider a specified angle in a specified cross section with respect to the center of the ring. The trajectory with angle θ_1 from radiation source at p_1 is collected by one pair of register counters associated with detectors D_i and D_j. At the next moment of inspiration, the radiation source from location p_1 moves to location p_2. The trajectory, with the angle θ_2, from the same radiation source at p_2 is collected by another pair of register counters associated with detectors D_i' and D_j'. The offset from D_iD_j to $D_i'D_j'$ is defined as the *trajectory disparity*. The trajectory disparity is determined by 1) the *location* of the radiation detector on the ring (e.g., register counters connected to detectors with small angle are affected more by respiration), 2) the cross sectional *shape* of the subject, especially the points (p_A, p_A') which the *trajectory* passes through and 3) the respiratory "*direction*", i.e., from expiration to inspiration, or from inspiration to expiration.

Considering a specified cross section, we temporarily limit our interest in the x-y space at a particular z level (similar to conventional PET data acquisition setup). Let us start with an ellipse to approximate the cross section of a subject; it is easy to establish a respiration-contour function by measured displacements as variables,

$$C(x,y,t) = f(\delta_x(t),\delta_y(t)) \qquad (5\text{-}3)$$

where δ_x and δ_y are the dynamically measured movement in the corresponding direction, and C is the contour function that can be derived from the measured movement signals.

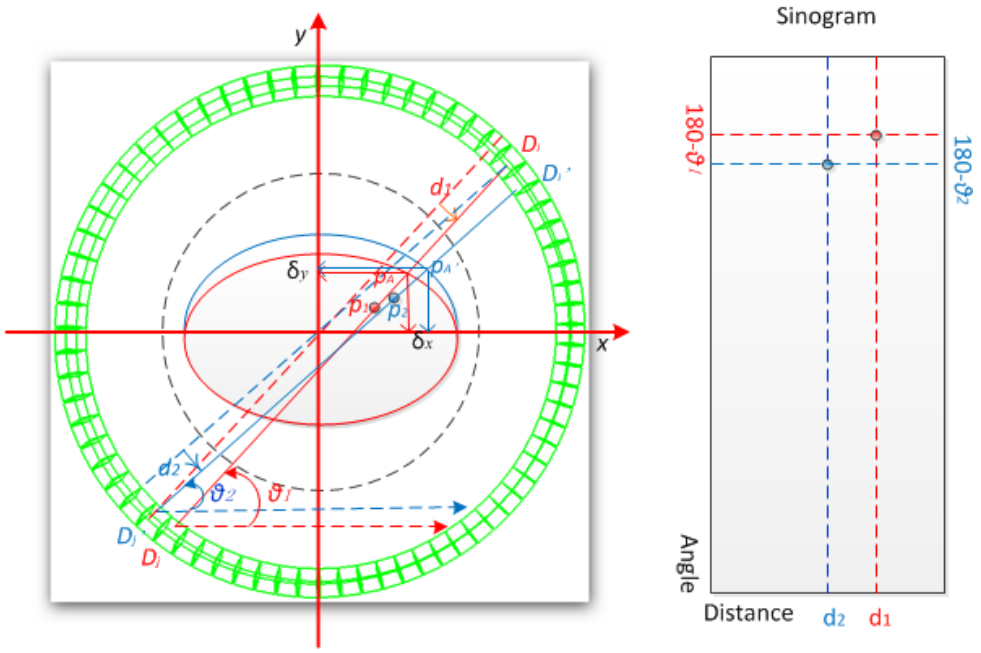

Figure 41: Illustration of the respiration movement

The defined contour does not predict the location of the internal organs/lesions. However, it does affect the tracks of trajectories. One can think of the CT projection profiles at two moments of respiration. For a specified moment, if we can estimate the "shape" of the subject, we can map the second projections "width" onto the first one's (not the "magnitude" because of unknown density distribution). That means $p_A(x, y)$ can be calculated from $p'_A(x, y)$. Applying this principle to PET data collection, we can correct the trajectory disparity. For a given SNR (Signal-Noise Ratio), the signal's shifting (trajectory disparity) correlates the axial-shape of the subject.

For a specific PET scanner, the inner radius *R* and detector size are all known. In this example, 72 pair detectors are equally distributed on a ring. Each detector occupies 2.5°. The arc length of each detector also can be calculated ($\frac{2.5\pi R}{180}$). From Figure 42, the coordinates of detector pairs D_iD_j can be calculated as follows:

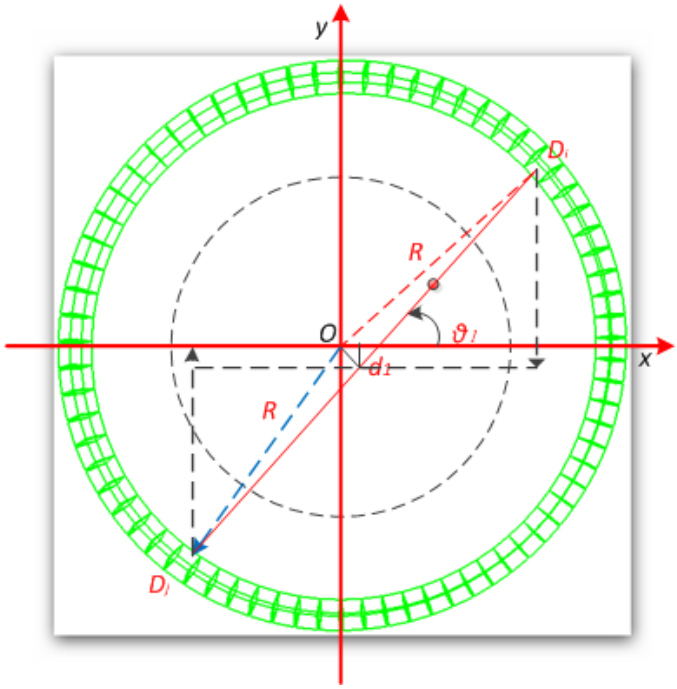

Figure 42: The coordinates calculation of detetor pairs

$$D_i \begin{pmatrix} x \\ y \end{pmatrix} = \begin{pmatrix} \sqrt{R^2 - d_1^2}\cos(\theta_1) + d_1 \sin(\theta_1) \\ \sqrt{R^2 - d_1^2}\sin(\theta_1) - d_1\cos(\theta_1) \end{pmatrix} \qquad (5\text{-}4)$$

$$D_j \begin{pmatrix} x \\ y \end{pmatrix} = \begin{pmatrix} -\sqrt{R^2 - d_1^2}\cos(\theta_1) + d_1 \sin(\theta_1) \\ -\sqrt{R^2 - d_1^2}\sin(\theta_1) - d_1\cos(\theta_1) \end{pmatrix} \qquad (5\text{-}5)$$

where R is the inner radius of the PET scanner, the value of d_1 is the perpendicular distance from the origin O to LOR D_iD_j, the sign of is d_1 determined by the projection direction. θ_1 is the angle between the LOR and the positive x-axis. The polar coordinate LOR D_iD_j (θ_1, d_1)also can be described as:

$$xsin(\theta_1) - ycos(\theta_1) = d_1 \qquad (5\text{-}6)$$

Similarly, the LOR of $D_i'D_j'$ can be described as follows:

$$xsin(\theta_2) - ycos(\theta_2) = d_2 \qquad (5\text{-}7)$$

$$D_i'\begin{pmatrix}x\\y\end{pmatrix} = \begin{pmatrix}\sqrt{R^2 - d_2^2}\cos(\theta_2) + d_2\sin(\theta_2)\\ \sqrt{R^2 - d_2^2}\sin(\theta_2) - d_2\cos(\theta_2)\end{pmatrix} \qquad (5\text{-}8)$$

$$D_j'\begin{pmatrix}x\\y\end{pmatrix} = \begin{pmatrix}-\sqrt{R^2 - d_2^2}\cos(\theta_2) + d_2\sin(\theta_2)\\ -\sqrt{R^2 - d_2^2}\sin(\theta_2) - d_2\cos(\theta_2)\end{pmatrix} \qquad (5\text{-}9)$$

Because the LOR of $D_i'D_j'$ is the movement result of LOR D_iD_j due to breathing, in two dimensions, their relationship can be defined as equation 5.11.

$$D_iD_j\begin{bmatrix}x\\y\\1\end{bmatrix} = \begin{bmatrix}cos\alpha & sin\alpha & t_x\\ -sin\alpha & cos\alpha & t_y\\ 0 & 0 & 1\end{bmatrix} D_i'D_j'\begin{bmatrix}x'\\y'\\1\end{bmatrix} \qquad (5\text{-}11)$$

Where α is the anti-clockwise rotation angle, here α equals θ_2 - θ_1 , t_x and t_y are the translation in x and y direction respectively.

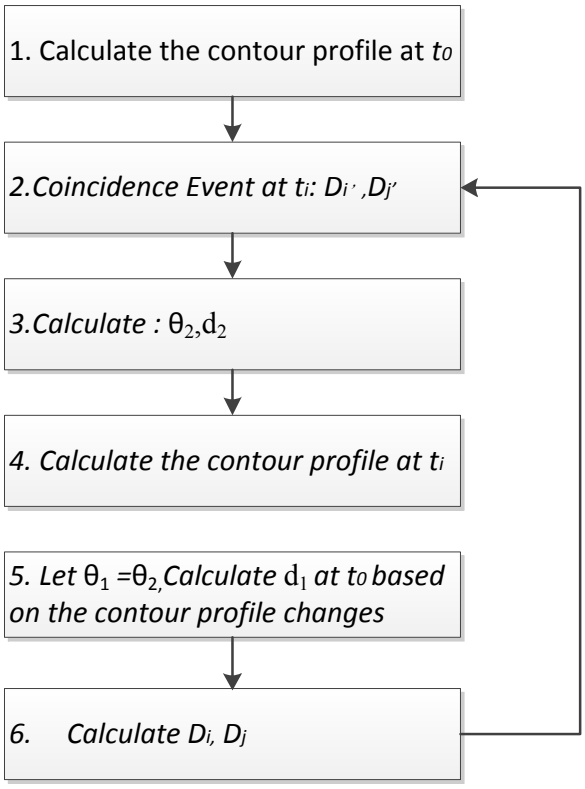

Figure 43: Work flow of the event-based dynamic justification method

In order to speed up the calculation, it is reasonable if we assume α=0, so t_x and t_y can be calculated based on the points on the contour profile. The work flow of the algorithm is shown in Figure 43. Steps 2 and 3 can be pre-calculated for a specific PET scanner and the result can be saved into a look-up table to accelerate real-time calculations. Normally, the approximate value $\bar{d}_1$ which is the calculation result of d_1 in real time, does not exactly match the pre-calculation result; this will bring a lot of round-off errors. Then D_i and D_j can be searched from the look-up table reversely based on $\bar{d}_1$ and θ_1.

5.4 NCAT PHANTOM

Now NURBS is one of the most common methods to model curves and surfaces in 3D graphical geometrics in computer models. A pth-degree NURBS [166] curve in the u direction is defined in Eq. 5-12. If qth-degree NURBS curve is also defined in the v direction at the same time, this will represent a NURBS surface (Eq. 5-13).

$$C(u) = \frac{\sum_{i=0}^{n} N_{i,p}(u) w_i P_i}{\sum_{i=0}^{n} N_{i,p}(u) w_i} \qquad 0 < u < 1 \qquad (5\text{-}12)$$

$$S(u,v) = \frac{\sum_{i=0}^{n}\sum_{j=0}^{m} N_{i,p}(u) N_{j,q}(v) w_{i,j} P_{i,j}}{\sum_{i=0}^{n}\sum_{j=0}^{m} N_{i,p}(u) N_{j,q}(v) w_{i,j}} \qquad 0 < u,v < 1 \qquad (5\text{-}13)$$

Where $\{P_i\}$,$\{P_{i,j}\}$ are control points set, $\{w_i\}$,$\{w_{i,j}\}$ are the weights and $\{N_{i,p}(u)\}$, $\{N_{j,q}(v)\}$ are B-spline base functions which can be defined by knot vectors. If we let the weights equal to one, a surface which is represented by NURBS includes 3 parts: U knot vector (Eq. 5-14), V knot vector (Eq.5-15) and control points set P.

$$U = \{\underbrace{0, \dots, 0}_{p+1}, u_{p+1}, \dots, u_{k-p-1}, \underbrace{1, \dots, 1}_{p+1}\} \quad k = n + p + 1 \qquad (5\text{-}14)$$

$$V = \{\underbrace{0, \ldots, 0}_{q+1}, v_{q+1}, \ldots, v_{l-q-1}, \underbrace{1, \ldots, 1}_{q+1}\} \quad l = m + q + 1 \qquad (5\text{-}15)$$

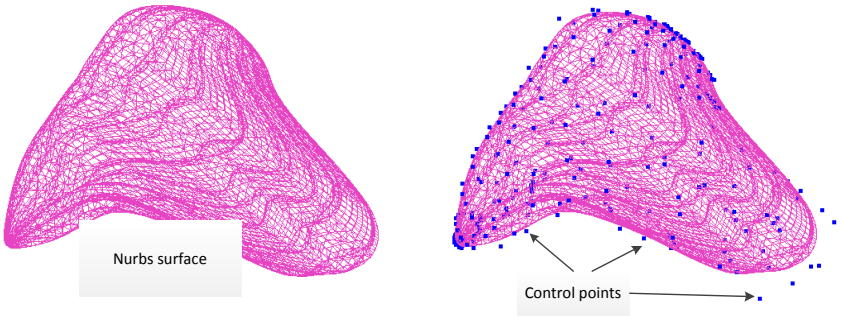

Figure 44: A NURBS surface and its control points

Figure 44 is an example which models a liver surface; the blue points in the right picture are the control points (dataset from NCAT, rendering in QGATE Designer).

Based on the CT dataset of the Visible Human Project [167] and other datasets, Segars, et al. [25] developed NCAT to model human anatomy, see Figure 45. Through applying affine transformation to the control points of relative organs, the respiration motion can be simulated.

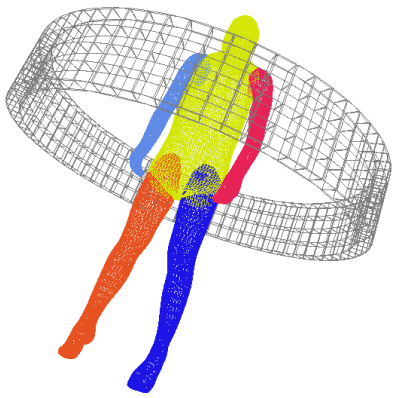

Figure 45: NCAT in QGATE Designer

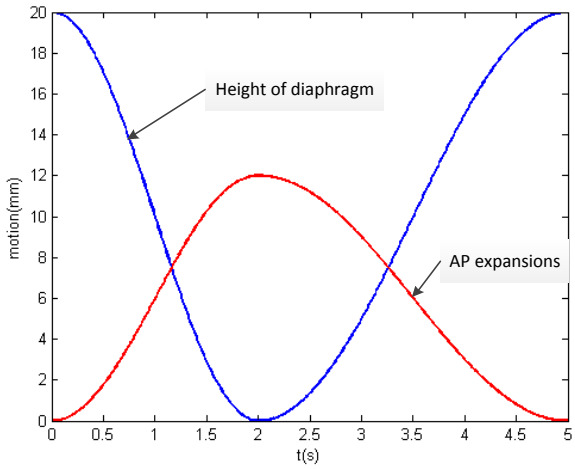

Figure 46: Normal breathing signal

Two motion equations were summed up for simulating normal respiration based on the breathing mechanics [25]. One is for the height changes of diaphragm, Δ_{HD} during a breathing cycle (Eq. 5-16); another is for AP expansions of chest wall, Δ_{AP} (Eq.5-17). In NCAT application package, an interface is introduced to help the user to utilize user-defined-data to simulate the motion of the diaphragm and AP expansions.

$$\Delta_{HD}(t) = \begin{cases} 10\cos(\frac{\pi t}{2}) + 10 & 0 \le t \le 2 \\ 10cos\left(\frac{\pi(5-t)}{3}\right) + 10 & 2 < t \le 5 \end{cases} \quad (5\text{-}16)$$

$$\Delta_{AP}(t) = \begin{cases} -\frac{N}{2}\cos\left(\frac{\pi t}{2}\right) + \frac{N}{2} & 0 \le t \le 2 \\ -\frac{N}{2}\cos\left(\frac{\pi(5-t)}{3}\right) + \frac{N}{2} & 2 < t \le 5 \end{cases} \quad (5\text{-}17)$$

where N is maximum expansion of AP. In normal breathing, N is set to 12 mm, and 20 mm is specified for the maximum height changes of the diaphragm. Figure 46 shows the motion curve in a normal breathing cycle.

5.5 REALISTIC HUMAN PHANTOMS PREPARATION

Unfortunately NCAT cannot be used directly in the GATE simulation. There are still no functions in GATE which can convert the NURBS data of NCAT into useful format too. Using the application provided by the NCAT software package, multi-frame phantoms with image-format can be generated. These phantoms include two corresponding parts. One part is for the activity distribution and the other part is for the attenuation coefficient. The number of frames can be determined by the period of the external respiratory signal. Each frame may include variable slices according to the user's needs and selection. In this study, 128 slices are chosen. These slices consist of human data set from neck to abdomen. Each slice thickness is 3.125mm and stored in 128 × 128 pixels. The value of each pixel is formatted by a 32 bit float data type. These image-format phantoms also cannot be used by GATE directly, because GATE only supports the image format of 16-bit unsigned integer pixel. So phantoms need to be converted first. Second, the original phantom has too many gray scales. This will also make those phantoms difficult to use and waste simulation time. The gray scale in this phantom should be trimmed down to a reasonable range.

The first principle of reducing the image's gray scales as less as possible is based on the density and linear attenuation coefficients of these tissues or organs at 511 kev (Table 9). Secondly, we consider clinical statistics of the radiation dose of these tissue or organs when ^{18}FDG is administrated intravenously. In clinical study, the standard dose using ^{18}FDG for adults is about 555 to 740MBq (15~20 mCi) [113]. Table 10 gives the estimation dose of different tissues or organs in the thorax of a 70-kg patient.

In Figure 47, the upper part shows a slice in the original activity distribution phantom and its histogram. The bottom part shows the re-binned phantom as a comparison. Figure 48 shows the original and the processed result of a slice of the attenuation phantom.

Tissue or Organ	Density ($g.cm^{-3}$)	$\mu(cm^{-1})$
Soft tissue	~1.04	~0.096
Adipose tissue	0.92~0.95	0.090
Lung (non-inflated)	1.05	~0.025~0.04
Smooth muscle	1.05	0.101
Skeletal muscle	1.05	0.024
Blood*	1.06	0.102
Heart*	1.05	0.101
Liver*	1.05	0.101
Kidney*	1.05	0.101
Spine Bone	1.42	0.136
Rib Bone *	1.92	0.184

Source: [168], [169] ;* *values are calculated based on* [169], *part of original data comes from* [115]

Table 9: Linear attenuation coefficient of related tissues or organs at 511keV

Radiation	Lung	Liver	Breast	Heart	Kidneys	Bone Marrow	Bone Surface
Dose(mGy/185MBp)	2.04	2.22	2.04	12.03	3.88	2.04	1.95

Source: [170]

Table 10: Estimated radiation dose of tissues or organs in thorax

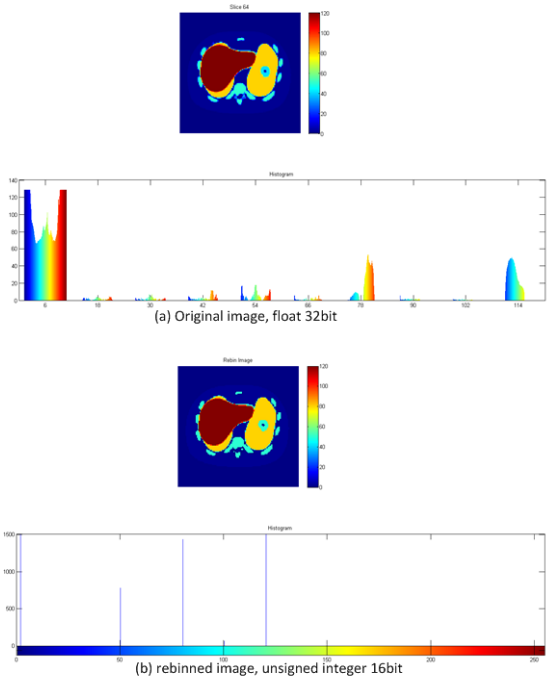

Figure 47: Comparison of the original and processed result of the activity distribution phantom

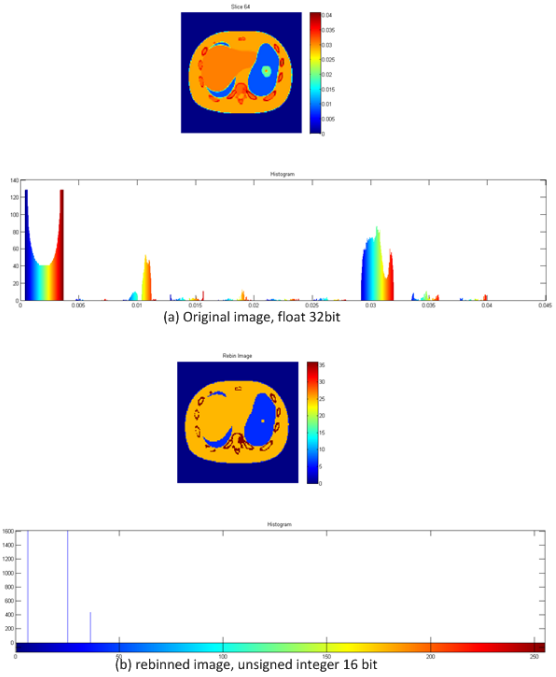

Figure 48: Comparison of the original and processed result of the attenuation phantom

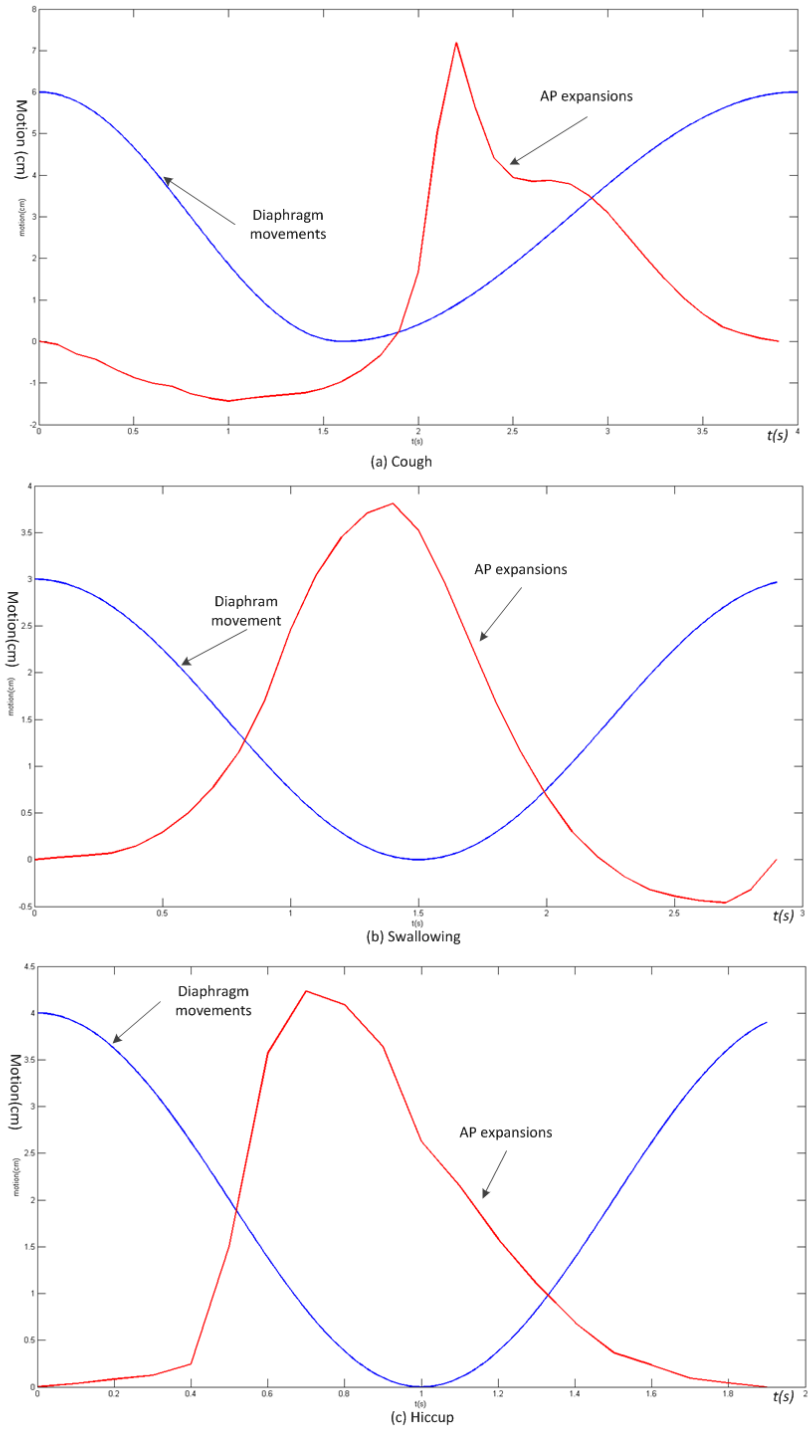

Figure 49: Simulation breathing signal in cough, swallowing and hiccup

5.6 SIMULATION RESULTS

In the simulation study, based on the captured signal of different respiratory states (Figure 49), a cycle signal of AP movement for each state is generated respectively. The signal of diaphragm movement for each state is also generated based on the signal of normal diaphragm movement. Figure 49 shows the respiratory signal of cough, swallowing, and hiccup in one period. The normal breathing signal can be found in Figure 46. Four realistic phantoms are generated based on NCAT. They are all converted to the format which can be recognized by GATE. Meanwhile they are all re-binned into appropriate gray scales. Table 10 gives the basic information of each simulation phantom used in this work.

Respiratory States	**Maximum Movement of Diaphragm (cm)**	**Maximum Expansions of AP (cm)**	**Period (s)**	**Phantom Frames**	**Slices of Each Frame**	**Slice Size**
Normal	2.4	1.2	5	10	128	128×128
Cough	6	7.2	4	12	128	128×128
Swallow	3	3.75	3	15	128	128×128
Hiccup	4	4.24	2	10	128	128×128

Table 11: Basic information of simulation phantoms

Lesion	Location	Diameter(mm)
A	Left Lung	30
B	Left Lung	20
C	Other	15
D	Liver	10
E	Right Lung	8
F	Right Lung	5

Table 12: Location and diameter of six different lesions

Frame	Lesion A	Lesion B	Lesion C	Lesion D	Lesion E	Lesion F
1	554	180	83	27	15	5
2	554	179	83	27	14	5
3	553	179	83	27	16	5
4	552	181	83	26	17	4
5	554	180	83	27	16	6
6	558	180	83	26	15	4
7	557	180	83	26	15	5
8	555	182	83	26	16	5
9	553	179	83	26	15	4
10	557	180	83	27	14	5
11	565	181	-	26	16	3
12	561	181	-	26	15	3
13	560	-	-	27	-	4
14	565	-	-	28	-	5
15	564	-	-	26	-	6
Average	**557.5**	**180.1**	**83**	**26.5**	**15.3**	**4.6**

Table 13: Volume size in pixel of each lesion in each frame

Six sphere lesions are defined. They have different diameters and locations in the phantoms. Table 12 gives their locations and diameters. Each phantom is assigned 3 different lesions. The real volume of each lesion in different frames is given in Table 13. It is important to calculate the total activity in a simulation study. The position of some lesions can be viewed in transverse, coronal and sagittal plane in each phantom. The animation of each phantom with lesion and without lesion can be viewed on-line.

Four simulation jobs have been tested for 1 second on the local server first. The output data are saved in ROOT format. The results are shown in Figure 50 to Figure 53. Due to the capability limitation of the local server, all jobs are transferred manually to the

Pegasus cluster located at the CCS (Center for Computational Science) at University of Miami [171]. Each job runs a 300-second simulation. The overall processing time of each job ranges from about 13 hours to 15 hours on a node of the cluster. Each node has 8 Xeon 2.6 GHz cores and 16 GB memory. Two results of each simulation job are provided; one is in normal condition; the other is using the event-based dynamic justification method. The final results are reconstructed using 3DRP (3D Re-Projection) algorithm [172] based on the source code of STIR (Software for Tomography Image Reconstruction) [173].

Lesion	Original	Normal(W×H)	Cough(W×H)	Swallow(W×H)	Hiccup(W×H)
A	72	13×21	—	12×15	—
B	32	10×17	9×16	—	9×15
C	18	11×8	—	—	7×7
D	8	—	—	—	—
E	5	—	—	—	—
F	2	—	—	—	—

Table 14: The center cross-section area of each lesion in pixel before justification

Lesion	Original	Normal(W×H)	Cough(W×H)	Swallow(W×H)	Hiccup(W×H)
A	72	14×14	—	13×13	—
B	32	10×10	9×10	—	11×12
C	18	8×8	—	—	7×7
D	8	—	—	—	—
E	5	—	3×4	—	—
F	2	—	—	4×4	—

Table 15: The center cross-section area of each lesion in pixel after justification

Table 14 and Table 15 give the estimation of the center cross-section area of each lesion in pixel before justification and after justification respectively. The estimation is based on the reconstruction images shown in Figure 50-53. In order to express the effect

of the new method, in Table 14 and Table 15, the data of each lesion are shown in width and height separately.

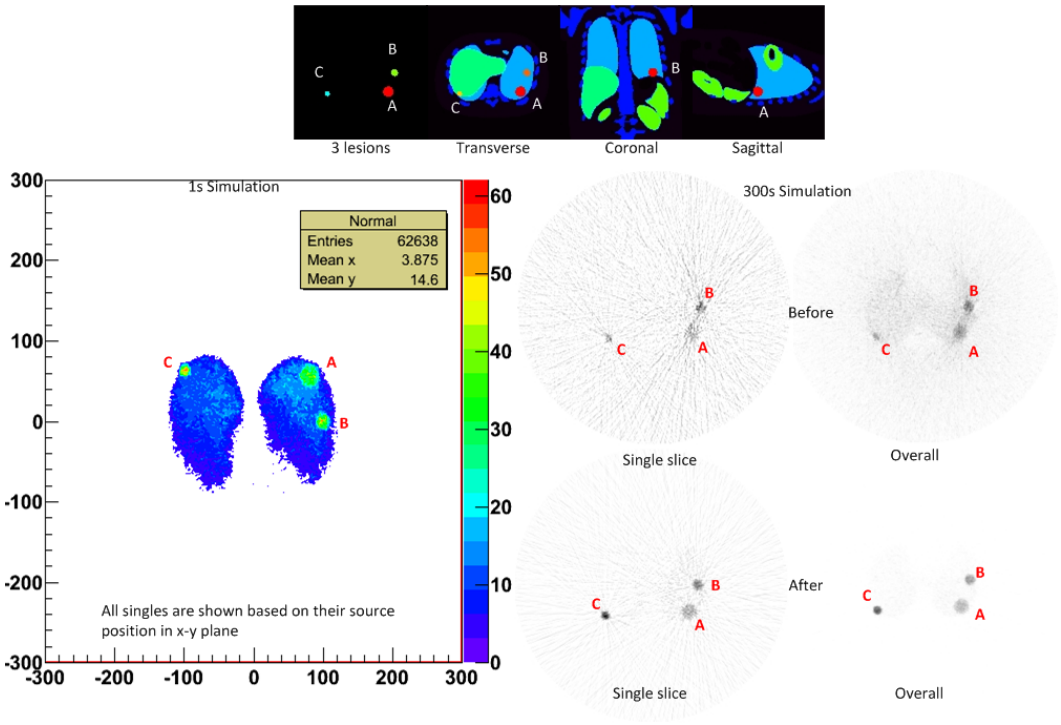

Figure 50: Lesions' distribution and simulation results of normal breathing

Figure 50 shows the phantom and results of normal breathing. The activity per pixel for lesions A, B and C is 35Bq, 50Bq and 60Bq respectively. Meanwhile, 3Bq/pixel activity is added to the lung area as the background activity. The overall average activity is 2.28×10^{5}Bq. From the results, the new method shows some improvement in motion-correction, especially in up-down direction for all lesions.

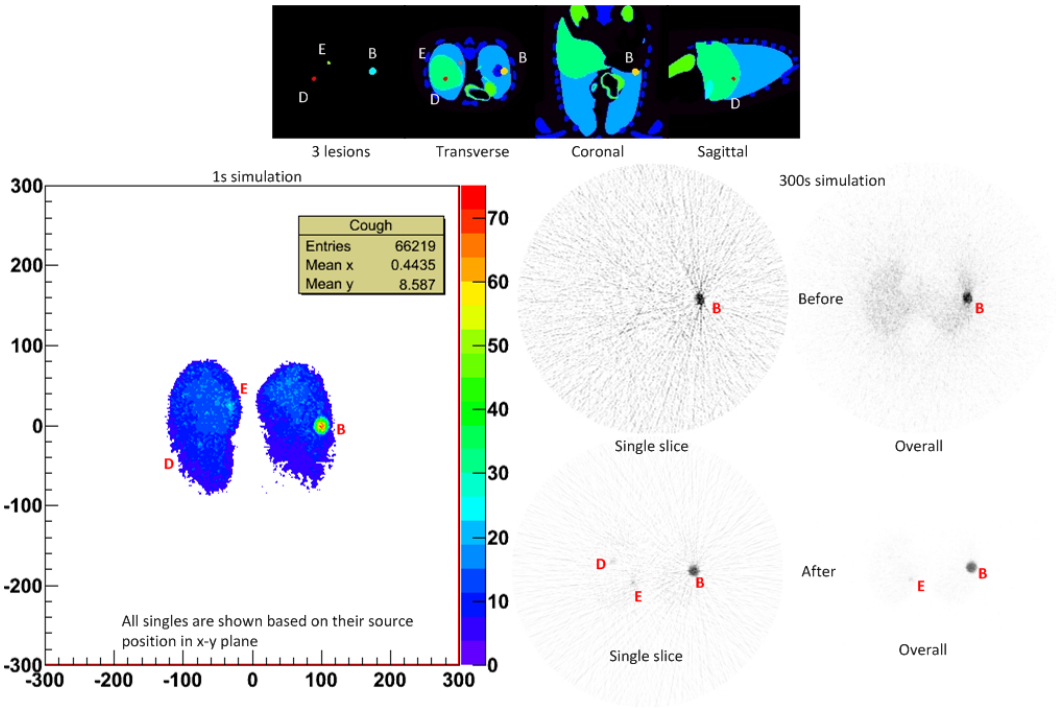

Figure 51: Lesions' distribution and simulation results of cough

Figure 51 gives the lesions' position in the phantom and the simulation results when coughing. The activity per pixel for lesions B, D and E is 60Bp, 50Bq, and 35Bq respectively. 3Bq/pixel is set for the lung area. The overall average activity is 2.31 $\times 10^5$Bq. Due to the small size, low activity and short simulation time (300s), lesions D and E cannot be observed in the results before justification. Lesion B has some shape deformation in the up-down direction because of motion. After justification, though D and E can be observed in a slice, as their diameters become larger. After the background is filtered out, lesion D cannot be observed in the overall result too. Only lesion B has a better result of motion-correction.

Figure 52 shows the lesions' position and the simulation results of the phantom when swallowing. 3Bq/pixel is specified for the lung area, The activity per pixel for

lesions A, D and F is set to 60Bq, 35Bq and 50Bq respectively. The overall activity is 2.35 $\times 10^5$Bq. From the result, lesion D cannot be observed, which may be caused by its low activity distribution and small size. The justification has impact on lesion F. Because F can be viewed in the overall result after justification, but cannot be seen before. Lesion A has a little bit of improvement.

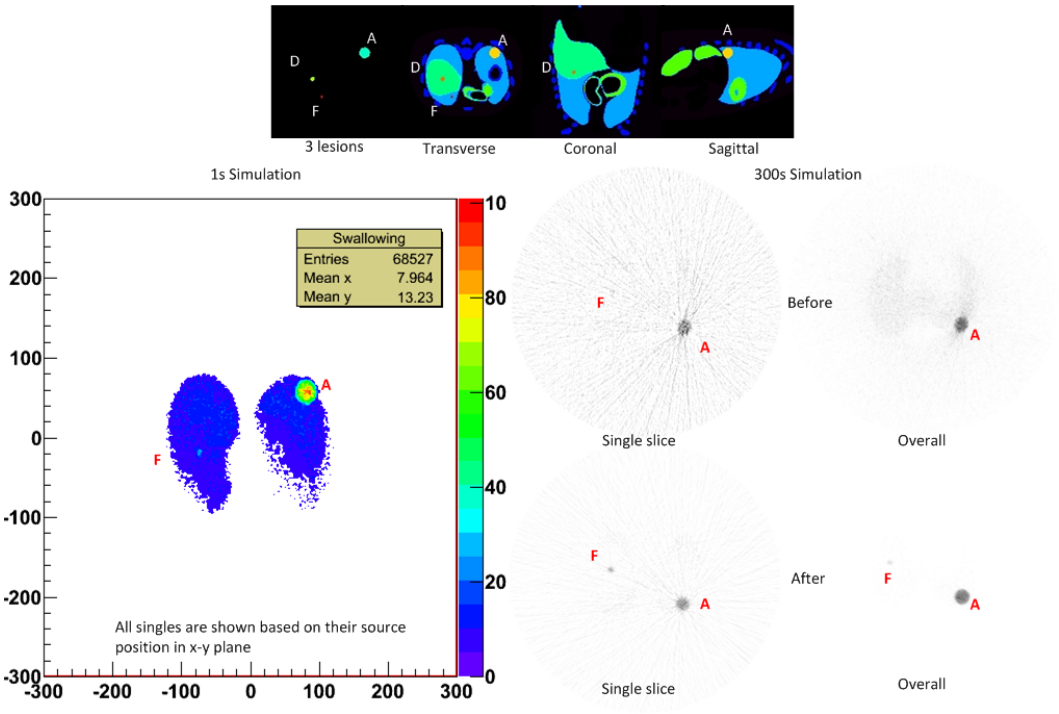

Figure 52: Lesions' distribution and simulation results when swallowing

In Figure 53, for the hiccupping phantom, the activity per pixel for lesions B, C and E is 60Bq, 35Bq and 50Bq respectively. As for the other three phantoms, 3Bq/pixel is also set for the lung area. The overall activity is 2.38 $\times 10^5$Bq.

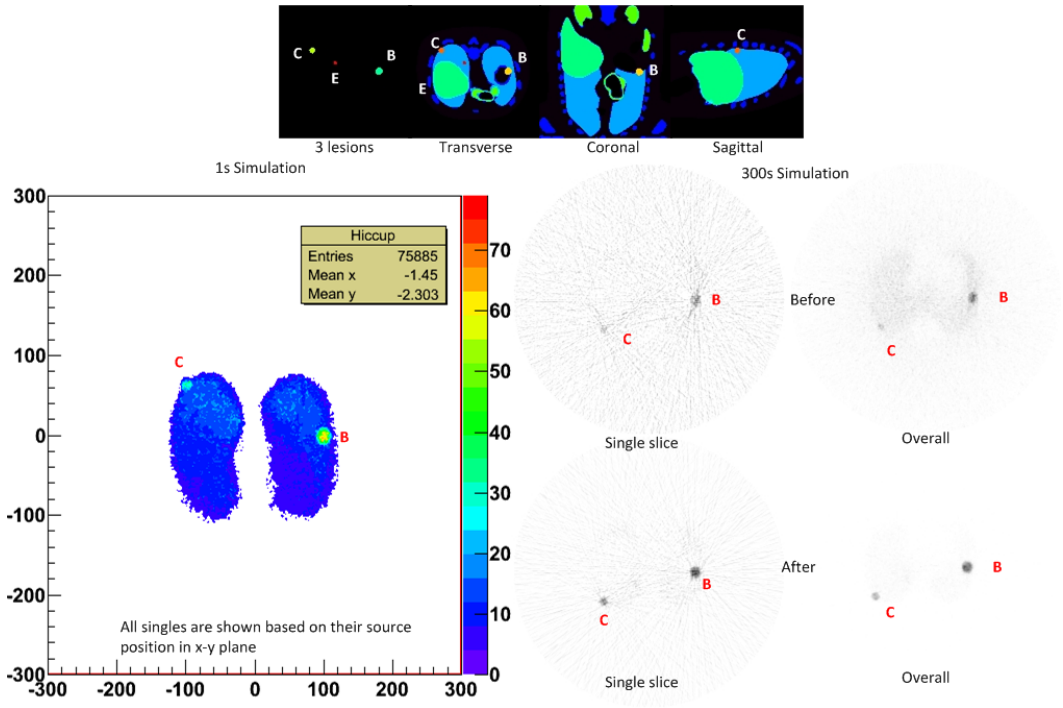

Figure 53: Lesions' distribution and simulation results when hiccuping

From the result, lesion D cannot be observed in both situations. The reason perhaps is the same as for the above analysis. By comparison with the result before justification, no obvious improvement can be seen from the result after justification. The reason is that the motion mainly comes from diaphragm movement in the z-direction which has little influence on the overall cross-section if the lesions are all located in the axial FOV.

5.7 DISCUSSION AND SUMMARY

From the simulation results, the event-based justification method shows its potential capability to help reduce motion influence of breathing in reconstruction image. Especially, to those lesions which have diameters larger than 15 mm, higher activity than background, and motion in the x-y plane. However, the improvement benefits a lot from

the simulation environment. Unlike the real experimental environment, the simulation has much more ideal conditions. First, the respiratory signal is always the same. Not only the contour changes are known, but also the exact position of any point in the phantom is known at any time. The position and movement of each lesion can be obtained. The lesions have been assigned much higher activity than the background. Meanwhile, the background has uniform activity distribution. It is easy to filter out the background in the final image. In addition, because only 2D cross-section information is considered in the new method, the z coordinate of the detectors is omitted. The PET scanner used in this simulation study has 32 rings, so that many cross-ring coincidence events are added to the center slice. Some of these events may come from the background decay in another slice and may be mistakenly added to the center slice as the coincidence events from a lesion. This is an important reason why the center slice has more counts than it should, and it makes the reconstruction result always much better than before justification. In addition, PET imaging simulation based on GATE is a very slow procedure. The calculation speed of event justification is not a problem, but in the real application, it may be a challenging job.

In this chapter, a new proposed method was tested based on the phantoms generated using different external breathing signals, though its real effectiveness needs to be further validated. This work shows that the prototype simulation platform can be used as a research platform as well as an education platform. The phantoms can be saved in the platform. They can be chosen by other users to carry out their own simulations. The

more user cases are accumulated in the platform, the more opportunity it can serve different users, more mature it will become.

CHAPTER 6 SUMMARY AND FUTURE PLAN

In this dissertation, three tasks have been complete: an education platform for medical imaging, a prototype simulation service platform and PET imaging simulation research based on the platform. Among them, the most important contribution is the simulation service platform. Based on the idea of Simulation as a Service (SaaS), a unique architecture has been built. It can manage different simulation applications agilely and flexibly. Its workflow is job-oriented, and like a bridge, it can connect complicated simulation applications with different level users together to facilitate the simulations. It can be used in education and also can be a useful tool in research and different training areas.

The education platform for medical imaging is another contribution. It has been used for several years by students in the BME department of the University of Miami. As a distributable software package, its architecture is kept in a relatively stable status. The evaluation and assessment output can help instructors adjust lecture content in the class. Different level evaluation questions can be picked out based on the students' performance in pre/post tests on-line. After several teaching/learning cycles, the evaluation questions are better suited for different assessment purposes. Finally, the questions related to basic concepts can be applied to build up a concept inventory for medical imaging education.

As a validated simulation software of PET imaging, GATE has become a widely used tool. QGATE client and the simulation service platform can facilitate its simulation work flow, from PET construction, crystal selection, phantom design, and different sources selection, etc. QGATE client provides a user-frendily GUI to help design the simulation scripts for students and educate them on how to conduct a simulation job.

Based on these, simulations have been carried out to serves double purposes. One is to verify the functions and capability of the simulation service platform. The other is to evaluate a new proposed acquisition method, event-based-justification. The processing of these simulations indicates that the simulation platform is competent and stable. At the same time, the results show the potential capability of the new method to reduce respiratory motion influence to get better quality in reconstruction images in PET imaging.

Though the frameworks and basic functions of the three projects have been built and implemented, as software related products, there is still a lot of work to be done in the future. First, because all the development is in the academic environment, there is no strict quality control during the development. Except for the fact that the education platform has been used and tested by students, the other two still need more time to test, verify and validate. However, the initial version has been downloaded many times from our website, no feedback has been collected yet.

Second, regarding the education platform, our objectives do not always match the students'; sometimes they may be in conflict. Based on the practice result, we find that those students lose interest quickly, so it is important to find out the common objectives between what we want them do and what they want to do. Aligning their interests with our objectives is the only way to keep our products growing. In the next step, we should focus on motivating their interests by providing more attractive and interactive high-quality contents. For example, some students may feel successful when they are challenged. Meanwhile we need let them know what they will benefit from it, so that they

may be more cooperative with us in the future research. The last consideration goes into the security, though the purpose of our development is for education and research, as network applications, it is also our responsibility to keep information and data as safe as possible.

REFERENCE

[1] B. Furht, A. Escalante and e. al., Handbook of Cloud, New York: Springer, 2010.

[2] R. Jennings, Cloud Computing with the Windows® Azure™ Platform, Indianapolis: Wiley Publishing, Inc., 2009.

[3] "Amazon Simple Storage Service (Amazon S3)," Amazon, [Online]. Available: http://aws.amazon.com/s3. [Accessed 12 09 2011].

[4] "Amazon Elastic Compute Cloud (Amazon EC2)," Amazon, [Online]. Available: http://aws.amazon.com/ec2. [Accessed 12 09 2011].

[5] "Google App Engine," Google, [Online]. Available: http://code.google.com/appengine/articles/. [Accessed 12 09 2011].

[6] "Google Apps," [Online]. Available: http://www.google.com/apps/intl/en/business/index.html. [Accessed 12 09 2011].

[7] "Microsoft Office Live," [Online]. Available: http://www.officelive.com/en-us/. [Accessed 12 09 2011].

[8] K. Delic and J. Riley, "Enterprise Knowledge Clouds: Next Generation KM Systems?," in *Proceedings of the 2009 International Conference Information, Process, and Knowledge Management*, Cancun, 2009.

[9] "Elastic-R," [Online]. Available: www.elasticr.net/portal. [Accessed 12 09 2011].

[10] "Scilab," [Online]. Available: http://www.scilab.org. [Accessed 12 09 2011].

[11] R. Brun and F. Rademakers, "ROOT - An Object Oriented Data Analysis Framework," in *Proceedings AIHENP Workshop, Nucl. Inst. and Meth. in Phys. Res. A*, 1996.

[12] "OpenGATE Collaboration," 2011. [Online]. Available: http://www.opengatecollaboration.org/ . [Accessed 06 2011].

[13] S. Agostinelli, J. Allison, K. Amako and e. al, "Geant4 - A Simulation Toolkit.," *Nucl. Instrum. and Meth. in Phys. Res,* vol. 506, no. 3, pp. 250-303, 2003.

[14] "Matlab Prices for Individual Licenses," The MathWorks, Inc., 2011. [Online]. Available: http://www.mathworks.com/store/productIndexLink.do. [Accessed 06 2011].

[15] "Qt – Cross-Platform Application and UI Framework," Nokia, [Online]. Available: http://qt.nokia.com/. [Accessed 06].

[16] F. Meas, A. Collignon, D. Vandermeulen, G. Marchal and P. Suetens, "Multimodality Image Registration by Maximization of Mutual Information," *IEEE Trans. Med. Imag.,* no. 16, pp. 187-198, 1997.

[17] S. Bacharach, "PET/CT Attenuation Correction: Breathing Lessons," *J. Nucl. Med.,* no. 48, pp. 677-679, 2007.

[18] M. Osman, C. Cohade, Y. Nakamoto and R. Wahl, "Respiratory Motion Artifacts on PET Emission Images Obtained Using CT Attenuation Correction on PET-CT," *Eur. J. Nucl. Med. Mol. Imag.,* no. 30, p. 603–606, 2003.

[19] P. Koepfli, T. Hany, C. Wyss, M. Namdar, C. Burger, K. Konstantinidis and e. al, "CT Attenuation Correction for Myocardial Perfusion Quantification using a PET/CT Hybrid Scanner," *J. Nucl. Med.,* no. 45, pp. 537-542, 2004.

[20] T. Pan, O. Mawlawi, S. Nehmeh, Y. Erdi, D. Luo, H. Liu and e. al., "Attenuation Correction of PET Images with Respiration-averaged CT Images in PET/CT," *J. Nucl. Med.,* no. 46, pp. 1481-1487, 2005.

[21] T. Pan, O. Mawlawi, D. Luo and e. al., "Attenuation Correction of PET Cardiac Data with Low-dose Average CT in PET/CT," *Med. Phys.,* no. 33, p. 3931–3938, 2006.

[22] R. Cook, G. Carnes, T. Lee and R. Wells, "Respiration-averaged CT for Attenuation Correction in Canine Cardiac PET/CT," *J. Nucl. Med.,* no. 48, pp. 811-818, 2007.

[23] Y. Erdi, S. Nehmeh, P. Tinsu, A. Pevsner, K. Rosenzweig, G. Mageras and e. al., "The CT Motion Quantification of Lung Lesions and Its Impact on PET-Measured SUVs," *J. Nucl. Med.,* no. 45, pp. 1287-1292, 2004.

[24] A. Alessio, S. Kohlmyer, K. Branch, G. Chen, J. Caldwell and K. Kinahan, "Cine CT for Attenuation Correction in Cardiac PET/CT," *J. Nucl. Med.,* no. 48, pp. 794-801, 2007.

[25] W. Segars, D. Lalush and B. Tsui, "Modeling Respiratory Mechanics in the MCAT and Spline-based MCAT Phantoms," *IEEE Trans. Nucl. Sci.,* no. 48, pp. 89-97, 2001.

[26] H. Watabe, K. Matsumoto, M. Senda and H. Iida, "Performance of List Mode Data Acquisition with ECAT EXACT HR and ECAT EXACT HR+ Positron Emission Scanners," *Ann. Nucl. Med.,* no. 20, pp. 189-194, 2006.

[27] R. Huesman, G. Klein, W. Moses, J. Qi, B. Reutter and P. Virador, "List-mode Maximum-likelihood Reconstruction Applied to Positron Emission Mammography (PEM) with Irregular Sampling," *IEEE Trans. Med. Imag.,* no. 19, pp. 532-537, 2000.

[28] J. Qi and R. Huesman, "List Mode Reconstruction for PET with Motion Compensation: A Simulation Study," in *IEEE International Symposium on Biomedical Imaging, Proceedings*, 2002.

[29] T. Nichols, J. Qi, E. Asma and R. Leahy, "Spatiotemporal Reconstruction of List-mode PET Data," *IEEE Trans. Med. Imag.,* no. 21, pp. 396 -404, 2002.

[30] E. Asma, N. TE, J. Qi and R. Leahy, "4D PET Image Reconstruction from List Mode Data," in *IEEE Nucl. Sci. Symp. Conf. Rec.*, 2000.

[31] Q. Li, E. Asma, S. Ahn and R. Leahy, "A Fast Fully 4-D Incremental Gradient Reconstruction Algorithm for List Mode PET Data," *IEEE Trans. Med. Imag.,* no. 26, pp. 58- 67, 2007.

[32] S. Nehmeh, Y. Erdi, K. Rosenzeig and e. al., "Effect of Respiratory Gating on Reducing Lung Motion Artifacts in PET Imaging of Lung Cancer," *Med. Phys.,* no. 29, pp. 336-37, 2002.

[33] S. Nehmeh, Y. Erdi, C. Ling, K. Rosenzweig, H. Schode, S. Larson and e. al., "Effect of Respiratory Gating on Quantifying PET Images of Lung Cancer," *J. Nucl. Med.,* no. 43, pp. 876-881, 2002.

[34] J. Wang, G. Wang and M. Jiang, "Blind Deblurring of Spiral CT Images Based on ENR and Wiener Filter," *J. X-ray Sci. and Tech.,* no. 13, p. 49–60, 2005.

[35] I. Naqa, D. Low, J. Bradley, M. Vicic and J. Deasy, "Deblurring of Breathing Motion Artifacts in Thoracic PET Images by Deconvolution Methods," *Am. Assoc. Phys. Med.,* no. 33, pp. 3587-3600, 2006.

[36] R. Puetter, T. Gosnell and A. Yahil, "Digital Image Reconstruction: Deblurring and Denoising," *Annu. Rev. Astron. Astrophys,* no. 43, p. 139–94, 2005.

[37] S. Jan, G. Santin, D. Strul and e. al., "GATE: A Simulation Toolkit for PET and SPECT," *Phys. Med. Biol.,* vol. 49, no. 19, p. 4543–4561, 2004.

[38] G. Santin, D. Strul, D. Lazaro and e. al., "GATE, A Geant4-based Simulation Platform for PET and SPECT Integrating Movement and Time Management," *IEEE Trans. Nucl. Sci.,* no. 50, p. 1516–1521, 2003.

[39] M. Gibbsons, "Engineering by the Numbers," [Online]. Available: http://www.asee.org/papers-and-publications/publications/college-profiles/2010-profile-engineering-statistics.pdf. [Accessed 09 2011].

[40] "White Paper," [Online]. Available: http://www.bmes.org/WhitakerArchives/academic/ugradbioimaging.pdf. [Accessed 06 2008].

[41] "BME Curriculum Database," [Online]. Available: ttp://bmes.seas.wustl.edu/Whitaker/. [Accessed 06 2008].

[42] L. Howard, "Adaptive Learning Technologies for Biomedical Engineering Education," *IEEE Eng. Med. Biol. Mag.,* no. 22, pp. 58-65, 2003.

[43] C. Paschal, "The Need for Effective Bomedical Engineering Education," *IEEE Eng. Med. Biol. Mag.,* no. 22, pp. 88-91, 2003.

[44] J. Holvikivi, "Logical Reasoning Ability in Engineering Students: A Case Study," *IEEE Trans. Educ.,* no. 50, pp. 367-372, 2007.

[45] I. Plaza and C. Medrano, "Continuous Improvement in Electronic Engineering Education," *IEEE Tran. Educ.,* no. 50, p. 259:265, 2007.

[46] J. Stewart and G. Stewart, "Educational Engineering Theory," 2004. [Online]. Available: http://educationalengineering.uark.edu/theory/ee-theory.pdf. [Accessed 05 2010].

[47] N. Carroll, L. Markauskaite and R. Calvo, "E-Portfolios for Developing Transferable Skills in A Freshman Engineering Course," *IEEE Trans. Educ.,* no. 50, pp. 360-366, 2007.

[48] K. Crawford , "E-learning and Activity: Supporting Communication, Cooperation and Coinvention," in *Proceedings of the 2nd IEEE International Workshop on Wireless and Mobile Technologies in Education (WMTE'04)*, 2004.

[49] B. Kerry, J. Isakson, P. Abraham, A. Arkatov, G. Bailey, J. Bingaman and e. al., "Report of the Web Based Education Commission to the President and Congress of the United States," 12 2000. [Online]. Available: http://www.ed.gov/offices/AC/WBEC/FinalReport/WBECReport.pdf. [Accessed 06 2010].

[50] "Virtual Imaging Laboratory," Duke University, [Online]. Available: http://dukemil.egr.duke.edu/. [Accessed 06 2009].

[51] M. Defrise, "A Short Reader's Guide to 3-D Tomographic Reconstruction," *Computerized Medical Imaging and Graphics,* no. 25, pp. 113-116, 2001.

[52] J. Ollinger and J. Fessler, "Positron Emission Tomography," *IEEE Signal Processing Magazine,* no. 14, pp. 43-55, 1997.

[53] G. Zeng, "Image Reconstruction - A Tutorial," *Computerized Medical Imaging and Graphics,* no. 25, pp. 97-103, 2001.

[54] A. Formiconi, A. Passeri, M. Guelfi, M. Masoni, A. Pupi and U. Meldolesi, "World Wide Web Interface for Advanced SPECT Reconstruction Algorithms Implemented on a Remote Massively Parallel Computer," *Intl. J.of Med. Info.,* no. 47, pp. 125-138, 1997.

[55] S. Vandenberghe, Y. Asseler, R. Van de Walle, T. Kauppinen, M. Koole, L. Bouwens, K. Van Laere, I. Lemahieu and R. Dierckx, "Iterative Reconstruction Algorithms in Nuclear Medicine," *Computerized Medical Imaging and Graphics,* no. 25, pp. 105-111, 2001.

[56] R. Acharya, R. Wasserman, J. Stevens and C. Hinojosa, "Biomedical Imaging Modalities: A Tutorial," *Computerized Medical Imaging and Graphics,* no. 19, pp. 3-25, 1995.

[57] D. Tweig, "The K-trajectory Formulation of the NMR Imaging Process with Applications in Analysis and Synthesis of Imaging Methods," *Med. Phys.,* no. 10, pp. 610-621, 1983.

[58] J. Ballinger, "Basic Concepts of MRI (Online Textbook)," [Online]. Available: http://www.mritutor.org/mritutor/index.html. [Accessed 06 2009].

[59] J. Hornak, "The Basics of MRI (online textbook)," [Online]. Available: http://www.cis.rit.edu/htbooks/mri/. [Accessed 06 2009].

[60] P. Alon, "Bringing the Internet and Multimedia Revolution to the Classroom," *Campus-Wide Information System,* no. 17, pp. 16-22, 2000.

[61] S. Athanasiou, I. Kouvaras, I. Poulakis, A. Kokorogiannis, P. Tsanakas and N. Koziris, "TALOS: An Interactive Web-enabled Educational Environment on Mobile Robot Technology," in *10th Meditmean Electrotechnical Conference*, 2000.

[62] R. Hake, "Interactive-engagement vs.Traditional Methods: A Six-thousand Student Survey of Mechanics Test Data for Introductory Physics Courses," *American Journal of Physics,* no. 6, pp. 64-75, 1998.

[63] J. Bransford, A. Brown and R. Cocking, How People Learn, Washington, D.C.: National Academy Press, 1999.

[64] M. Roblyer and L. Ekhaml, "How Interactive are YOUR Distance Courses? A Rubric for Assessing Interaction in Distance Learning," *Online Journal of Distance Learning Administration,* no. 3, 2000.

[65] M. Roubidoux, C. Chapman and M. Pointek, "Development and Evaluation of an Interactive Web-based Breast Imaging Game for Medical Students," *Acad. Radiol.,* no. 9, pp. 169-1178, 2002.

[66] I. Plaza and C. Medrano, "Continuous Improvement in Electronic Engineering Education," *IEEE Tran. Educ.,* no. 50, p. 259:265, 2007.

[67] G. Allan and J. Zylinski, "TheTeaching of Computer Programming and Digital Image Processing in Radiography," *Intl. J.of Med. Info.,* no. 139-143, p. 50, 1998.

[68] M. Grunewald, R. Heckemann, H. Gebhard, M. Lell and W. Bautz, "COMPARE Radiology:Creating an Interactive Web-based Training Program for Radiology with Multimedia Authoring Software," *Acad. Radiol.,* no. 10, pp. 543-553, 2003.

[69] M. Litzkow and G. Moses, "An Easy to Use Tool for Augmenting Multi-media Lectures with Accessible Self-assessment Exercises," in *Frontiers in Education Conference*, Indianapolis, 2005.

[70] M. Urban-Lurainl, G. Albertelli and G. Kortemeyer, "Work in Progress - Using Information Technology to Author, Administer, and Evaluate Performance-based Assessments," in *Frontiers in Education Conference*, Indianapolis, 2005.

[71] J. Gentry, What is Experiential Learning? Guide to Business Gaming and Experiential Learning, East Brunswick: Nichols/GP Publishing, 1990, pp. 9-20.

[72] D. Kolb, "Experiential Learning Theory and the Learning Style Inventory: A Reply to Freedman and Stumpf," *Academy of Management Review,* vol. 6, no. 2, pp. 289-96, 1981.

[73] D. Kolb, Experiential Learning, Englewood Cliffs: Prentice-Hall, 1984.

[74] D. Hestenes, M. Wells and G. Swackhamer, "Force Concept Inventory," *The Physics Teacher,* vol. 30, no. 3, p. 141–158, 1992.

[75] C. Mcloughlin, "The Implications of the Research Literature on Learning Styles for the Design of Instructional Material," *Australian Journal of Educational Technology,* vol. 15, no. 3, pp. 222-241, 1999.

[76] S. Elrod and S. Obispo, "Genetics Concepts Inventory," [Online]. Available: http://bioliteracy.net/Readings/papersSubmittedPDF/Elrod.pdf. [Accessed 11 03 2008].

[77] K. Wage, J. Buck, C. Wright and T. Welch, "The Signals and Systems Concept Inventory," *IEEE Trans. Educ.,* no. 48, pp. 448-461, 2005.

[78] A. Stone, K. Allen, T. Rhoads, T. Murphy, R. Shehab and C. Saha, "The Statistics Concept Inventory: A Pilot Study," in *Proceedings of the 33rd ASEE/IEEE Frontiers in Education Conference*, Boulder, 2003.

[79] J. Richardson, P. Steif, J. Morgan and J. Dantzler, "Development of A Concept Inventory for Strength of Materials," in *33rd ASEE/IEEE Frontiers in Education Conference.*, 2003.

[80] S. Krause, J. Birk, R. Bauer, B. Jenkins and M. Pavelich, "Development, Testing, and Application of A Chemistry Concept Inventory," in *34th ASEE/IEEE Frontiers in Education Conference*, 2004.

[81] D. Mulford and W. Robinson, "An Inventory for Alternate Conceptions among First-semester General Chemistry Students," *Journal of Chemical Education,* vol. 79, no. 6, pp. 739-744, 2002.

[82] T. Rhoads and R. Roedel, "The Wave Concept Inventory - A Cognitive Instrument Based on Bloom's Taxonomy," in *29th ASEE/IEEE Frontiers in Education Conference*, 1999.

[83] C. Caruana and J. Plaskek, "An Inventory of Biomedical Imaging Physics Elements-of-Competence for Diagnostic Radiography Education in Europe," *Radiography,* no. 12, pp. 189-202, 2006.

[84] G. Kuder and M. Richardson, "The Theory of the Estimation of Test Reliability," *Psychometrika,* vol. 2, no. 3, pp. 151-160, 1937.

[85] L. Cronbach, "Test "Reliablity": Its Meaning and Determination," *Psychometrika,* no. 12, pp. 1-16, 1947.

[86] L. Cronbach, "Coefficient Alpha and the Internal Structure of Tests," *Psychometrika,* no. 16, pp. 297-334, 1951.

[87] L. Guttman, "A Basis for Analyzing Test-Retest Reliability," *Psychometrika,* vol. 10, no. 4, pp. 255-282, 1945.

[88] K. Allen, T. Rhoads, R. Terry, T. Murphy and A. Stone, "Coefficient Alpha: An Engineer's Interpretation of Test Reliability," *J. Eng. Educ.,* no. 1, pp. 87-94, 2008.

[89] "Apache Web Server," [Online]. Available: http://httpd.apache.org/download.cgi. [Accessed 06 2011].

[90] "PHP: Hypertext Preprocessor," [Online]. Available: http://php.net/downloads.php. [Accessed 06 2011].

[91] "MySQL," [Online]. Available: http://dev.mysql.com/. [Accessed 06 2011].

[92] "Discuz," Comsenz Technology Co., Ltd, [Online]. Available: http://www.discuz.net/. [Accessed 06 2011].

[93] "phpBB," phpBB Limited, [Online]. Available: http://www.phpbb.com. [Accessed 06].

[94] M. Kofler, The Definitive Guide to MySQL 5, Berkley: Apress, 2005.

[95] W. Huda and R. Slone, Review of Radiologic Physics, Philadelphia: Lippincott Williams and Wilkins, 2003.

[96] J. Bushberg, J. Seibert, E. Leidholdt and J. Boone, The Essential Physics of Medical Imaging (Second Edition), Philadelphia: Lippincott Williams and Wilkins, 2002.

[97] X. Li and W. Zhao, "Work in Progress - Internet Accessible, Interactive Teaching Software and Tracking System for Medical Imaging Education," in *39th ASEE/IEEE Frontiers in Education Conference*, San Antonio, 2009.

[98] X. Li, F. Manns and W. Zhao, "Work in Progress - Medical Imaging Education by A Multi-level Module-based Online Teaching and Assessment System," in *40th ASEE/IEEE Frontiers in Education Conference*, Washington, DC, 2010.

[99] W. Zhao, X. Li and F. Manns, "Medical Imaging Teaching Software and Dynamic Assessment Tracking System for Biomedical Engineering Program”," in *American Society for Engineering Education*, 2011.

[100] D. Dewhurst, J. Hardcastle, P. Hardcastle and E. Stuart, "Comparison of A Computer Simulation Program and the Principles of Intestinal Absorption a Traditional Laboratory Practical Class for Teaching," *Advan. in Phys. Educ.,* no. 267, pp. S95-S104, 1994.

[101] P. Morgan, D. Cleave-Hogg, J. Mcilroy and J. Devitt, "Simulation Technology: A Comparison of Experiential and Visual Learning for Undergraduate Medical Students," *Anesthesiology,* vol. 96, no. 1, pp. 10-16, 2002.

[102] "Foldit Solve Puzzles for Science," [Online]. Available: http://fold.it/portal/. [Accessed 22 09 2011].

[103] F. Khatib, F. DiMaio, Foldit and e. al., "Crystal Structure of A Monomeric Retroviral ProteaseSolved by Protein Folding Game Players," *Nature Structural and Molecular Biology,* vol. 18, no. 10, pp. 1175-1177, 2011.

[104] A. McDaniel, Perl and Apache: Your Visual Blueprint for Developing Dynamic Web Content, Indianapolis: Wiley Publishing, Inc, 2010.

[105] S. Guelich, S. Gundavaram and G. Birznieks, CGI Programming with Perl, Second Edition, O'Reilly Media, 2000.

[106] R. Carver and K. Tai, Modern Multithreading:Implementing, Testing, and Debugging Multithreaded Java and C++/Pthreads/Win32 Programs, Hoboken: John Wiley & Sons, Inc., 2006.

[107] R. Netzer and B. Miller, "Optimal Tracing and Replay for Debugging Message Passing Parallel Programs," *Journal of Supercomputing,* vol. 8, no. 4, pp. 371-388, 1994.

[108] "Unix," [Online]. Available: http://www.unix.org. [Accessed 23 09 2011].

[109] M. Wernick and J. Aarsvold, Emission Tomography: the Fundamentals of PET and SPECT, London: Elsevier Academic Press, 2004.

[110] P. Valk, D. Delbeke, D. Bailey, D. Townsend and M. Maisey, Positron Emission Tomography: Clinical Practice, London : Springer-Verlag London Limited , 2006.

[111] D. Bailey, D. Townsend, P. Valk and M. Maisey, Positron Emission Tomography: Basic Sciences, London : Springer-Verlag London Limited , 2005.

[112] M. Burn, "PET Market Appears Poised for Continued Strong Growth," *Diag. Imag.,* no. 25, p. 93, 2003.

[113] T. Lynch, PET/CT in Clinical Practice, London: Springer-Verlag, 2007.

[114] H. Johns and J. Cunningham, The Physics of Radiology, Fourth Edition, Springfield: Charles C Thomas , 1983.

[115] J. Hubbel and S. Seltzer, "NIST: X-Ray Mass Attenuation Coefficients," Ionizing Radiation Division, Physics Laboratory, NIST, 2004. [Online]. Available: http://www.nist.gov/pml/data/xraycoef/index.cfm. [Accessed 22 09 2011].

[116] M. Phelps, S. Cherry and M. Dahlbom, PET Physics,Instrumentation, and Scanners, New York: Springer Science,Business Media, LLC, 2006.

[117] "BGO, LYSO and GSO Crystal Scintillators," Omega Pizeo, [Online]. Available: http://www.omegapiezo.com/crystal_scintillators.html. [Accessed 11 10 2011].

[118] G. Tarantola, F. Zito and P. Gerundini, "PET Instrumentation and Reconstruction Algorithms in Whole-body Applications," *J. Nucl. Med.,* no. 44, pp. 756-769, 2003.

[119] S. Strother, M. Casey and E. Hoffman, "Measuring PET Scanner Sensitivity: Relating Countrates to Image Signal-to-noise Ratios Using Noise Equivalent Counts," *IEEE Trans. Nucl. Sci.,* vol. 37, p. 783–788., 1990.

[120] M. Daube-Witherspoon, J. Karp, M. Casey, F. DiFilippo, H. Hines, G. Muehllehner, V. Simcic, C. Stearns, P. Vernon, L. Adam, S. Kohlmyer and V. Sossi, "PET Performance Measurements Using the NU 2–2001 Standard," *J. Nucl. Med.,* vol. 43, p. 1398–1409, 2002.

[121] D. Strul, G. Santin, D. Lazaro, V. Breton and C. Morel, "GATE (Geant4 Application for Tomographic Emission): A PET/SPECT General-Purpose Simulation Platform," *Nucl. Phys. B (Proc. Suppl.),* vol. 125, pp. 75-79, 2003.

[122] K. Assié, V. Breton, I. Buvat and e. al, "Monte Carlo Smulation in PET and SPECT Instrumentation using GATE," *Nucl. Instrum. and Meth. in Phys. Res. A,* no. 527, p. 180–189, 2004.

[123] S. Jan, C. Comtat, D. Strul, G. Santin and R. Trebossen, "Monte Carlo Simulation for the ECAT EXACT HR+ System Using GATE," *IEEE Trans. Nucl. Sci.,* vol. 52, pp. 627-633, 2005.

[124] K. Assié, I. Gardin, P. Véra and I. Buvat, "Validation of the Monte Carlo Simulator GATE for Indium-111 Imaging," *Phys. Med. Biol.,* vol. 50, p. 3113–3125, 2005.

[125] P. Gonias, N. Bertsekas, N. Karakatsanis and e. al., "Validation of A GATE Model for the Simulation of the Siemens Biograph 6 PET Scanner," *Nucl. Instrum. and Meth. in Phys. Res. A,* no. 571, pp. 263-266, 2007.

[126] F. Rannou, V. Kohli, D. Prout and A. Chatziioannou, "Investigation of OPET Performance Using GATE, A Geant4-based Simulation Software," *IEEE Trans. Nucl. Sci.,* no. 51, pp. 2713-2716, 2004.

[127] L. Simon, D. Strul, G. Santin, M. Krieguer and C. Morel, "Simulation of Time Curves in Small Animal PET using GATE," *Nucl. Instrum. and Meth. in Phys. Res. A,* no. 527, p. 90–194, 2004.

[128] I. Buvat and D. Lazaro, "Monte Carlo Simulations in Emission Tomography and GATE: An Overview," *Nucl. Instrum. and Meth. in Phys. Res. A,* no. 569, p. 323–329, 2006.

[129] J. He, G. O'Keefe, G. Jones and e. al., "The Application of GATE and NCAT to Respiratory Motion Simulation in Allegro PET," in *Proceedings of IEEE Nucl. Sci. Symp.*, 2006.

[130] N. Sakellios, J. Rubio, N. Karakatsanis and e. al., "GATE Simulations for Small Animal SPECT/PET using Voxelized Phantoms and Rotating-head Detectors," in *Proceedings of IEEE Nucl. Sci. Symp.*, 2006.

[131] A. Konik, M. Madsen and J. Sunderland, "GATE Simulations of Human and Small Animal PET for Determination of Scatter Fraction as A Function of Object Size," *IEEE Trans. Nucl. Sci.,* no. 57, pp. 2558-2563, 2010.

[132] E. Yoshida, T. Yamaya, K. Shibuya, F. Nishikido, N. Inadama and H. Murayama, "Simulation Study on Sensitivity and Count Rate Characteristics of “OpenPET” Geometries," *IEEE Trans. Nucl. Sci.,* no. 57, pp. 111-116, 2010.

[133] N. Karakatsanis, G. Loudos and K. Nikita, "A Methodology for Optimizing the Acquisition Time of A Clinical PET Scan Using GATE," in *Proceedings of IEEE Nucl. Sci. Symp. Conference*, 2009.

[134] J. De Beenhouwer, D. Kruecker, S. Staelens, L. Ferrer, A. Chatziioannou and F. Rannou, "Distributed Computing Platform for PET and SPECT Simulations with GATE," in *Proceedings of IEEE Nucl. Sci. Symp. Conference*, 2005.

[135] X. Li and W. Zhao, " QGATE: A New Graphical Simulation Client-Server Application Based on GATE," in *IEEE-NSS/MIC*, Knoxville, 2010.

[136] X. Li and W. Zhao, "QGATE: An Educational Environment to Learn and Perform Nuclear Medicine Imaging Simulation with GATE," *The Open Medical Imaging Journal,* vol. July, 2011.

[137] J. West, Respiratory Physiology: The Essentials, 8th Edition, San Diego: Lippincott Williams & Wilkins, 2008.

[138] Q. Hamid, J. Shannon and J. Martin, Physiologic Basis of Respiratory Disease, Hamilton: BC Decker Inc, 2005.

[139] B. Horn, Robot Vision, Cambridge: The MIT Press, 1986.

[140] D. Ballard and C. Brown, Computer Vision, Englewood Cliffs: Prentice-Hall, 1982.

[141] G. Klein, B. Reutter and R. Huesman, "Four-Dimensional Affine Registration Models for Respiratory-gated PET," *IEEE Trans. Nucl. Sci.,* no. 48, pp. 756-760, 2001.

[142] S. Nehmeh, Y. Erdi, T. Pan and e. al, "Four Dimensional (4D) PET/CT Imaging of the Thorax.," *Med. Phys.,* no. 31, p. 3179–3186, 2004.

[143] T. Pan, T. Lee, E. Rietzel and e. al, "4D-CT Imaging of A Volume Influenced by Respiratory Motion on Multi-slice CT," *Med. Phys.,* no. 31, p. 333–340, 2004.

[144] T. Yamazaki, H. Ue, I. Haneish, A. Hirayama, T. Sato and S. Nawano, "An Attenuation Correction Method for Respiratory-gated PET/CT Image," in *IEEE Nuc. Sci. Symp. Conf. Rec.*, 2006.

[145] G. Meirelles, Y. Erdi, S. Nehmeh, O. Squire, S. Larson, J. Humm and e. al., "Deep-inspiration Breath-hold PET/CT: Clinical Findings with A New Technique for Detection and Characterization of Thoracic Lesions," *J. Nucl. Med.,* no. 48, pp. 712-719, 2007.

[146] R. Bundschuh, A. Martínez-Moeller, M. Essler, M. Martínez, S. Nekolla, S. Ziegler and e. al., "Post-acquisition Detection of Tumor Motion in the Lung and Upper Abdomen using List-mode PET Data: A Feasibility Study," *J. Nucl. Med.,* no. 48, pp. 758-763, 2007.

[147] K. Thielemans, S. Mustafovic and L. Schnorr, "Image Reconstruction of Motion Corrected Sinograms," in *IEEE Nucl. Sci. Symp. Conf. Rec.*, 2003.

[148] H. Kubo, P. Len, S. Minohara and H. Mostafavi, "Breathing-synchronized Radiotherapy Program at the University of California Davis Cancer Center," *Med. Phys.,* no. 27, p. 346–353, 2000.

[149] S. Nehmeh and Y. Erdi, "Respiratory Motion in Positron Emission Tomography/Computed Tomography: A Review," *Semin Nucl. Med.,* pp. 38:167-176, 2008.

[150] B. Reutter, G. Klein and R. Huesman, "Automated 3D Segmentation of Respiratory-gated PET Transmission Images," *IEEE Trans. Nucl. Sci.,* no. 44, pp. 2473-2476, 1997.

[151] J. Starck and E. Pantin, "Deconvolution in Astronomy: A Review," *Publication of the Astronomical Society of the Pacific,* no. 114, p. 1051–1069, 2002.

[152] S. Woo, T. Song, J. Chop, K. Hong, Y. Choi, K. Lee and e. al, "Development of A Motion Detecting System for Respiratory-gated PET Using Laser Optical Displacement Sensor," in *IEEE Nucl. Sci. Symp. Conf. Rec.*, 2003.

[153] M. Georgiou, S. Carleo, A. Locascio, P. Tarjan, S. Ezuddin and G. Sfakianakis, "A Respiratory Gating System for PET Imaging," *J. Nucl. Med.,* p. 46:485P, 2005.

[154] M. Georgiou, W. Zhao, J. Bohorquez, Q. Shen, S. Ezuddin and G. Sfakianakis, "A PET Gated System for Respiratory Motion Compensation for Lung Lesion," *J. Nucl. Med.,* p. 48:163P, 2007.

[155] R. Manjeshwar, X. Tao, E. Asma and K. Thielemans, "Motion Compensated Image Reconstruction of Respiratory Gated PET/CT," in *3rd IEEE International Symposium on Biomedical Imaging: Nano to Macro*, 2006.

[156] H. Ue, H. Haneishi, H. Iwanaga and K. Suga, "Nonlinear Motion Correction of Respiratory-gated Lung SPECT Images," *IEEE Trans. Med. Imag.,* no. 25, pp. 486-495, 2006.

[157] N. Detorie and M. Dahlbom, "Motion Correction for Respiratory Gated PET Images," in *IEEE Nuc. Sci. Symp. Conf. Rec.*, 2006.

[158] M. Menke, M. Atkins and K. Buckley, "Compensation Methods for Head Motion Detected During PET Scans," in *IEEE Nucl. Sci. Symp. and Med. Imag. Conf. Rec.*, 1994.

[159] S. Nehmeh, Y. Erdi, K. Rosenzweig, H. Schoder, S. Larson, O. Squire and J. Humm, "Reduction of Respiratory Motion Artifacts in PET Imaging of Lung Cancer by Respiratory Correlated Dynamic PET: Methodology and Comparison with Respiratory Gated PET," *J. Nucl. Med.,* no. 44, pp. 1644-1648, 2003.

[160] M. Bertero and P. Boccacci, Introduction to Inverse Problems in Imaging, London: Inst. Phys., 1998.

[161] A. Katsaggelos, Digital Image Restoration, Berlin: Springer, 1991.

[162] A. Katsaggelos and K. Lay, "Image Identification and Image Restoration Based on the Expectation-maximization Algorithm.," *Opt. Eng. Bellingham,* no. 29, pp. 436-445, 1990.

[163] V. Mesarovic, N. Galatsanos and M. Wernick, "Iterative Linear Minimum Mean-square-error Image Restoration from Partially Known Blur," *J. Opt. Soc. Am,* no. 17, p. 711–723, 2000.

[164] I. Naqa, D. Low, J. Bradley, M. Vicic and J. Deasy, "Compensation of Breathing Motion Artifacts in Thoracic PET Images by Wavelet-based Deconvolution," in *3rd IEEE International Symposium on Biomedical Imaging: Nano to Macro*, 2006.

[165] K. Knesaurek and J. Machac, "Improving Detection of Small Lung Nodules in PET Imaging using Fourier-wavelet Deconvolution," in *IEEE Nucl. Sci. Symp. Conf. Rec.*, 2003.

[166] L. Piegl and W. Tiller, The NURBS Book,Second Edition, New York: Springer-Verlag, 2000.

[167] "The Visible Human Project," [Online]. Available: http://www.nlm.nih.gov/research/visible/visible_human.html. [Accessed 22 09 2011].

[168] P. Kinahan, D. Townsend, T. Beyer and D. Sashin, "Attenuation Correction for A Combined 3D PET/CT Scanner," *Med. Phys.,* vol. 25, no. 10, p. 2046–2053., 1998.

[169] C. Bai, L. Shao, A. Silva and Z. Zhao, "A Generalized Model for the Conversion from CT Numbers to Linear Attenuation Coefficients," *IEEE Trans. Nucl. Sci.,* vol. 50, no. 5, pp. 1510-1515, 2003.

[170] P. Oehr, H. Biersack and R. Coleman, PET and PET/CT in Oncology, Berlin: Springer-Verlag, 2004.

[171] "Center for Computational Science," [Online]. Available: http://www.ccs.miami.edu/hpc/Pegasus_intro.html. [Accessed 12 10 2011].

[172] P. Kinahan and J. Rogers, "Analytic 3D Image Reconstruction Using All Detected Events," *IEEE Tran. Nucl. Sci.,* vol. 36, no. 1, pp. 964 - 968, 1989.

[173] "STIR," [Online]. Available: http://stir.sourceforge.net/. [Accessed 12 06 2011].